Eur. Phys. J. Plus (2022) 137:914
https://doi.org/10.1140/epjp/s13360-022-03114-7

THE EUROPEAN PHYSICAL JOURNAL PLUS

Regular Article

Solitons, breath-wave transitions, quasi-periodic waves and asymptotic behaviors for a (2+1)-dimensional Boussinesq-type equation

Juan Yue, Zhonglong Zhao[a]

College of Mathematics, North University of China, Taiyuan 030051, Shanxi, People's Republic of China

Received: 23 March 2022 / Accepted: 26 July 2022

Abstract In this paper, the N-soliton solutions of a (2+1)-dimensional Boussinesq-type equation are obtained by the Hirota's bilinear method, and one-, two-, three-soliton solutions and their clear images are given in detail. Then, one breath-wave solution and two breath-wave solution are obtained by taking the complex conjugate of soliton solutions. The transformation mechanism of the breath-waves is analyzed systematically. Through the multi-dimensional Riemann theta function and bilinear method, the quasi-periodic wave solutions are obtained. Among these periodic waves, the high-dimensional complex three-periodic waves are firstly presented, the one-periodic waves are often applied to one-dimensional models of periodic waves in shallow water, the two-periodic waves and three-periodic waves are the generalization of one-periodic waves. The asymptotic behaviors of one-, two-, three-periodic waves and the relations between periodic wave solutions and soliton wave solutions are strictly established and proved by a limiting procedure. The characteristic line method is developed to analyze the dynamical characteristics of the quasi-periodic waves.

1 Introduction

Nonlinear science is a basic subject to study the commonness of nonlinear phenomena. As we all know, the research subjects of nonlinear science are chaos, solitons and fractals. Among them, solitons represent unpredictable organized behaviors in nonlinear science, which is the result of the balance between dispersion and nonlinearity in nonlinear dynamic systems. As a typical nonlinear phenomenon, it frequently appears in nonlinear optics [1–4], electromagnetism [5–8], plasma physics, condensed matter physics and biophysics [9–13].

The nonlinear Boussinesq equation plays an important role in marine research. The classical Boussinesq equation describes the propagation of long waves in shallow water. In addition, the Boussinesq equation also simulates the large-scale atmospheric and ocean currents leading to cold fronts and jets. The Boussinesq equation of surface gravity wave has been proved to be an effective tool for simulating wave propagation in coastal and marine areas [14]. In the past decades, researchers have given the exact analytical solutions [15], bright and dark soliton solutions [16], rogue wave solutions [17] and degenerate breather solutions [18] of the Boussinesq equation.

Quasi-periodic wave solutions have always been a hot topic of research in the field of integrable systems [19–22]. Some scholars have given the existence of quasi-periodic wave solutions of coupled Duffing-type equation [23], Vanderpol-Mathieu equation [24], etc. [25, 26]. The quasi-periodic wave solutions of algebraic geometry are constructed in a unified way on the basis of finite gap theory [27]. The quasi-periodic wave solutions of Kadomtsev-Petviashvili (KP) equation are obtained by Baker-Akhiezer functions when seeking compatible solution [28]. The quasi-periodic wave solutions of Saweda-Kotera-Kadomtsev-Petviashvili equation (SKKP) are gained by asymptotic analysis [29]. The quasi-periodic wave solutions have been also obtained via bilinear Bäcklund transformation [30], the Riemann-Bäcklund method [31] and the Riemann theta function [32]. In addition, the quasi-periodic wave solutions appear in many fields of science and technology [33, 34], including optics, electromagnetism, etc.

The Boussinesq equation is usually written in the form of $u_{tt}+u_{xx}-(u^2)_{xx}+\frac{1}{3}u_{xxxx}=0$, where the index x and t present partial derivatives. By the transformation $u\to u+1$, $(u+1)_{tt}+(u+1)_{xx}-((u+1)^2)_{xx}+\frac{1}{3}(u+1)_{xxxx}=0$, $u_{tt}+u_{xx}-(u^2+2u+1)_{xx}+\frac{1}{3}u_{xxxx}=0$, we have got another widely used Boussinesq equation $u_{tt}-u_{xx}-(u^2)_{xx}+\frac{1}{3}u_{xxxx}=0$, this equation was introduced by Boussinesq in 1871 [35, 36] to study the propagation of long waves in shallow water. In this paper, we devote to considering the following (2+1)-dimensional Boussinesq-type equation

$$u_{tt}+c_1u_{xx}+c_2u_{xy}+c_3\left(6u_x^2+6uu_{xx}+u_{xxxx}\right)=0, \tag{1}$$

where $u=u(x,y,t)$. Eq. (1) is integrable nonlinear partial differential equations in the sense of the theory of bilinear, the N-soliton solutions of Eq. (1) are obtained in the following statement, and it is a generalization of classical (2+1)-dimensional Boussinesq

[a] emails: zhaozlhit@163.com; zhaozl@nuc.edu.cn (corresponding author)

Published online: 11 August 2022

equation [37–39]. When $c_3 = 1$, Eq. (1) can be written into the form of another (2+1)-dimensional Boussinesq-type equation [40]. When $c_2 = 0$, the above equation reduces to a generalized two dimensional Boussinesq equation [41, 42]. The lump and rogue wave solutions of this generalized Boussinesq equation have been discussed in [40, 41]. However, there was no discussion about the breath-wave transitions and quasi-periodic wave solutions, especially the high-dimensional Riemann theta function quasi-periodic wave solutions. In this work, we shall investigate solitons, transformation mechanism of the breath-waves and quasi-periodic wave solutions in detail.

The organization of this paper is as follows. In Sect. 2, we briefly introduce the Hirota's bilinear method and derive the bilinear form and N-soliton solutions of Eq. (1) and present the Riemann theta function and its properties. In Sect. 3, we obtain one and two breath-wave solutions via taking the complex conjugate of soliton solutions and briefly introduce the breath-wave transitions. In Sections 4,5,6, we apply the Hirota's bilinear method and Riemann theta function to construct one-, two- and three-periodic wave solutions of Eq. (1). We further apply the limiting method and characteristic line method to analyze the characteristics and asymptotic behaviors of one-, two- and three-periodic wave solutions in detail. It is strictly proved that under a "small-amplitude" limit, the periodic wave solutions tend to the known soliton solutions. Finally, some conclusions are given in the last section.

2 Bilinear form and the Riemann theta function

In this section, we briefly introduce the bilinear form of Eq. (1) and some brief conclusions of the Riemann theta function.

2.1 Bilinear form of Eq. (1)

The Hirota's bilinear method [43–48] is an important tool for constructing exact solutions of many nonlinear equations. If a nonlinear equation is transformed into a bilinear form by a dependent variable transformation, the multi-soliton solutions are often obtained.

By the dependent variable transformation

$$u = 2(\ln f(x, y, t))_{xx},$$

Eq. (1) can be transformed into a bilinear form

$$\left(D_t^2 + c_1 D_x^2 + c_2 D_x D_y + c_3 D_x^4\right) f(x, y, t) f(x, y, t) = 0, \tag{2}$$

where the bilinear differential operators D_x, D_y and D_t are defined by

$$D_x^m D_y^n D_t^p f(x, y, t) g(x, y, t) = (\partial x - \partial x')^m (\partial y - \partial y')^n (\partial t - \partial t')^p f(x, y, t) g(x', y', t')|_{x'=x, y'=y, t'=t}.$$

These operators have a great property when applying to exponential function, that is

$$D_x^m D_y^n D_t^p \mathrm{e}^{\tau_1} \mathrm{e}^{\tau_2} = (\varepsilon_1 - \varepsilon_2)^m (\eta_1 - \eta_2)^n (\omega_1 - \omega_2)^p \mathrm{e}^{\tau_1 + \tau_2},$$

where $\tau_j = \varepsilon_j x + \eta_j y + \omega_j t + \upsilon_j$ $(j = 1, 2)$. Furthermore, we have

$$B(D_x, D_y, D_t) \mathrm{e}^{\tau_1} \mathrm{e}^{\tau_2} = B(\varepsilon_1 - \varepsilon_2, \eta_1 - \eta_2, \omega_1 - \omega_2) \mathrm{e}^{\tau_1 + \tau_2}, \tag{3}$$

where $B(D_x, D_y, D_t)$ is a polynomial about D_x, D_y and D_t. This property plays an important role in the subsequent construction of periodic wave solutions.

The N-soliton solutions of Eq. (1) can be found by applying Hirota's bilinear theory. It can be written in the form of

$$f = f_N = \sum_{\mu=0,1} \exp\left(\sum_{j=1}^{N} \mu_j \sigma_j + \sum_{j<s}^{N} \mu_j \mu_s A_{js}\right),$$

with phase variable $\sigma_j = k_j x + l_j y + \sqrt{-c_2 k_j l_j - c_3 {k_j}^4 - c_1 {k_j}^2} t + \delta_j$, k_j, l_j and δ_j are free constants,

$$\begin{aligned} e^{A_{js}} =& \Big(c_2 k_s l_j + c_2 k_j l_s + 4c_3 k_s^3 k_j + 4c_3 k_j^3 k_s - 6c_3 k_s^2 k_j^2 + 2c_1 k_s k_j \\ &+ 2\sqrt{-c_3 k_s^4 - c_1 k_s^2 - c_2 k_s l_s} \times \sqrt{-c_2 k_j l_j - c_3 k_j^4 - c_1 k_j^2}\Big) \Big/ \Big(c_2 k_j l_s + c_2 k_s l_j + 4c_3 k_s^3 k_j \\ &+ 6c_3 k_s^2 k_j^2 + 4c_3 k_j^3 k_s + 2c_1 k_s k_j + 2\sqrt{-c_3 k_s^4 - c_1 k_s^2 - c_2 k_s l_s}\sqrt{-c_2 k_j l_j - c_3 k_j^4 - c_1 k_j^2}\Big). \end{aligned}$$

The mark $\sum_{\mu=0,1}$ means summation over all possible combinations of $\mu_j = 0, 1$ $(j = 1...N)$, the $\sum_{j<s}^{N}$ summation is over all possible combinations of N elements in the specific condition $j < s$.

Therefore, the one-soliton solution of Eq. (1) has the form of

$$u_1 = 2\left(\ln(1 + \mathrm{e}^{\sigma})\right)_{xx}, \tag{4}$$

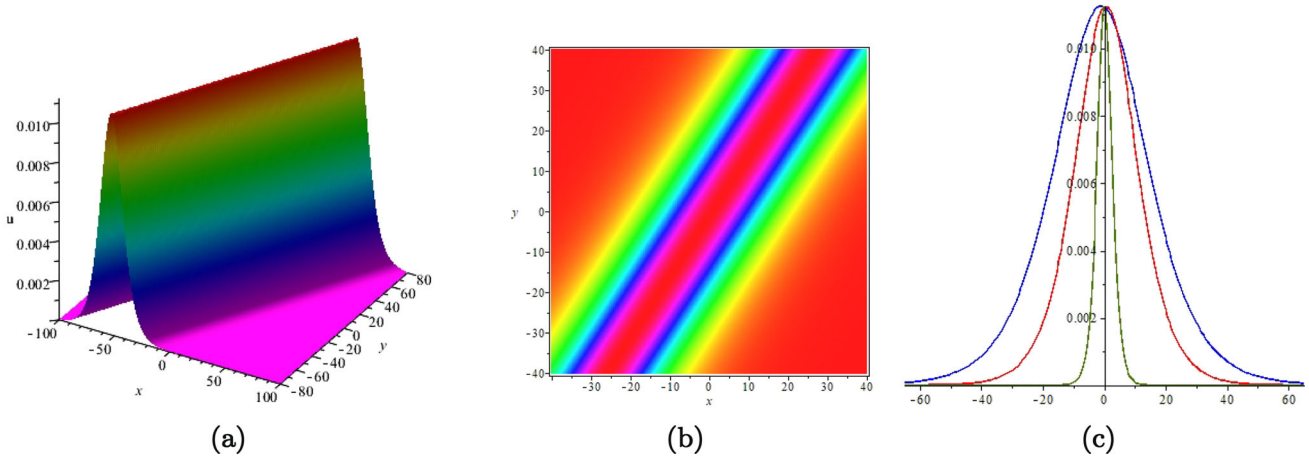

Fig. 1 (Color online) One-soliton wave Eq. (4) with parameters $c_1 = -10, c_2 = 10, c_3 = -20, k = 0.15, l = -0.1, \delta = -0.1$. **a** Three-dimensional stereogram of one-soliton wave when $t = 0$. **b** Vertical view of (**a**). **c** The wave moves along the x-axis$(-65 \le x \le 65)$(red) when $y = 0, t = 0$, y-axis$(-65 \le y \le 65)$(blue) when $x = 0, t = 0$, t-axis$(-65 \le t \le 65)$(green) when $x = 0, y = 0$

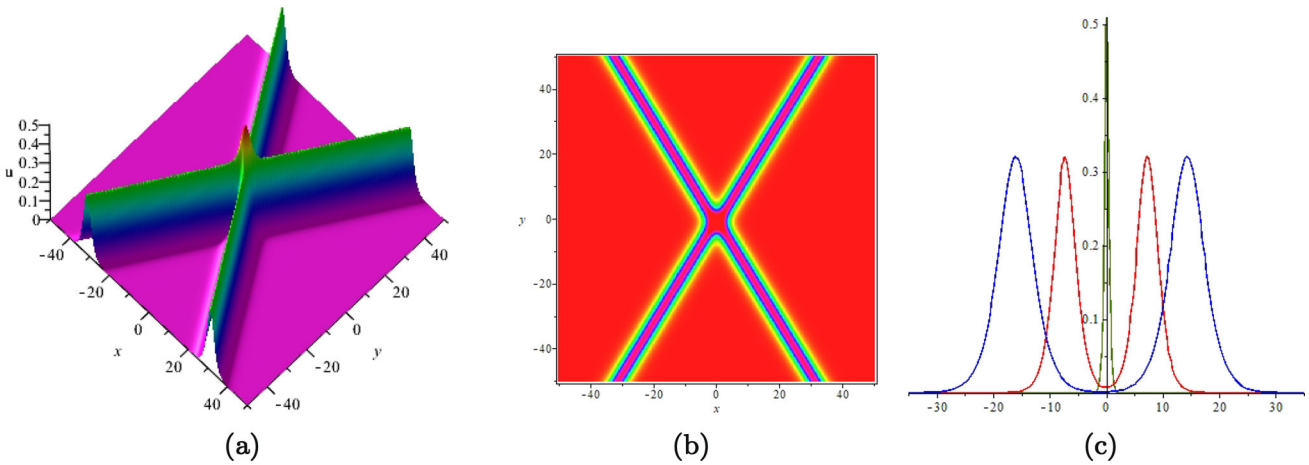

Fig. 2 (Color online) Two-soliton wave Eq. (5) with parameters $c_1 = -10, c_2 = 1, c_3 = -20, k_1 = -0.8, l_1 = 0.5, k_2 = 0.8, l_2 = 0.5, \delta_1 = 0, \delta_2 = 0$. **a** Three-dimensional stereogram of two-soliton wave when $t = 0$. **b** Vertical view of (**a**). **c** The wave moves along the x-axis$(-35 \le x \le 35)$(red) when $y = 0, t = 0$, y-axis$(-35 \le y \le 35)$(blue) when $x = 0, t = 0$, t-axis$(-35 \le t \le 35)$(green) when $x = 0, y = 0$

where phase variable $\sigma = kx + ly + \sqrt{-c_2kl - c_3k^4 - c_1k^2}t + \delta$, k, l and δ are free constants (Fig. 1).

While the two-soliton solution has the form of

$$u_2 = 2\Big(\ln(1 + e^{\alpha_1} + e^{\alpha_2} + e^{\sigma_1+\sigma_2+A_{12}})\Big)_{xx}, \tag{5}$$

(Fig. 2) with phase variable $\sigma_j = k_jx + l_jy + \sqrt{-c_2k_jl_j - c_3{k_j}^4 - c_1{k_j}^2}t + \delta_j$ $(j = 1, 2)$, $e^{A_{12}} = e^{A_{js}}(j = 1, s = 2)$.

Based on the above analysis, the three-soliton solution has the form of

$$u_3 = 2\Big(\ln\Big(1 + e^{\sigma_1} + e^{\sigma_2} + e^{\sigma_3} + e^{\sigma_1+\sigma_2+A_{12}} + e^{\sigma_2+\sigma_3+A_{23}} + e^{\sigma_1+\sigma_3+A_{13}} + e^{\sigma_1+\sigma_2+\sigma_3+A_{12}+A_{23}+A_{13}}\Big)\Big)_{xx}, \tag{6}$$

(Fig. 3) with phase variable σ_j $(j = 1, 2, 3)$, $e^{A_{12}} = e^{A_{js}}(j = 1, s = 2)$, $e^{A_{23}} = e^{A_{js}}(j = 2, s = 3)$, $e^{A_{13}} = e^{A_{js}}(j = 1, s = 3)$.

In order to construct the multi-periodic wave solutions, we consider

$$u = u_0 + 2(\ln\varphi(\tau))_{xx}, \tag{7}$$

where u_0 is a constant solution of Eq. (1), and phase variable τ has the form of $\tau = (\tau_1, \tau_2, ..., \tau_N)^T$, $\tau_j = \varepsilon_jx + \eta_jy + \omega_jt + \upsilon_j$ $(j = 1, 2, ..., N)$. By substituting Eq. (7) into Eq. (1) and integrating about variable x, we obtain the following bilinear form

$$B(D_x, D_y, D_t)\varphi(\tau)\varphi(\tau) = \big(D_t^2 + c_1D_x^2 + c_2D_xD_y + c_3D_x^4 + 6u_0D_x^2 + c\big)\varphi(\tau)\varphi(\tau) = 0, \tag{8}$$

where c is an integration constant.

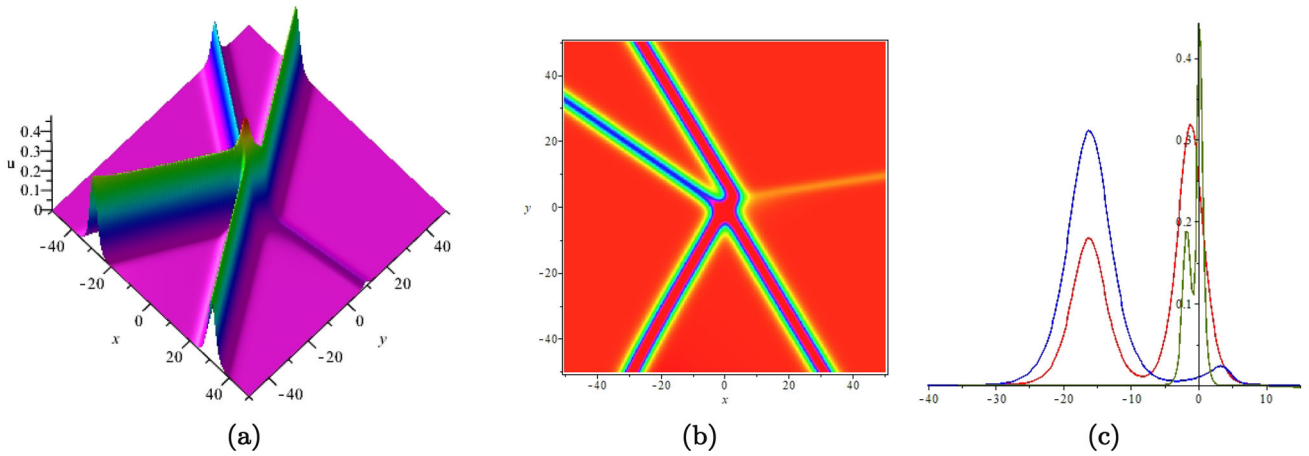

Fig. 3 (Color online) Three-soliton wave Eq. (6) with parameters $c_1 = -10, c_2 = 1, c_3 = -20, k_1 = -0.8, l_1 = 0.5, k_2 = 0.8, l_2 = 0.5, k_3 = 0.6, l_3 = 0.9, \delta_1 = 0, \delta_2 = 0, \delta_3 = 0$. **a** Three-dimensional stereogram of three-soliton wave when $t = 0$. **b** Vertical view of (**a**). **c** The wave moves along the x-axis($-40 \le x \le 15$)(red) when $y = 0, t = 0$, y-axis($-40 \le y \le 15$)(blue) when $x = 0, t = 0$, t-axis($-40 \le t \le 15$)(green) when $x = 0, y = 0$

2.2 Riemann theta function and its periodicity

Definition 1. The multi-dimensional Riemann theta function of genus N is defined as the form of

$$\varphi(\tau) = \varphi(\tau, a) = \sum_{n \in Z^N} \mathrm{e}^{-\pi \langle an, n \rangle + 2\pi \mathrm{i} \langle \tau, n \rangle}, \tag{9}$$

where the integer value vector $n = (n_1, n_2, ..., n_N)^T \in Z^N$, and complex phase variable $\tau = (\tau_1, \tau_2, ..., \tau_N)^T \in C^N$. Furthermore, for two vectors $h = (h_1, h_2, ..., h_N)^T$ and $p = (p_1, p_2, ..., p_N)^T$, their inner product is defined by $< h, p >= h_1 p_1 + h_2 p_2 + \cdots + h_N p_N$. The $a = (a_{ij})$ is a positive definite and real-valued symmetric $N \times N$ matrix.

Proposition 1 Let e_j be the jth column of $N \times N$ identity matrix I_N, a_j be the jth column of positive matrix a, a_{jj} be the element in row j, column j. Then the theta function $\varphi(\tau)$ has the following periodic properties:

$$\begin{aligned}
&(1)\ \varphi(\tau + \mathrm{e}_j, a) = \varphi(\tau, a),\\
&(2)\ \varphi(\tau + \mathrm{i}a_j, a) = \mathrm{e}^{-2\pi \mathrm{i}\tau_j + \pi a_{jj}} \varphi(\tau, a),\\
&(3)\ \left(\ln \varphi(\tau + \mathrm{e}_j, a)\right)_{\tau_j \tau_j} = (\ln \varphi(\tau, a))_{\tau_j \tau_j},\ j = 1, ..., N,\\
&(4)\ (\ln \varphi(\tau + \mathrm{i}a_j, a))_{\tau_j \tau_j} = (\ln \varphi(\tau, a))_{\tau_j \tau_j},\ j = 1, ..., N.
\end{aligned}$$

3 Breath-wave solutions and their transitions

3.1 The one-breath-wave solution of Eq. (1)

In this section, we obtain the one breath-wave solution of Eq. (1) by taking complex conjugate about real parameters of two-soliton solution(5), that is, letting

$$k_1 = a_1 + b_1 \mathrm{i},\ k_2 = a_1 - b_1 \mathrm{i},\ l_1 = p_1 + q_1 \mathrm{i},\ l_2 = p_1 - q_1 \mathrm{i},\ \delta_1 = \ln \frac{\alpha_1}{2} + \beta_1 + \gamma_1 \mathrm{i},\ \delta_2 = \ln \frac{\alpha_1}{2} + \beta_1 - \gamma_1 \mathrm{i}, \tag{10}$$

where $a_1, b_1, p_1, q_1 \neq 0, \alpha_1 > 0, \beta_1$ and γ_1 are arbitrary real constants. By letting $f_2 = (1 + \mathrm{e}^{\alpha_1} + \mathrm{e}^{\alpha_2} + \mathrm{e}^{\alpha_1 + \alpha_2 + \mathrm{A}_{12}})$ in Eq. (5), and substituting Eq. (10) into f_2, we obtain the following expression of the one breath-wave solution

$$f_2 \sim 2\sqrt{\alpha_2} \cosh(\theta_1 + \frac{1}{2} \ln \alpha_2) + \alpha_1 \cos(\Lambda_1), \tag{11}$$

where

$$\begin{aligned}
\theta_1 =& a_1 x + p_1 y + h_1 t + \beta_1,\ \Lambda_1 = b_1 x + q_1 y + d_1 t + \gamma_1,\ \alpha_2 = \frac{\alpha_1^2 G_1}{4},\\
G_1 =& \frac{-2c_1(a_1^2 + b_1^2) + 2c_2(a_1 p_1 + b_1 q_1) + 2c_3(a_1^4 - 7b_1^4 - 6a_1^2 b_1^2) + 2\sqrt{\Lambda_3^2 + \Lambda_4^2}}{-2c_1(a_1^2 + b_1^2) + 2c_2(a_1 p_1 + b_1 q_1) + 2c_3(7a_1^4 - b_1^4 + 6a_1^2 b_1^2) + 2\sqrt{\Lambda_3^2 + \Lambda_4^2}},
\end{aligned}$$

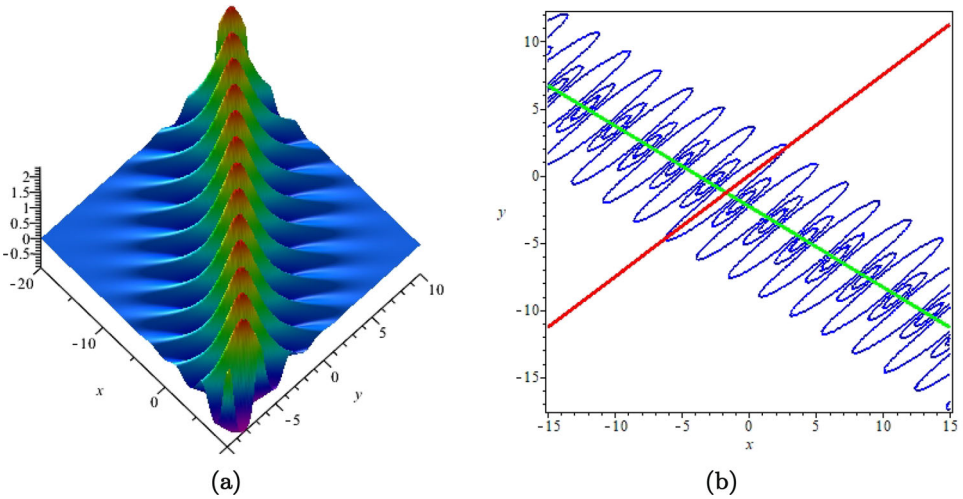

Fig. 4 (Color online) **a** One breath-wave of Eq. (1) with parameters $c_1 = c_2 = c_3 = 1, a_1 = 0.3, b_1 = 1.5, p_1 = 0.5, q_1 = -2, \alpha_1 = 2, \beta_1 = 0, \gamma_1 = 0$. This figure is three-dimensional stereogram of one breath-wave when $t = 0$. **b** the corresponding contour figure of (**a**), the red line $(1.5x - 2y = 0)$ and the green line $(0.3x + 0.5y + 1.153310513 = 0)$ are two characteristic lines of one breath wave

$$\Lambda_3 = -c_1(a_1^2 - b_1^2) - c_2(a_1p_1 - b_1q_1) - c_3(a_1^4 - 6a_1^2b_1^2 + b_1^4),$$
$$\Lambda_4 = -c_1(2a_1b_1) - c_2(b_1p_1 + a_1q_1) - c_3(4a_1^3b_1 - 4a_1b_1^3),$$
$$\sqrt{\Lambda_3 + \Lambda_4 \mathrm{i}} = h_1 + d_1\mathrm{i},\ \sqrt{\Lambda_3 - \Lambda_4 \mathrm{i}} = h_1 - d_1\mathrm{i}.$$

Then, by substituting Eq. (11) into Eq. (5), we obtain the one breath-wave solution of Eq. (1) as follows,

$$u_2 = \frac{2(2\sqrt{\alpha_2}\cosh(\theta_1 + \frac{1}{2}\ln\alpha_2)a_1{}^2 - \alpha_1\cos(\Lambda_1)b_1{}^2)}{2\sqrt{\alpha_2}\cosh(\theta_1 + \frac{1}{2}\ln\alpha_2) + \alpha_1\cos(\Lambda_1)} - \frac{2(2\sqrt{\alpha_2}\sinh(\theta_1 + \frac{1}{2}\ln\alpha_2)a_1 - \alpha_1 sin(\Lambda_1)b_1)^2}{(2\sqrt{\alpha_2}\cosh(\theta_1 + \frac{1}{2}\ln\alpha_2) - \alpha_1\cos(\Lambda_1))^2}. \tag{12}$$

Based on the work of the transitions of the breath-waves for the (2+1)-dimensional Ito equation [49], one breath-wave solution (12) of Eq. (1) has the following characteristics.

(1) It can be seen from expression (12) that the one breath-wave solution includes a hyperbolic function (cosh, sinh) and a trigonometric function (sin, cos), in which the hyperbolic function controls the local properties of one breath-wave, and the periodic properties are dominated by trigonometric function, so one breath-wave can be regarded as the combination of soliton and periodic wave.

(2) It is obviously noticed that the wave velocity of soliton along x-axis is $v_x^s = -\frac{a_1h_1}{a_1{}^2+p_1{}^2}$, and the wave velocity of soliton along y-axis is $v_y^s = -\frac{p_1h_1}{a_1{}^2+p_1{}^2}$, the velocity of periodic wave along x-axis is $v_x^p = -\frac{b_1d_1}{b_1{}^2+q_1{}^2}$, the velocity of periodic wave along y-axis is $v_y^p = -\frac{q_1d_1}{b_1{}^2+q_1{}^2}$,

(3) From Eq. (12), the one breath-wave has two characteristic lines: $\theta_1 + \frac{1}{2}\ln\alpha_2 = a_1x + p_1y + h_1t + \beta_1 + \frac{1}{2}\ln\alpha_2 = 0,\ \Lambda_1 = b_1x + q_1y + d_1t + \gamma_1 = 0$.

(i) If one has the following relation of $\begin{vmatrix} a_1 & p_1 \\ b_1 & q_1 \end{vmatrix} \neq 0$, the two characteristic lines are not parallel, as shown in Fig. (4).

(ii) If one has the following relation of $\begin{vmatrix} a_1 & p_1 \\ b_1 & q_1 \end{vmatrix} = 0$, that is the two characteristic lines are parallel, as shown in Fig. (5). Based on this special condition, the one breath-wave can be transformed into a series of nonlinear waves including quasi-anti-dark soliton, M-shaped soliton, oscillation M-shaped soliton, multi-peak soliton, quasi-sine wave, quasi-periodic W-shaped wave, quasi-periodic anti-dark soliton wave and quasi-periodic wave. In Fig. 5a and b, quasi-anti-dark soliton ($\frac{b_1}{a_1} < 0.4$) has only one characteristic line and is symmetrical about extreme line. In Fig. 5c and d, M-shaped soliton ($0.4 \leq \frac{b_1}{a_1} \leq 1$) has two peaks, one valley, three characteristic lines and is asymmetrical about extreme line. With the value of $\frac{b_1}{a_1}$ increasing, the one breath-wave becomes a asymmetrical oscillation M-shaped soliton $\left(1 < \frac{b_1}{a_1} \leq 2.5\right)$, and the number of characteristic lines also increases, if the value of $\frac{b_1}{a_1}$ increases continuously, the oscillation becomes acute, and the one breath-wave becomes a asymmetrical multi-peak soliton $\left(\left\{2.5 < \frac{b_1}{a_1} < 50\right\}\right)$, as shown in Fig. 5e–h. When the value of $\frac{b_1}{a_1}$ becomes very large, the one breath-wave transforms quasi-sine wave ($\frac{b_1}{a_1} \geq 50$), quasi-periodic W-shaped wave $\left(\frac{b_1}{a_1} \approx 1000\right)$, quasi-periodic anti-dark soliton wave $\left(\frac{b_1}{a_1} \approx 1000\right)$ and quasi-periodic wave $\left(\frac{b_1}{a_1} \geq 1500\right)$. Their locality

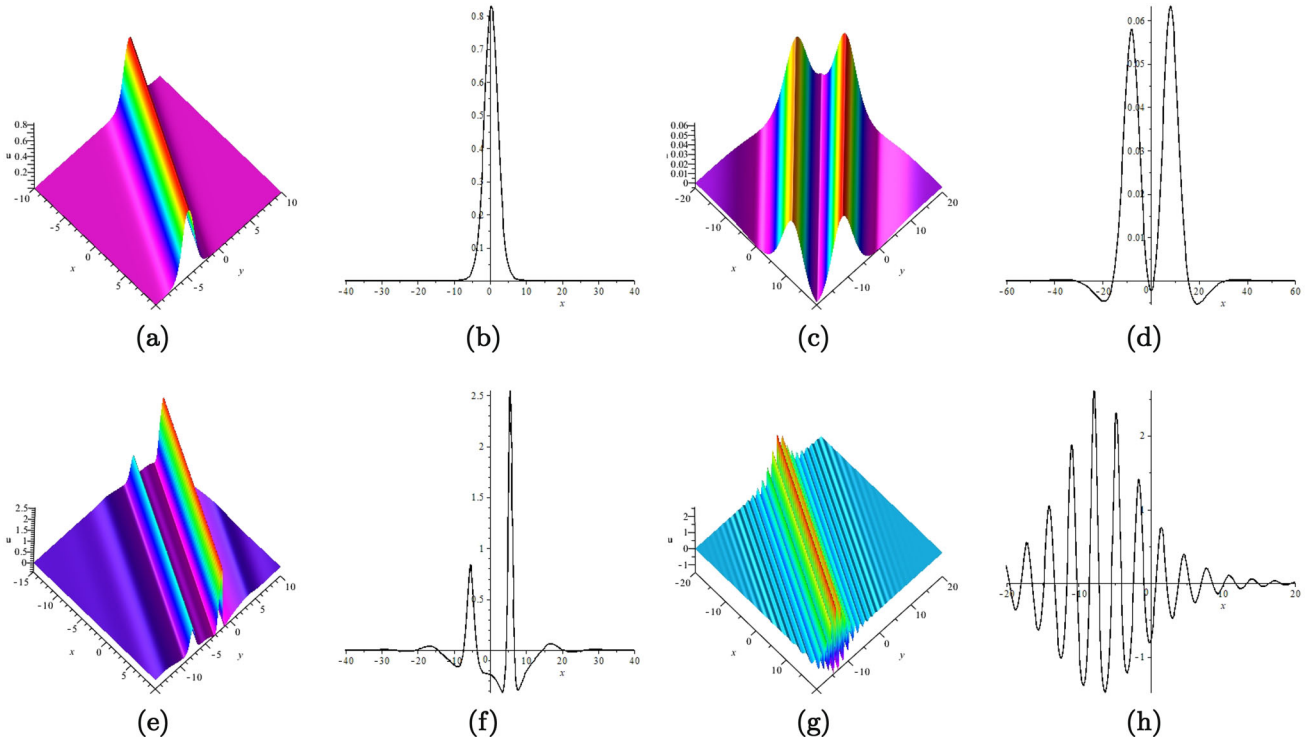

Fig. 5 (Color online) One breath-wave transformation of Eq. (1) with parameters $c_1 = c_2 = c_3 = 1$. **a** $a_1 = 1, b_1 = 0.01, p_1 = 2, q_1 = 0.02, \alpha_1 = 2, \beta_1 = 0, \gamma_1 = 0$. This figure is three-dimensional stereogram of one breath-wave transformation when $t = 0$. **b** The wave moves along the x-axis when $y = 0, t = 0$. **c** $a_1 = 0.2, b_1 = 0.2, p_1 = 0.2, q_1 = 0.2, \alpha_1 = 2, \beta_1 = 0, \gamma_1 = 0$. **d** The wave moves along the x-axis when $y = 0, t = 0$. **e** $a_1 = 0.2, b_1 = 0.5, p_1 = 0.4, q_1 = 1, \alpha_1 = 2, \beta_1 = 0, \gamma_1 = 0$. **f** The wave moves along the x-axis when $y = 0, t = 0$. **g** $a_1 = 0.2, b_1 = 2, p_1 = 0.4, q_1 = 4, \alpha_1 = 2, \beta_1 = 0, \gamma_1 = 0$. **h** The wave moves along the x-axis when $y = 0, t = 0$

almost disappears and the periodicity becomes more and more obvious, as shown in Fig. 6. Finally, the distribution of diverse transformed nonlinear waves is given in Fig. 7(a).

3.2 The two breath-wave solution of Eq. (1)

In this section, the two breath-wave solution of Eq. (1) is obtained by a similar method as one. The four-soliton solution has the form of

$$\begin{aligned} f_4 =& 1 + \mathrm{e}^{\sigma_1} + \mathrm{e}^{\sigma_2} + \mathrm{e}^{\sigma_3} + \mathrm{e}^{\sigma_4} + \mathrm{e}^{\sigma_1+\sigma_2+\mathrm{A}_{12}} + \mathrm{e}^{\sigma_1+\sigma_3+\mathrm{A}_{13}} \\ &+ \mathrm{e}^{\sigma_1+\sigma_4+\mathrm{A}_{14}} + \mathrm{e}^{\sigma_2+\sigma_3+\mathrm{A}_{23}} + \mathrm{e}^{\sigma_2+\sigma_4+\mathrm{A}_{24}} + \mathrm{e}^{\sigma_3+\sigma_4+\mathrm{A}_{34}} \\ &+ \mathrm{e}^{\sigma_1+\sigma_2+\sigma_3+\mathrm{A}_{12}+\mathrm{A}_{23}+\mathrm{A}_{13}} + \mathrm{e}^{\sigma_1+\sigma_2+\sigma_4+\mathrm{A}_{12}+\mathrm{A}_{24}+\mathrm{A}_{14}} \\ &+ \mathrm{e}^{\sigma_1+\sigma_3+\sigma_4+\mathrm{A}_{13}+\mathrm{A}_{34}+\mathrm{A}_{14}} + \mathrm{e}^{\sigma_2+\sigma_3+\sigma_4+\mathrm{A}_{23}+\mathrm{A}_{34}+\mathrm{A}_{24}} \\ &+ \mathrm{e}^{\sigma_1+\sigma_2+\sigma_3+\sigma_3+\mathrm{A}_{12}+\mathrm{A}_{23}+\mathrm{A}_{13}+\mathrm{A}_{23}+\mathrm{A}_{34}+\mathrm{A}_{24}}. \end{aligned} \tag{13}$$

By letting

$$k_3 = a_2 + b_2\mathrm{i},\ k_4 = a_2 - b_2\mathrm{i},\ l_3 = p_2 + q_2\mathrm{i},\ l_4 = p_2 - q_2\mathrm{i},\ \delta_3 = \ln\frac{\alpha_3}{2} + \beta_2 + \gamma_2\mathrm{i},\ \delta_4 = \ln\frac{\alpha_3}{2} + \beta_2 - \gamma_2\mathrm{i}, \tag{14}$$

where $a_2, b_2, p_2, q_2 \neq 0, \alpha_3 > 0, \beta_2$ and γ_2 are arbitrary real constants and substituting (14) into f_4, we obtain the another expression of

$$\begin{aligned} f_4 =& 1 + \alpha_1 e^{\theta_1}\cos(\Lambda_1) + \frac{\alpha_1^2 G_1 e^{2\theta_1}}{4} + \alpha_3 e^{\theta_2}\cos(\Lambda_2) + \frac{\alpha_3^2 G_2 e^{2\theta_2}}{4} \\ &+ \frac{\alpha_1^2\alpha_3^2 G_1 G_2}{16} e^{2\theta_1+2\theta_2}\left(H_{3R}^2 + H_{3I}^2\right)\left(H_{4R}^2 + H_{4I}^2\right) \\ &+ \frac{\alpha_1\alpha_3}{2} e^{\theta_1+\theta_2}\left(H_{3R}\cos(\Lambda_1+\Lambda_2) - H_{3I}\sin(\Lambda_1+\Lambda_2)\right) \end{aligned}$$

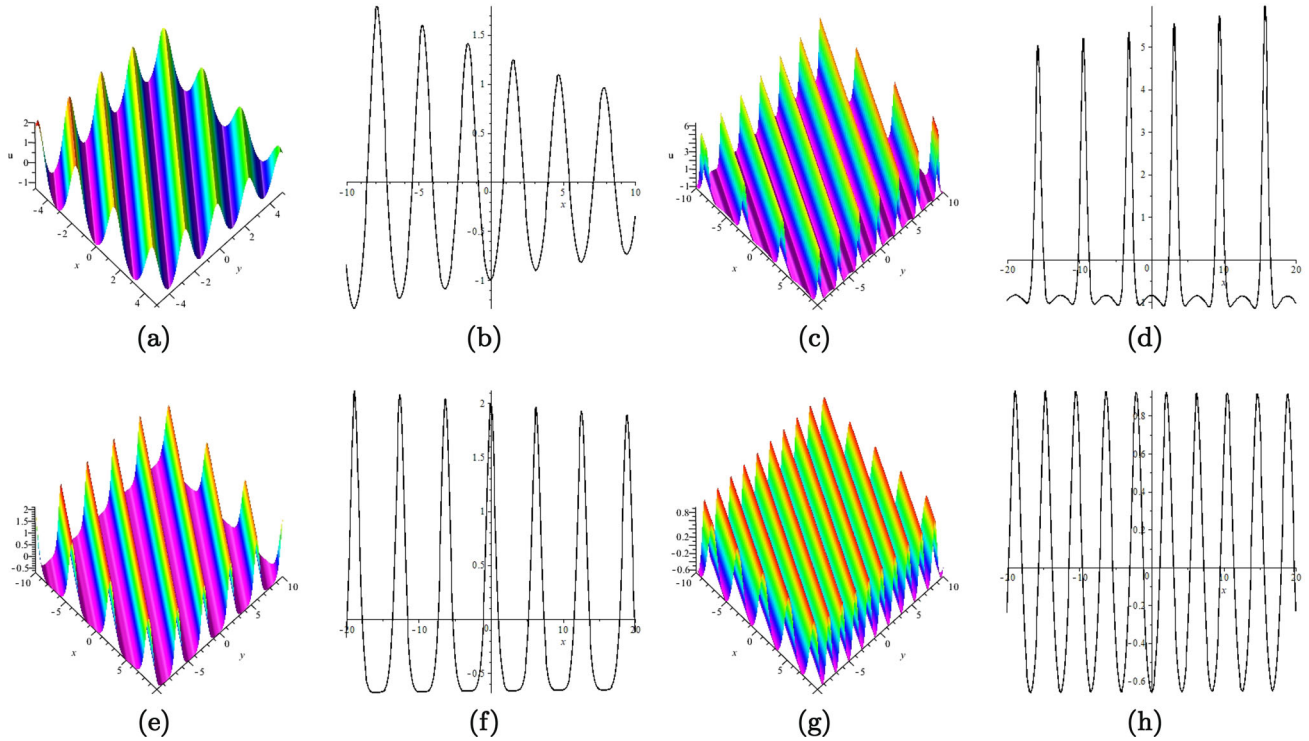

Fig. 6 (Color online) One breath-wave transformation of Eq. (1) with parameters $c_1 = c_2 = c_3 = 1$. **a** $a_1 = 0.04, b_1 = 2, p_1 = 0.05, q_1 = 2.5, \alpha_1 = 2, \beta_1 = 0, \gamma_1 = 0$. This figure is three-dimensional stereogram of one breath-wave transformation when $t = 0$. **b** The wave moves along the x-axis when $y = 0, t = 0$. **c** $a_1 = 0.001, b_1 = 1, p_1 = 0.002, q_1 = 2, \alpha_1 = 0.6, \beta_1 = 0, \gamma_1 = 0$. **d** The wave moves along the x-axis when $y = 0, t = 0$. **e** $a_1 = 0.001, b_1 = 1, p_1 = 0.0015, q_1 = 1.5, \alpha_1 = 0.6, \beta_1 = 0, \gamma_1 = 0$. **f** The wave moves along the x-axis when $y = 0, t = 0$. **g** $a_1 = 0.0015, b_1 = 1.5, p_1 = 0.002, q_1 = 3, \alpha_1 = 0.6, \beta_1 = 0, \gamma_1 = 0$. **h** The wave moves along the x-axis when $y = 0, t = 0$

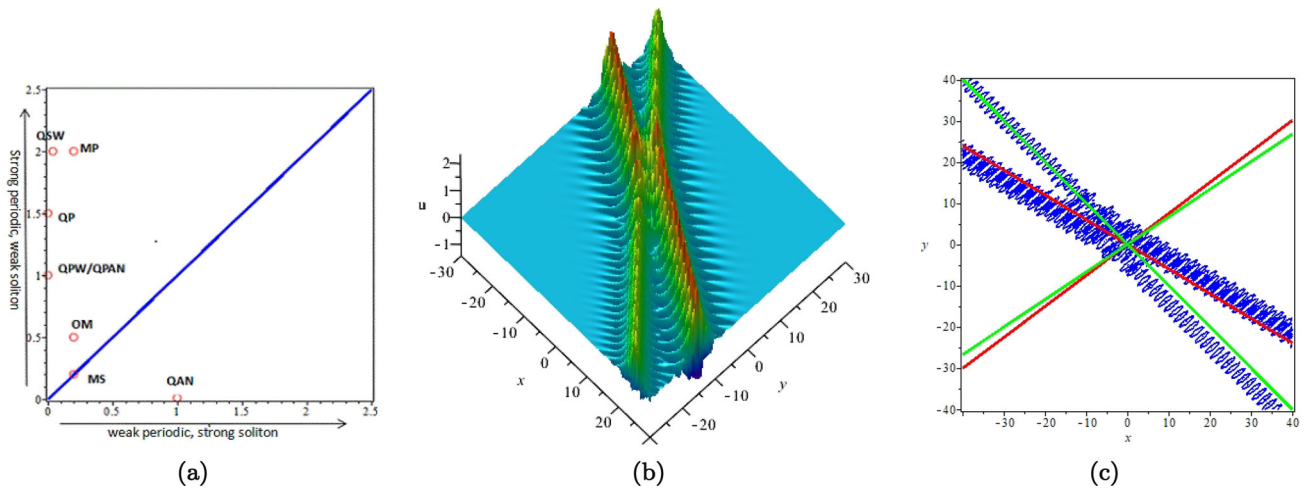

Fig. 7 (Color online) **a** The distributions of diverse transformed nonlinear waves, in which "QAN" represents quasi-anti-dark soliton, "MS"(M-shaped soliton), "OM"(oscillation M-shaped soliton), "QPW"(quasi-periodic W-shaped soliton", "QPAN"(quasi-periodic anti-dark soliton), "QP"(quasi-periodic wave), "MP"(multi-peak soliton) and "QSW"(quasi-sine wave). **b** Two breath-wave of Eq. (1) with parameters $c_1 = c_2 = c_3 = 1, a_1 = 0.3, b_1 = 1.5, p_1 = 0.5, q_1 = -2, a_2 = 0.5, b_2 = 2, p_2 = 0.5, q_2 = -3, \alpha_1 = 2, \beta_1 = 0, \gamma_1 = 0, \alpha_3 = 2, \beta_2 = 0, \gamma_2 = 0$. This figure is three-dimensional stereogram of two breath-wave when $t = 0$. **c** the corresponding contour figure of (**b**), the red lines ($1.5x - 2y = 0, 0.3x + 0.5y = 0$) and the green lines ($0.5x + 0.5y = 0, 2x - 3y = 0$) are two sets of characteristic lines of two breath-wave

$$+\frac{\alpha_1\alpha_3}{2}e^{\theta_1+\theta_2}(H_{4R}\cos(\Lambda_1-\Lambda_2)-H_{4I}\sin(\Lambda_1-\Lambda_2))$$
$$+\frac{\alpha_1^2\alpha_3 G_1}{4}e^{2\theta_1+\theta_2}((H_{3R}H_{4R}+H_{3I}H_{4I})\cos(\Lambda_2)-(H_{3I}H_{4R}-H_{3R}H_{4I})\sin((\Lambda_2))$$

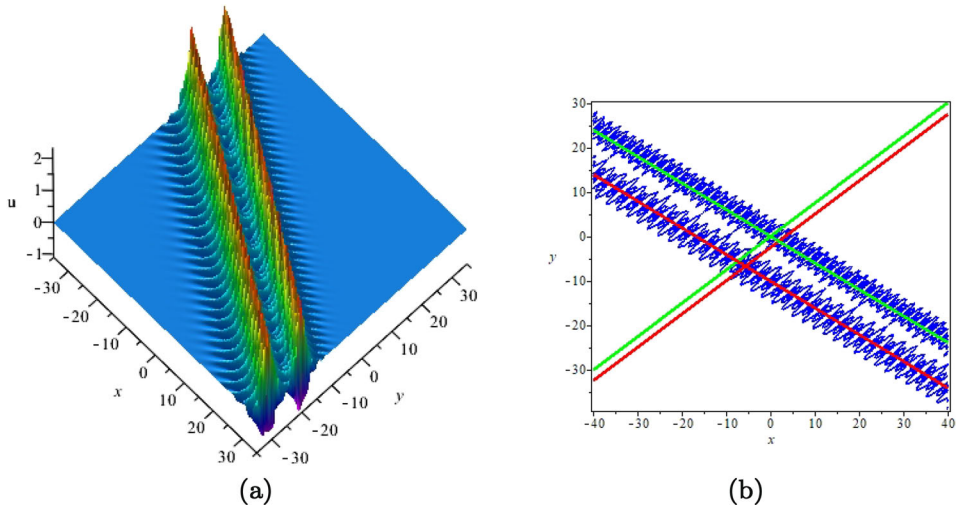

Fig. 8 (Color online) **a** Two breath-wave of Eq. (1) with parameters $c_1 = c_2 = c_3 = 1, a_1 = 0.3, b_1 = 1.5, p_1 = 0.5, q_1 = -2, a_2 = 0.4, b_2 = 2, p_2 = \frac{2}{3}, q_2 = -\frac{8}{3}, \alpha_1 = 0.7, \beta_1 = 5, \gamma_1 = -5, \alpha_3 = 2, \beta_2 = 0, \gamma_2 = 0$. This figure is three-dimensional stereogram of two breath-wave when $t = 0$. **b** the corresponding contour figure of (**a**), the red lines $(0.3x + 0.5y + 5 = 0, 1.5x - 2y - 5 = 0)$ and the green lines $(0.4x + 0.6666666667y = 0, 2x - \frac{8}{3}y = 0)$ are two sets of characteristic lines of two-breath wave

$$+\frac{\alpha_1\alpha_3^2 G_2}{4}e^{\theta_1+2\theta_2}((H_{3R}H_{4R}-H_{3I}H_{4I})\cos(\Lambda_1)-(H_{3I}H_{4R}+H_{3R}H_{4I})\sin(\Lambda_1)), \tag{15}$$

where

$$\theta_2 = a_2x + p_2y + h_2t + \beta_2,\ \ \Lambda_2 = b_2x + q_2y + d_2t + \gamma_2,$$

$$G_2 = \frac{-2c_1(a_2^2+b_2^2)+2c_2(a_2p_2+b_2q_2)+2c_3(a_2^4-7b_2^4-6a_2^2b_2^2)+2\sqrt{\Lambda_5^2+\Lambda_6^2}}{-2c_1(a_2^2+b_2^2)+2c_2(a_2p_2+b_2q_2)+2c_3(7a_2^4-b_2^4+6a_2^2b_2^2)+2\sqrt{\Lambda_5^2+\Lambda_6^2}},$$

$$H_{3R} = \mathrm{Re}(e^{A_{13}}),\ H_{3I} = \mathrm{Im}(e^{A_{13}}),\ H_{4R} = \mathrm{Re}(e^{A_{14}}),\ H_{4I} = \mathrm{Im}(e^{A_{14}}),$$

$$\Lambda_5 = -c_1(a_2^2-b_2^2)-c_2(a_2p_2-b_2q_2)-c_3(a_2^4-6a_2^2b_2^2+b_2^4),$$

$$\Lambda_6 = -c_1(2a_2b_2)-c_2(b_2p_2+a_2q_2)-c_3(4a_2^3b_2-4a_2b_2^3),\ \sqrt{\Lambda_5+\Lambda_6 i}$$

$$= h_2 + d_2 i,\ \sqrt{\Lambda_5-\Lambda_6 i} = h_2 - d_2 i.$$

It is different from the one breath-wave solution, in Figs. 7, 8, the two breath-wave solution has two sets of characteristic lines: $\theta_1 = a_1x + p_1y + h_1t + \beta_1 = 0,\ \Lambda_1 = b_1x + q_1y + d_1t + \gamma_1 = 0$ and $\theta_2 = a_2x + p_2y + h_2t + \beta_2 = 0,\ \Lambda_2 = b_2x + q_2y + d_2t + \gamma_2 = 0$.

(1) If two breather waves have

$$\begin{vmatrix} a_1 & p_1 \\ a_2 & p_2 \end{vmatrix} = 0,\ \begin{vmatrix} b_1 & q_1 \\ b_2 & q_2 \end{vmatrix} = 0,\ \begin{vmatrix} a_1 & p_1 \\ b_1 & q_1 \end{vmatrix} \neq 0,\ \begin{vmatrix} a_2 & p_2 \\ b_2 & q_2 \end{vmatrix} \neq 0,$$

the two breather waves are parallel, as shown in Fig. 8.

(2) If two breather waves have

$$\begin{vmatrix} a_1 & p_1 \\ a_2 & p_2 \end{vmatrix} \neq 0,\ \begin{vmatrix} b_1 & q_1 \\ b_2 & q_2 \end{vmatrix} \neq 0,$$

the waves are not parallel.

(i) If

$$\begin{vmatrix} a_1 & p_1 \\ b_1 & q_1 \end{vmatrix} \neq 0,\ \begin{vmatrix} a_2 & p_2 \\ b_2 & q_2 \end{vmatrix} \neq 0,$$

the two breather waves collide, as shown in Fig. 7. Then, in Figs. 9, 10, 11, 12, 13, 14, and 15, the transformation mechanism of two breath-wave is discussed in detail as follows.

(ii) If

$$\begin{vmatrix} a_1 & p_1 \\ b_1 & q_1 \end{vmatrix} = 0,\ \begin{vmatrix} a_2 & p_2 \\ b_2 & q_2 \end{vmatrix} \neq 0,$$

one of the breather waves can be transformed into a series of nonlinear waves including quasi-anti-dark soliton, M-shaped soliton and quasi-periodic wave. In Fig. 9, the two breather waves are transformed into one breather wave and quasi-anti-dark

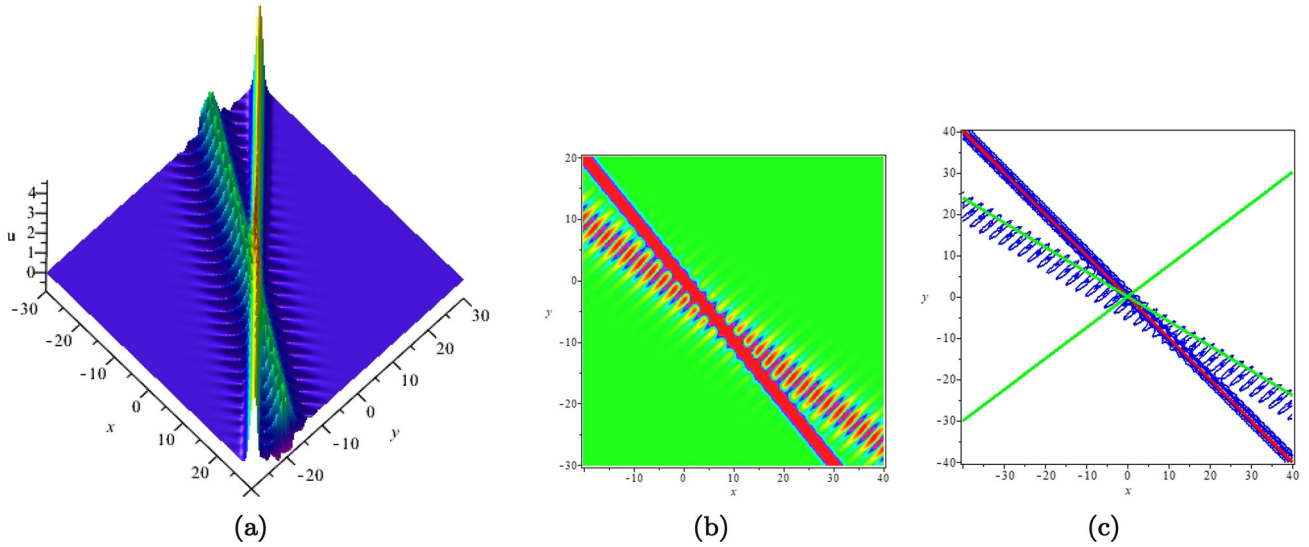

Fig. 9 (Color online) **a** Two breath-wave transformation of Eq. (1) with parameters $c_1 = c_2 = c_3 = 1, a_1 = 2.3, b_1 = 0.23, p_1 = 2.3, q_1 = 0.23, a_2 = 0.3, b_2 = 1.5, p_2 = 0.5, q_2 = -2, \alpha_1 = 2, \beta_1 = 0, \gamma_1 = 0, \alpha_3 = 2, \beta_2 = 0, \gamma_2 = 0$. This figure is three-dimensional stereogram of two breath-wave transformation when $t = 0$. **b** Vertical view of (**a**). **c** The corresponding contour figure of (**a**), the red line $(2.3x + 2.3y = 0)$ is characteristic line of quasi-anti-dark soliton, the green lines $(0.3x + 0.5y = 0, 1.5x - 2y = 0)$ are two characteristic lines of one breath wave

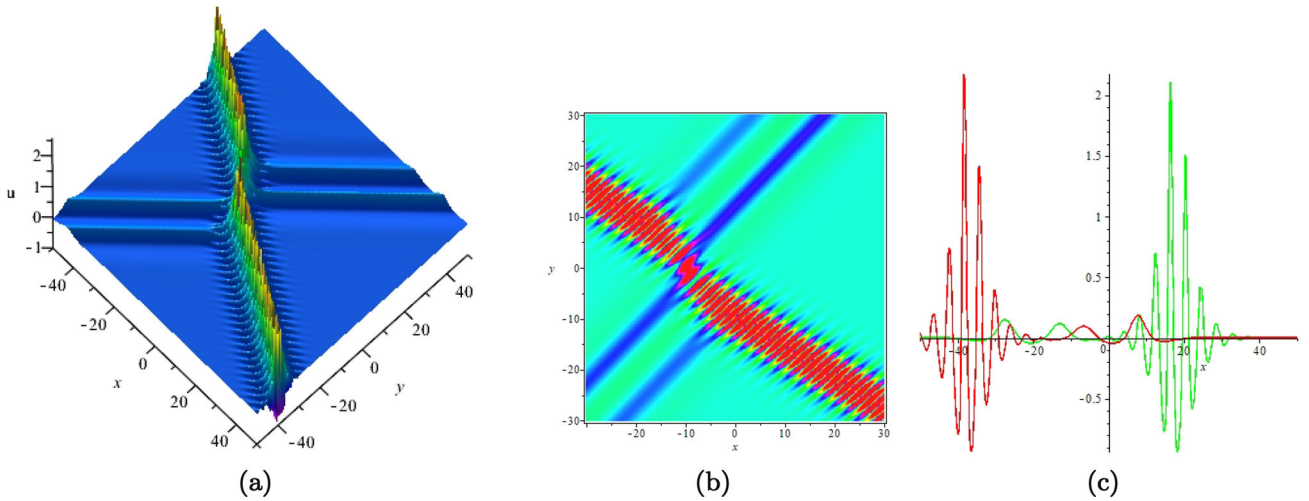

Fig. 10 (Color online) **a** Two breath-wave transformation of Eq. (1) with parameters $c_1 = c_2 = c_3 = 1, a_1 = 0.2, b_1 = 0.3, p_1 = -0.2, q_1 = -0.3, a_2 = 0.3, b_2 = 1.5, p_2 = 0.5, q_2 = -2, \alpha_1 = 2, \beta_1 = 0, \gamma_1 = 0, \alpha_3 = 2, \beta_2 = 0, \gamma_2 = 0$. This figure is three-dimensional stereogram of two breath-wave transformation when $t = 0$. **b** Vertical view of (**a**). **c** The wave moves along the x-axis when $y = -20, t = 0$(green), x-axis when $y = 20, t = 0$(red)

soliton $\left(\left|\frac{a_1}{b_1}\right| = \left|\frac{p_1}{q_1}\right| = 10\right)$. In Fig. 10, the two breather waves are transformed into one breather wave and M-shaped soliton $\left(\left|\frac{a_1}{b_1}\right| = \left|\frac{p_1}{q_1}\right| \approx 1\right)$. In Fig. 11a and b, the two breather waves are transformed into one breather wave and quasi-periodic wave $\left(\left|\frac{a_1}{b_1}\right| = \left|\frac{p_1}{q_1}\right| \leq 0.01\right)$.

(iii) If

$$\begin{vmatrix} a_1 & p_1 \\ b_1 & q_1 \end{vmatrix} = 0, \quad \begin{vmatrix} a_2 & p_2 \\ b_2 & q_2 \end{vmatrix} = 0,$$

the two breather waves can be transformed into a series of nonlinear waves. In Fig. 12, the two breather waves are transformed into two nonparallel quasi-anti-dark solitons $\left(\left|\frac{a_1}{b_1}\right| = \left|\frac{p_1}{q_1}\right| = \left|\frac{a_2}{b_2}\right| = \left|\frac{p_2}{q_2}\right| = 10\right)$. In Fig. 13, the two breather waves are transformed into quasi-anti-dark soliton $\left(\left|\frac{a_2}{b_2}\right| = \left|\frac{p_2}{q_2}\right| \approx 10\right)$ and M-shaped soliton $\left(\left|\frac{a_1}{b_1}\right| = \left|\frac{p_1}{q_1}\right| = 1\right)$. In Fig. 14, the two breather waves are transformed into two nonparallel M-shaped solitons $\left(\left|\frac{a_1}{b_1}\right| = \left|\frac{p_1}{q_1}\right| = \left|\frac{a_2}{b_2}\right| = \left|\frac{p_2}{q_2}\right| = 1\right)$. In Fig. 15, the two breather

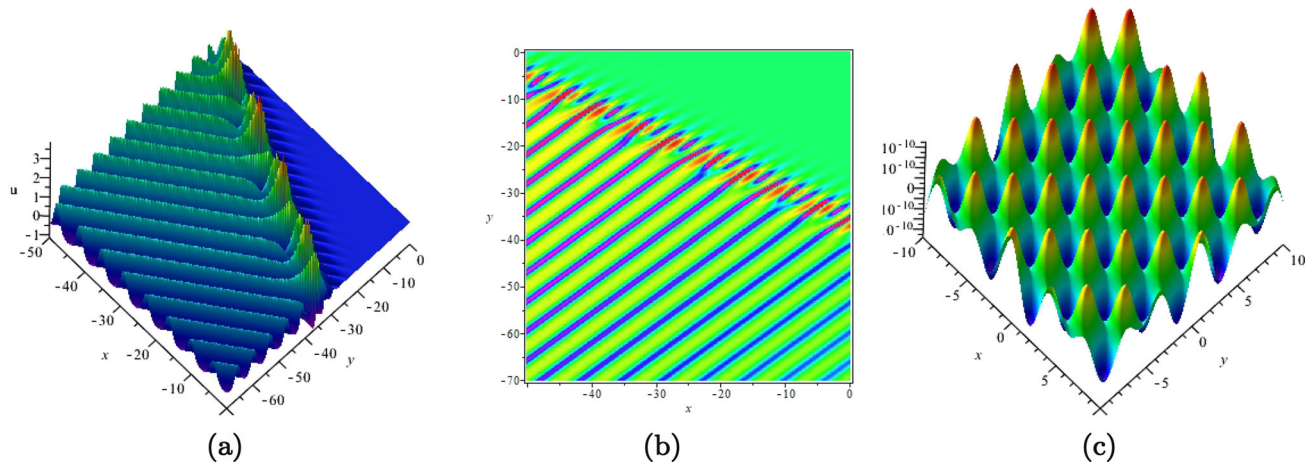

Fig. 11 (Color online) **a** Two breath-wave transformation of Eq. (1) with parameters $c_1 = c_2 = c_3 = 1, a_1 = 0.01, b_1 = 1, p_1 = -0.01, q_1 = -1, a_2 = 0.3, b_2 = 1.5, p_2 = 0.5, q_2 = -2, \alpha_1 = 2, \beta_1 = 0, \gamma_1 = 0, \alpha_3 = 2, \beta_2 = 0, \gamma_2 = 0$. This figure is three-dimensional stereogram of two breath-wave transformation when $t = 0$. **b** Vertical view of (**a**). **c** Two breath-wave transformation of Eq. (1) with parameters $c_1 = c_2 = c_3 = 1, a_1 = 0.01, b_1 = 1, p_1 = -0.01, q_1 = -1, a_2 = 0.01, b_2 = 1.5, p_2 = -0.01, q_2 = 1.5, \alpha_1 = 2, \beta_1 = 0, \gamma_1 = 0, \alpha_3 = 2, \beta_2 = 0, \gamma_2 = 0$. This figure is three-dimensional stereogram of two breath-wave transformation when $t = 0$

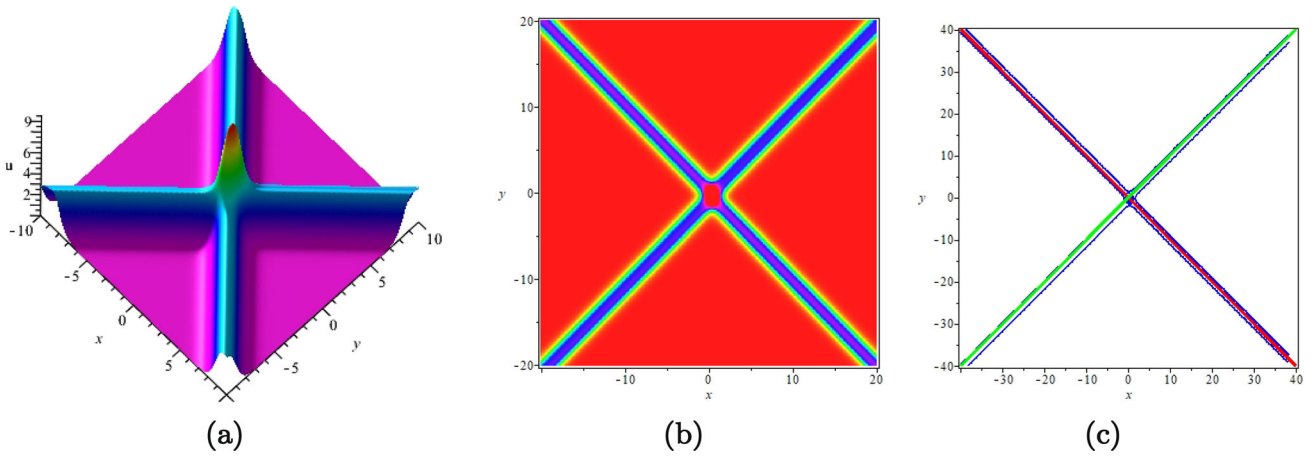

Fig. 12 (Color online) **a** Two breath-wave transformation of Eq. (1) with parameters $c_1 = c_2 = c_3 = 1, a_1 = 2.3, b_1 = 0.23, p_1 = 2.3, q_1 = 0.23, a_2 = 2.3, b_2 = 0.23, p_2 = -2.3, q_2 = -0.23, \alpha_1 = 2, \beta_1 = 0, \gamma_1 = 0, \alpha_3 = 0.6, \beta_2 = 0, \gamma_2 = 0$. This figure is three-dimensional stereogram of two breath-wave transformation when $t = 0$. **b** Vertical view of (**a**). **c** The corresponding contour figure of (**a**), the red line ($2.3x + 2.3y = 0$) and the green line ($2.3x - 2.3y = 0$) are characteristic lines of two quasi-anti-dark solitons

waves are transformed into quasi-periodic wave $\left(\left|\frac{a_2}{b_2}\right| = \left|\frac{p_2}{q_2}\right| \leq 0.01\right)$ and M-shaped soliton $\left(\left|\frac{a_1}{b_1}\right| = \left|\frac{p_1}{q_1}\right| = 1\right)$. In Fig. 11c, the two breather waves are transformed into bright and dark solitons $\left(\left|\frac{a_1}{b_1}\right| = \left|\frac{p_1}{q_1}\right| \leq 0.01\right)$, $\left(\left|\frac{a_2}{b_2}\right| = \left|\frac{p_2}{q_2}\right| \leq 0.01\right)$. Based on the above analysis, as the radio of a_j and b_j, p_j and q_j decreases, the periodicity of the two breather waves becomes obvious, the locality almost disappears.

4 One-periodic waves and asymptotic properties

In this section, one-periodic wave solution of Eq. (1) is obtained via bilinear method and Riemann theta function. When $N = 1$, the theta function degenerates the following Fourier series

$$\varphi(\tau, a) = \sum_{n=-\infty}^{+\infty} \mathrm{e}^{2\pi i n\tau - \pi n^2 a}, \tag{16}$$

with phase variable $\tau = \varepsilon x + \eta y + \omega t + \upsilon$, and the first-order matrix $a > 0$.

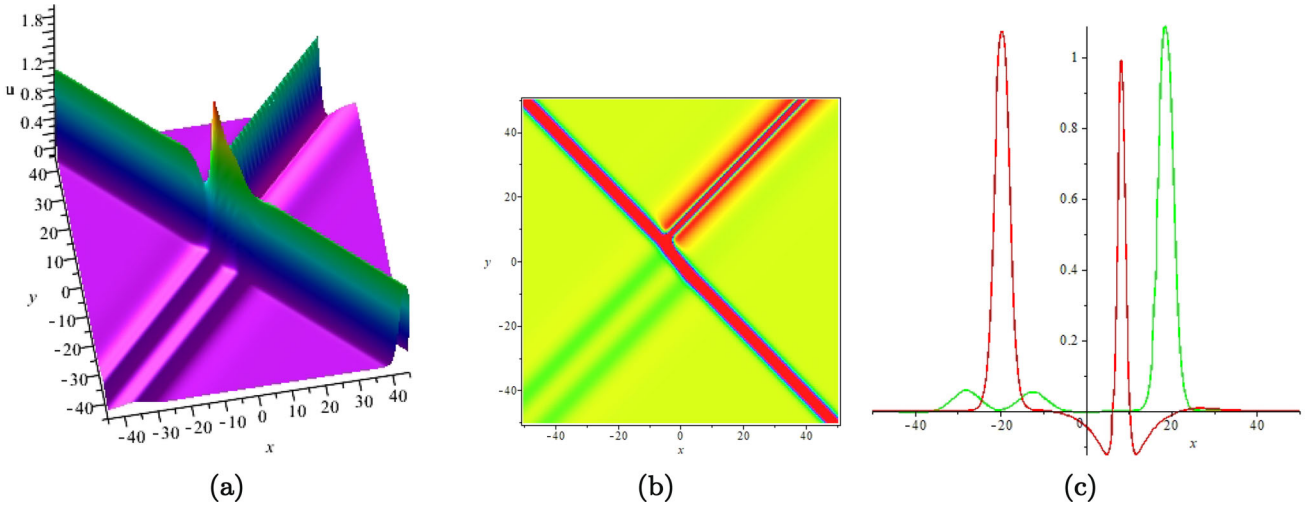

Fig. 13 (Color online) **a** Two breath-wave transformation of Eq. (1) with parameters $c_1 = c_2 = c_3 = 1, a_1 = 1.2, b_1 = 0.1, p_1 = 1.2, q_1 = 0.1, a_2 = 0.2, b_2 = 0.2, p_2 = -0.2, q_2 = -0.2, \alpha_1 = 2, \beta_1 = 0, \gamma_1 = 0, \alpha_3 = 2, \beta_2 = 0, \gamma_2 = 0$. This figure is three-dimensional stereogram of two breath-wave transformation when $t = 0$. **b** Vertical view of (**a**). **c** The wave moves along the x-axis when $y = -20, t = 0$ (green), x-axis when $y = 20, t = 0$(red)

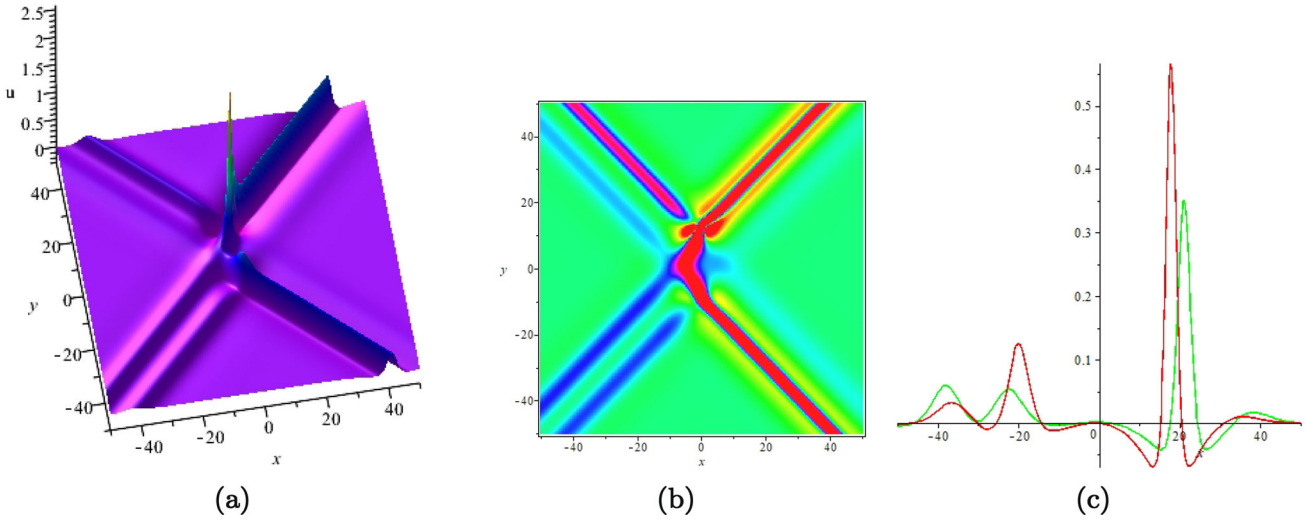

Fig. 14 (Color online) **a** Two breath-wave transformation of Eq. (1) with parameters $c_1 = c_2 = c_3 = 1, a_1 = 0.2, b_1 = 0.2, p_1 = 0.2, q_1 = 0.2, a_2 = 0.2, b_2 = 0.2, p_2 = -0.2, q_2 = -0.2, \alpha_1 = 0.9, \beta_1 = 0, \gamma_1 = 0, \alpha_3 = 2, \beta_2 = 0, \gamma_2 = 0$. This figure is three-dimensional stereogram of two breath-wave transformation when $t = 0$. **b** Vertical view of (**a**). **c** The wave moves along the x-axis when $y = -30, t = 0$(green), x-axis when $y = 30, t = 0$(red)

4.1 Construction of one-periodic waves

In order to obtain one-periodic wave solution, we take Eq. (16) into Eq. (8), and gain the following relation through Eq. (3):

$$
\begin{aligned}
B(D_x, D_y, D_t)\varphi(\tau, a)\varphi(\tau, a) &= \sum_{n=-\infty}^{+\infty}\sum_{m=-\infty}^{+\infty} B(D_x, D_y, D_t)e^{2\pi i n\tau - \pi n^2 a} e^{2\pi i m\tau - \pi m^2 a} \\
&= \sum_{n=-\infty}^{+\infty}\sum_{m=-\infty}^{+\infty} B(2\pi i(n-m)\varepsilon, 2\pi i(n-m)\eta, 2\pi i(n-m)\omega)e^{2\pi i(n+m)\tau - \pi(n^2+m^2)a} \\
&\overset{m=m'-n}{=} \sum_{m'=-\infty}^{+\infty}\left\{\sum_{n=-\infty}^{+\infty} B(2\pi i(2n-m')\varepsilon, 2\pi i(2n-m')\eta, 2\pi i(2n-m')\omega)e^{-\pi[n^2+(n-m')^2]a}\right\} \\
&\times e^{2\pi i m'\tau} = \sum_{m'=-\infty}^{+\infty} \overline{B}(m')e^{2\pi i m'\tau},
\end{aligned}
\tag{17}
$$

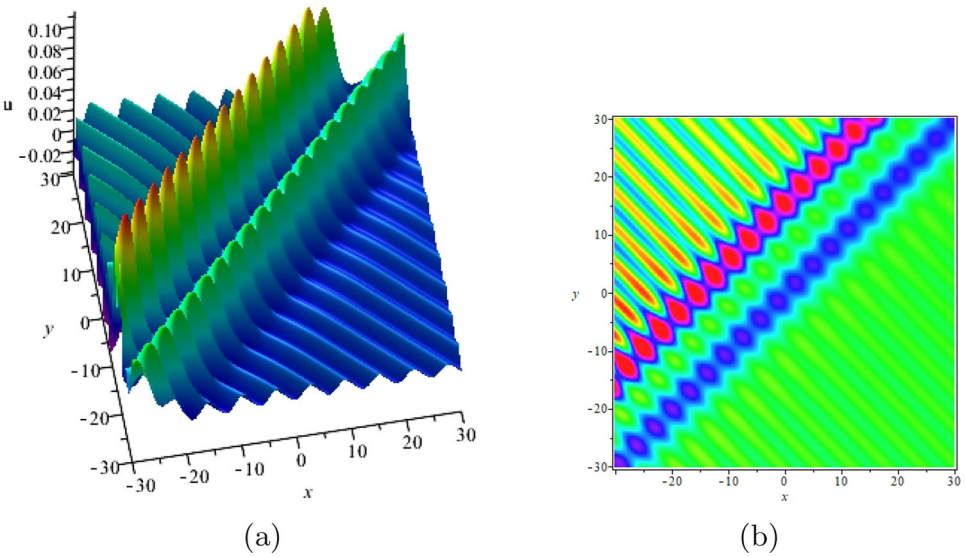

Fig. 15 (Color online) **a** Two breath-wave transformation of Eq. (1) with parameters $c_1 = c_2 = c_3 = 1, a_1 = 0.01, b_1 = -1.01, p_1 = 0.01, q_1 = -1.01, a_2 = 0.2, b_2 = 0.2, p_2 = -0.2, q_2 = -0.2, \alpha_1 = 2, \beta_1 = 0, \gamma_1 = 0, \alpha_3 = 2, \beta_2 = 0, \gamma_2 = 0$. This figure is three-dimensional stereogram of two breath-wave transformation when $t = 0$. **b** Vertical view of (**a**)

where

$$\overline{B}(m') = \sum_{n=-\infty}^{+\infty} B(2\pi \mathrm{i}(2n - m')\varepsilon, 2\pi \mathrm{i}(2n - m')\eta, 2\pi \mathrm{i}(2n - m')\omega)\mathrm{e}^{-\pi[n^2+(n-m')^2]a}. \tag{18}$$

Letting the summation index $n = n' + 1$, Eq. (18) have the following form of

$$\begin{aligned}\overline{B}(m') = &\sum_{n'=-\infty}^{+\infty} B(2\pi \mathrm{i}(2n' - (m' - 2))\varepsilon, 2\pi \mathrm{i}(2n' - (m' - 2))\eta, 2\pi \mathrm{i}(2n' - (m' - 2))\omega)\\ &\times \mathrm{e}^{-\pi a[n'^2+(n'-(m'-2))^2]} \times \mathrm{e}^{-2\pi(m'-1)a} = \overline{B}(m' - 2)\mathrm{e}^{-2\pi(m'-1)a} = \ldots\\ = &\begin{cases} \overline{B}(0)\mathrm{e}^{-\frac{\pi a m'^2}{2}}, & m' \text{ is even},\\ \overline{B}(1)\mathrm{e}^{-\frac{\pi a(m'^2-1)}{2}}, & m' \text{ is odd}, \end{cases}\end{aligned}$$

which shows that $\overline{B}(m'), m' \in Z$ is entirely determined by two formulas $\overline{B}(0)$ and $\overline{B}(1)$, that is, if the following two equations are satisfied

$$\overline{B}(0) = \overline{B}(1) = 0, \tag{19}$$

then $\overline{B}(m') = 0, (m' \in Z)$, so $B(D_x, D_y, D_t)\varphi(\tau, a)\varphi(\tau, a) = 0$. According to Eq. (18), Eq. (19) has the following form of

$$\begin{aligned}\overline{B}(0) = &\sum_{n=-\infty}^{+\infty} B(2\pi \mathrm{i}(2n - 0)\varepsilon, 2\pi \mathrm{i}(2n - 0)\eta, 2\pi \mathrm{i}(2n - 0)\omega)\mathrm{e}^{-2n^2\pi a}\\ = &\sum_{n=-\infty}^{+\infty} (-16\pi^2 n^2\omega^2 - 16\pi^2 n^2\varepsilon^2 c_1 - 16\pi^2 n^2\varepsilon\eta c_2 + 256\pi^4 n^4\varepsilon^4 c_3 - 96\pi^2 n^2\varepsilon^2 u_0 + c)\mathrm{e}^{-2n^2\pi a} = 0,\\ \overline{B}(1) = &\sum_{n=-\infty}^{+\infty} B(2\pi \mathrm{i}(2n - 1)\varepsilon, 2\pi \mathrm{i}(2n - 1)\eta, 2\pi \mathrm{i}(2n - 1)\omega)\mathrm{e}^{-(2n^2-2n+1)\pi a}\\ = &\sum_{n=-\infty}^{+\infty} (-4\pi^2(2n - 1)^2\omega^2 - 4\pi^2(2n - 1)^2\varepsilon^2 c_1 - 4\pi^2(2n - 1)^2\varepsilon\eta c_2 + 16\pi^4(2n - 1)^4\varepsilon^4 c_3\\ &- 24\pi^2(2n - 1)^2\varepsilon^2 u_0 + c)\mathrm{e}^{-(2n^2-2n+1)\pi a} = 0.\end{aligned} \tag{20}$$

By introducing the marks as

$$\psi = \mathrm{e}^{-\pi a},\ a_{11} = -\sum_{n=-\infty}^{+\infty} 16\pi^2 n^2 \psi^{2n^2},\ a_{12} = \sum_{n=-\infty}^{+\infty} \psi^{2n^2},$$

$$a_{21} = -\sum_{n=-\infty}^{+\infty} 4\pi^2(2n-1)^2\psi^{2n^2-2n+1},\ a_{22} = \sum_{n=-\infty}^{+\infty} \psi^{2n^2-2n+1},$$
$$b_1 = \sum_{n=-\infty}^{+\infty} (16\pi^2n^2\varepsilon^2c_1 + 16\pi^2n^2\varepsilon\eta c_2 - 256\pi^4n^4\varepsilon^4c_3 + 96\pi^2n^2\varepsilon^2u_0)\psi^{2n^2},$$
$$b_2 = \sum_{n=-\infty}^{+\infty} (4\pi^2(2n-1)^2\varepsilon^2c_1 + 4\pi^2(2n-1)^2\varepsilon\eta c_2 - 16\pi^4(2n-1)^4\varepsilon^4c_3 + 24\pi^2(2n-1)^2\varepsilon^2u_0)\psi^{2n^2-2n+1}, \quad (21)$$

Eq. (19) can be written as the form of a system of linear equations about frequency ω and integration constant c, that is

$$\begin{pmatrix} a_{11} & a_{12} \\ a_{21} & a_{22} \end{pmatrix}\begin{pmatrix} \omega^2 \\ c \end{pmatrix} = \begin{pmatrix} b_1 \\ b_2 \end{pmatrix}. \quad (22)$$

Then solve Eq. (22), we get the frequency and integration constant, that is

$$\omega^2 = \frac{b_1a_{22} - b_2a_{12}}{a_{11}a_{22} - a_{12}a_{21}}, \quad c = \frac{b_2a_{11} - b_1a_{21}}{a_{11}a_{22} - a_{12}a_{21}},$$

so we obtain the one-periodic wave solution of Eq. (1)

$$u = u_0 + 2(\ln\varphi(\tau, a))_{xx}, \quad (23)$$

where the theta function $\varphi(\tau, a)$ is given by Eq. (16), the other parameters $c_1, c_2, c_{3,}a, \varepsilon, \eta, u_0$ and υ are free, the three parameters a, ε and η play a major role in one-periodic waves.

4.2 Characteristics of one-periodic waves

(1) It is bounded for all complex variables (x, y, t).
(2) It has two fundamental periods 1 and ia about the phase variable τ.
(3) Equation (17) can be written as the following form of

$$B(D_x, D_y, D_t)\varphi(\tau, a)\varphi(\tau, a) = \sum_{n=-\infty}^{+\infty}\sum_{m=-\infty}^{+\infty} B(D_x, D_y, D_t)\mathrm{e}^{2\pi in\tau - \pi n^2a}\mathrm{e}^{2\pi im\tau - \pi m^2a}$$
$$= \sum_{m'=-\infty}^{+\infty} \overline{B}(m')\mathrm{e}^{2\pi im'\tau} = \sum_{m'=-\infty}^{+\infty} \overline{B}(m')cos(m'\tau). \quad (24)$$

It can be seen from expression (24) that the one-periodic wave solution has one characteristic line: $\tau = \varepsilon x + \eta y + \omega t + \upsilon = 0$, the propagation direction of wave is completely determined by τ, and $\frac{v_x}{v_y} = \frac{\varepsilon}{\eta}$, where v_x and v_y are the propagation velocity along the x-axis and y-axis, respectively. In Fig. 16a, the points (x, y) $(\varepsilon x + \eta y = 2k\pi, k = 0, 1, 2, ...)$ are the peak points of one-periodic waves, and the points (x, y) $(\varepsilon x + \eta y = 2k\pi + \pi, k = 0, 1, 2, ...)$ are the trough points of one-periodic waves.

4.3 Asymptotic properties of one-periodic waves

In what follows, we further analyze asymptotic properties of the one-periodic wave solution by solving Eq. (22) and taking a limit condition. In order to solve Eq. (22), one makes

$$\begin{pmatrix} a_{11} & a_{12} \\ a_{21} & a_{22} \end{pmatrix} = M_0 + M_1\psi + M_2\psi^2 + \cdots, \quad \begin{pmatrix} b_1 \\ b_2 \end{pmatrix} = N_0 + N_1\psi + N_2\psi^2 + \cdots, \quad \begin{pmatrix} \omega^2 \\ c \end{pmatrix} = X_0 + X_1\psi + X_2\psi^2 + \cdots,$$

then taking $u_0 = 0$ and expanding a_{ij}, b_j $(i, j = 1, 2)$ into the sum of ψ

$$a_{11} = -32\pi^2(\psi^2 + 4\psi^8 + 9\psi^{18} + \cdots),\ a_{12} = 1 + 2\psi^2 + 2\psi^8 + 2\psi^{18} + \cdots,$$
$$a_{21} = -8\pi^2(\psi + 9\psi^5 + 25\psi^{13} + \cdots),\ a_{22} = 2\psi + 2\psi^5 + 2\psi^{13} + 2\psi^{25} + \cdots,$$
$$b_1 = (32\pi^2\varepsilon^2c_1 + 32\pi^2\varepsilon\eta c_2 - 512\pi^4\varepsilon^4c_3)\psi^2 + (32\pi^2\varepsilon^2c_1 + 32\pi^2\varepsilon\eta c_2 - 2048\pi^4\varepsilon^4c_3)4\psi^8 + \cdots,$$
$$b_2 = (8\pi^2\varepsilon^2c_1 + 8\pi^2\varepsilon\eta c_2 - 32\pi^4\varepsilon^4c_3)\psi + (8\pi^2\varepsilon^2c_1 + 8\pi^2\varepsilon\eta c_2 - 288\pi^4\varepsilon^4c_3)9\psi^5 + \cdots,$$

we have

$$M_0 = \begin{pmatrix} 0 & 1 \\ 0 & 0 \end{pmatrix},\ M_1 = \begin{pmatrix} 0 & 0 \\ -8\pi^2 & 2 \end{pmatrix},\ M_2 = \begin{pmatrix} -32\pi^2 & 2 \\ 0 & 0 \end{pmatrix},\ M_3 = M_4 = 0,\ M_5 = \begin{pmatrix} 0 & 0 \\ -72\pi^2 & 2 \end{pmatrix}, \cdots,$$

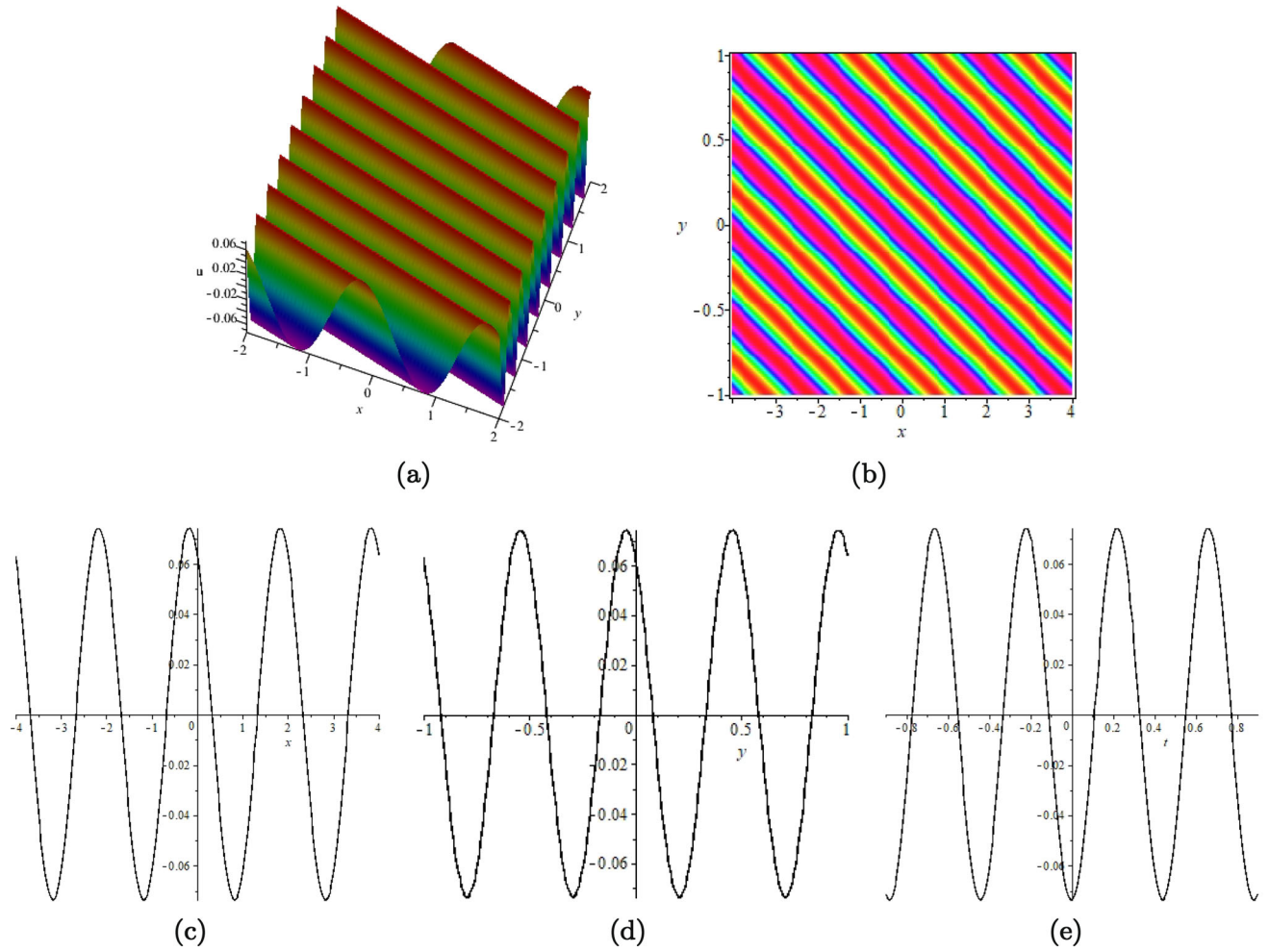

Fig. 16 (Color online) A one-periodic wave of Eq. (1) with parameters $c_1 = 1,\ c_2 = 2,\ c_3 = 3,\ a = 2, \varepsilon = 0.5, \eta = 2$. This figure can be regarded as a superposition of a series of soliton waves. **a** Three-dimensional stereogram of one-periodic wave when $t = 0$. **b** Vertical view of plot (**a**). **c** The wave moves along the x-axis when $y = 0, t = 0$. **d** The wave moves along the y-axis when $x = 0, t = 0$. **e** The wave moves along t-axis when $x = 0, y = 0$

$$N_0 = 0,\quad N_1 = \begin{pmatrix} 0 \\ 8\pi^2\varepsilon^2 c_1 + 8\pi^2\varepsilon\eta c_2 - 32\pi^4\varepsilon^4 c_3 \end{pmatrix},\quad N_2 = \begin{pmatrix} 32\pi^2\varepsilon^2 c_1 + 32\pi^2\varepsilon\eta c_2 - 512\pi^4\varepsilon^4 c_3 \\ 0 \end{pmatrix},$$
$$N_3 = N_4 = 0,\quad N_5 = \begin{pmatrix} 0 \\ 72\pi^2\varepsilon^2 c_1 + 72\pi^2\varepsilon\eta c_2 - 2592\pi^4\varepsilon^4 c_3 \end{pmatrix}, \ldots.$$

Therefore, one has

$$X_0 = \begin{pmatrix} -\varepsilon^2 c_1 - \varepsilon\eta c_2 + 4\pi^2\varepsilon^4 c_3 \\ 0 \end{pmatrix},\quad X_1 = X_3 = 0,\quad X_2 = \begin{pmatrix} -96\pi^2\varepsilon^4 c_3 \\ -384\pi^4\varepsilon^4 c_3 \end{pmatrix},\quad X_4 = \begin{pmatrix} -288\pi^2\varepsilon^4 c_3 \\ -2304\pi^4\varepsilon^4 c_3 \end{pmatrix}. \tag{25}$$

Interestingly, the relation of the one-soliton wave solution and one-periodic wave solution is given as follows.

Theorem 1 If one-periodic wave solution Eq. (23) satisfies the condition of

$$u_0 = 0,\quad \varepsilon = \frac{k}{2\pi \mathrm{i}},\quad \eta = \frac{l}{2\pi \mathrm{i}},\quad \upsilon = \frac{\delta + \pi a}{2\pi \mathrm{i}}, \tag{26}$$

where k, l and δ are given by Eq. (4), we have the following asymptotic properties:

$$c \to 0,\quad \tau \to \frac{\sigma + \pi a}{2\pi \mathrm{i}},\quad \varphi(\tau, a) \to 1 + \mathrm{e}^{\alpha},\quad \psi \to 0.$$

Proof By applying Eq. (25), we obtain

$$\omega^2 = (-\varepsilon^2 c_1 - \varepsilon\eta c_2 + 4\pi^2\varepsilon^4 c_3) - 96\pi^2\varepsilon^4 c_3\psi^2 - 288\pi^2\varepsilon^4 c_3\psi^4 + o(\psi^4),$$

$$c = -384\pi^4\varepsilon^4 c_3\psi^2 - 2304\pi^4\varepsilon^4 c_3)\psi^4 + o(\psi^4),$$

and by using condition (26), we have

$$c \to 0,\ 2\pi \mathrm{i}\omega \to \sqrt{-4\pi^2(-\varepsilon^2 c_1 - \varepsilon\eta c_2 + 4\pi^2\varepsilon^4 c_3)} = \sqrt{-c_2 kl - c_3 k^4 - c_1 k^2},\ \psi \to 0.$$

Then expanding the theta function

$$\varphi(\tau, a) = 1 + \psi(\mathrm{e}^{2\pi \mathrm{i}\tau} + \mathrm{e}^{-2\pi \mathrm{i}\tau}) + \psi^4(\mathrm{e}^{4\pi \mathrm{i}\tau} + \mathrm{e}^{-4\pi \mathrm{i}\tau}) + \cdots,$$

by applying condition (26), we have

$$\varphi(\tau, a) = 1 + \mathrm{e}^{\tau'} + \psi^2(\mathrm{e}^{-\tau'} + \mathrm{e}^{2\tau'}) + \psi^6(\mathrm{e}^{-2\tau'} + \mathrm{e}^{3\tau'}) + \ldots \to 1 + \mathrm{e}^{\tau'},\ \psi \to 0. \tag{27}$$

where

$$\tau' = 2\pi \mathrm{i}\tau - \pi a \to kx + ly + \sqrt{-c_2 kl - c_3 k^4 - c_1 k^2}t + \delta = \sigma,\ \psi \to 0. \tag{28}$$

What is more, $\tau \to \frac{\sigma + \pi a}{2\pi \mathrm{i}}$, finally, combining Eq. (27) and Eq. (28), we obtain

$$\varphi(\tau, a) \to 1 + \mathrm{e}^{\sigma},\ \psi \to 0.$$

Therefore, one-periodic wave solution tends to one-soliton solution under the condition of $\psi \to 0$. □

5 Two-periodic waves and asymptotic properties

In this section, two-periodic wave solution of Eq. (1) is similar to the one-periodic wave solution. When $N = 2$, the theta function degenerates the following Fourier series

$$\varphi(\tau, a) = \varphi(\tau_1, \tau_2, a) = \sum_{n=-\infty}^{+\infty} \mathrm{e}^{2\pi \mathrm{i} < \tau, n > - \pi < an, n >}, \tag{29}$$

with phase variable $\tau_1 = \varepsilon_1 x + \eta_1 y + \omega_1 t + \upsilon_1,\ \tau_2 = \varepsilon_2 x + \eta_2 y + \omega_2 t + \upsilon_2$, where $n = (n_1, n_2)^T \in Z^2$, $\tau = (\tau_1, \tau_2)^T \in C^2$, and a is a positive definite and real-valued symmetric 2×2 matrix, that is $a = \begin{pmatrix} a_{11} & a_{12} \\ a_{21} & a_{22} \end{pmatrix}$, where $a_{11} > 0$, $a_{22} > 0$ and $a_{11}a_{22} - {a_{12}}^2 > 0$.

5.1 Construction of two-periodic waves

In order to obtain two-periodic wave solution, we take Eq. (29) into Eq. (8) and finally gain the following relation through Eq. (3):

$$\begin{aligned} B(D_x, D_y, D_t)\varphi(\tau_1, \tau_2, a)\varphi(\tau_1, \tau_2, a) &= \sum_{n=-\infty}^{+\infty}\sum_{m=-\infty}^{+\infty} B(D_x, D_y, D_t)\mathrm{e}^{2\pi \mathrm{i} < \tau, n > - \pi < an, n >}\mathrm{e}^{2\pi \mathrm{i} < \tau, m > - \pi < am, m >} \\ &= \sum_{n=-\infty}^{+\infty}\sum_{m=-\infty}^{+\infty} B(2\pi \mathrm{i} < n - m, \varepsilon >, 2\pi \mathrm{i} < n - m, \eta >, 2\pi \mathrm{i} < n - m, \omega >)\mathrm{e}^{2\pi \mathrm{i} < \tau, n+m > - \pi(< an, n > + < am, m >)} \\ &\overset{m=m'-n}{=} \sum_{m'=-\infty}^{+\infty}\left\{\sum_{n=-\infty}^{+\infty} B(2\pi \mathrm{i} < 2n - m', \varepsilon >, 2\pi \mathrm{i} < 2n - m', \eta >, 2\pi \mathrm{i} < 2n - m', \omega >)\right. \\ &\quad \left.\times \mathrm{e}^{-\pi[< a(n-m'), n-m' > + < an, n >]}\right\} \times \mathrm{e}^{2\pi \mathrm{i} < \tau, m' >} = \sum_{m'=-\infty}^{+\infty} \overline{B}(m_1', m_2')\mathrm{e}^{2\pi \mathrm{i} < \tau, m' >}\ (m, n \in Z^2), \end{aligned} \tag{30}$$

where

$$\overline{B}({m_1}', {m_2}') = \sum_{n=-\infty}^{+\infty} B(2\pi \mathrm{i} < 2n - m', \varepsilon >, 2\pi \mathrm{i} < 2n - m', \eta >, 2\pi \mathrm{i} < 2n - m', \omega >)\mathrm{e}^{-\pi[< a(n-m'), n-m' > + < an, n >]}. \tag{31}$$

Letting the summation index $n_j = {n_j}' + \delta_{jl}$, where $\delta_{jl} = \begin{cases} 0, & l \neq j \\ 1, & l = j \end{cases}$, Eq. (31) has the form of

$$\overline{B}({m_1}', {m_2}') = \sum_{n=-\infty}^{+\infty} B(2\pi \mathrm{i}\sum_{j=1}^{2}[2{n_j}' - ({m_j}' - 2\delta_{jl})]\varepsilon_j, 2\pi \mathrm{i}\sum_{j=1}^{2}[2{n_j}' - ({m_j}' - 2\delta_{jl})]\eta_j, 2\pi \mathrm{i}\sum_{j=1}^{2}[2{n_j}' - ({m_j}' - 2\delta_{jl})]\omega_j)$$

$$\times \mathrm{e}^{-\pi \sum_{j,k=1}^{2}(n_j{}'+\delta_{jl})a_{jk}(n_k{}'+\delta_{kl})-\pi \sum_{j,k=1}^{2}[(m_j{}'-2\delta_{jl}-n_j{}')+\delta_{jl}]a_{jk}[(m_k{}'-2\delta_{kl}-n_k{}')+\delta_{kl}]}$$

$$= \begin{cases} \overline{B}(m_1{}'-2, m_2{}')\mathrm{e}^{2\pi a_{11}-2\pi(a_{11}m_1{}'+a_{12}m_2{}')}, & l=1, \\ \overline{B}(m_1{}', m_2{}'-2)\mathrm{e}^{2\pi a_{22}-2\pi(a_{12}m_1{}'+a_{22}m_2{}')}, & l=2, \end{cases}$$

which shows that $\overline{B}(m_1{}', m_2{}')$ $(m_1{}' \in Z^2, m_2{}' \in Z^2)$ is entirely determined by four formulas $\overline{B}(0,0)$, $\overline{B}(0,1)$, $\overline{B}(1,0)$, $\overline{B}(1,1)$. That is, if the following four equations are satisfied

$$\overline{B}(0,0) = \overline{B}(0,1) = \overline{B}(1,0) = \overline{B}(1,1) = 0, \tag{32}$$

then $\overline{B}(m_1{}', m_2{}') = 0$ $(m_1{}' \in Z^2, m_2{}' \in Z^2)$, so $B(D_x, D_y, D_t)\varphi(\tau_1, \tau_2, a)\varphi(\tau_1, \tau_2, a) = 0$. Then introducing the marks as

$$M = (a_{jl})_{4\times 5},\ b = (b_1, b_2, b_3, b_4)^T,\ a_{j1} = \sum_{n_1,n_2\in Z^2} -4\pi^2(2n_1 - s_1^j)^2 v_j(n),\ a_{j2} = \sum_{n_1,n_2\in Z^2} -4\pi^2(2n_2 - s_2^j)^2 v_j(n),$$

$$a_{j3} = \sum_{n_1,n_2\in Z^2} -24\pi^2 < 2n - s^j, \varepsilon >^2 v_j(n),\ a_{j4} = \sum_{n_1,n_2\in Z^2} v_j(n),\ a_{j5} = \sum_{n_1,n_2\in Z^2} -8\pi^2(2n_1 - s_1^j)(2n_2 - s_2^j)v_j(n),$$

$$b_j = \sum_{n_1,n_2\in Z^2} (4\pi^2 c_1 < 2n - s^j, \varepsilon >^2 + 4\pi^2 c_2 < 2n - s^j, \varepsilon >< 2n - s^j, \eta > -16\pi^4 c_3 < 2n - s^j, \varepsilon >^4)v_j(n),$$

$$v_j(n) = {\psi_1}^{{n_1}^2+(n_1-s_1^j)^2}{\psi_2}^{{n_2}^2+(n_2-s_2^j)^2}{\psi_3}^{n_1n_2+(n_1-s_1^j)(n_2-s_2^j)},\ \psi_1 = \mathrm{e}^{-\pi a_{11}},\ \psi_2 = \mathrm{e}^{-\pi a_{22}},\ \psi_3 = \mathrm{e}^{-2\pi a_{12}},$$

$$s^1 = (0,0),\ s^2 = (0,1),\ s^3 = (1,0),\ s^4 = (1,1),\ s^j = (s_1^j, s_2^j),$$

Eq. (32) can be written as the form of a system of linear equations about frequency ω_1, ω_2, constant u_0 and integration constant c, that is

$$M({\omega_1}^2, {\omega_2}^2, u_0, c, \omega_1\omega_2) = b, \tag{33}$$

so we obtain the two-periodic wave solution of Eq. (1)

$$u = u_0 + 2(\ln \varphi(\tau_1, \tau_2, a))_{xx}, \tag{34}$$

where the theta function $\varphi(\tau_1, \tau_2, a)$ is given by Eq. (29), u_0 is determined by formula (33), the other parameters $c_1, c_2, c_3, a_{11}, a_{12}, a_{22}, \varepsilon_1, \eta_1, \varepsilon_2, \eta_2, \upsilon_1$ and υ_2 are free, the seven parameters $a_{11}, a_{22}, a_{12}, \varepsilon_1, \eta_1, \varepsilon_2$ and η_2 play a major role in two-periodic waves. Figures 17, 18, 19, and 20 systematically show the dynamic characteristics of two-periodic waves.

5.2 Characteristics of two-periodic waves

(1) It is bounded for all complex variables (x, y, t).

(2) It is obvious that two-periodic waves are the generalization of the one-periodic waves, but there are two phase variables τ_1 and τ_2, it has two independent periods in two independent horizontal directions, respectively, and it can be regarded as the superposition of a periodic wave propagating along the x-axis and y-axis, respectively.

(3) It has $2N$ fundamental periods $\{e_j, j = 1, 2, ..., N\}$ and $\{\mathrm{i}a_j, j = 1, 2, ..., N\}$ in (τ_1, τ_2). Its velocity of the propagation has the form of

$$\frac{\mathrm{d}x}{\mathrm{d}t} = \frac{\omega_2\varepsilon_1 - \omega_1\varepsilon_2}{\varepsilon_1\eta_2 - \varepsilon_2\eta_1}, \quad \frac{\mathrm{d}y}{\mathrm{d}t} = \frac{\omega_1\eta_2 - \omega_2\eta_1}{\varepsilon_1\eta_2 - \varepsilon_2\eta_1}.$$

(4) Eq. (30) can be written as the form of

$$B(D_x, D_y, D_t)\varphi(\tau_1, \tau_2, a)\varphi(\tau_1, \tau_2, a) = \sum_{m'=-\infty}^{+\infty} \overline{B}(m_1{}', m_2{}')\mathrm{e}^{2\pi\mathrm{i}<\tau, m'>} = \sum_{m'=-\infty}^{+\infty} \overline{B}(m_1{}', m_2{}')\cos(\tau_1 m_1{}')\cos(\tau_2 m_2{}').$$

According to the above formula, two-periodic wave has two characteristic lines: $\tau_1 = \varepsilon_1 x + \eta_1 y + \omega_1 t + \upsilon_1 = 0$ and $\tau_2 = \varepsilon_2 x + \eta_2 y + \omega_2 t + \upsilon_2 = 0$.

(i) If we give the following relations of $\begin{vmatrix} \varepsilon_1 & \eta_1 \\ \varepsilon_2 & \eta_2 \end{vmatrix} \neq 0$, that is the two characteristic lines are not parallel. In one case, the included angle of the characteristic line is a general angle, that is $\frac{\varepsilon_1}{\eta_1} \neq \frac{\varepsilon_2}{\eta_2}$, as shown in Fig. 17, and in the other case, the included angle is a right angle, that is $\frac{\varepsilon_1}{\eta_1} = -\frac{\eta_2}{\varepsilon_2}$, as shown in Fig. 20. What they have in common is the collision of phase variables τ_1 and τ_2 makes the two-periodic waves appear honeycomb, and these hill-shaped bulges propagate periodically along the x-axis and y-axis, the points (x, y) $(\varepsilon_1 x + \eta_1 y = 2k\pi, \varepsilon_2 x + \eta_2 y = 2k\pi, k = 0, 1, 2, ...)$ are the peak points of two-periodic waves, the points (x, y) $(\varepsilon_1 x + \eta_1 y = 2k\pi + \pi, \varepsilon_2 x + \eta_2 y = 2k\pi + \pi, k = 0, 1, 2, ...)$ are the trough points of two-periodic waves. The different is that Fig. 17 has two strict periods along x-axis and y-axis, whereas Fig. 20 has one period along x-axis and y-axis.

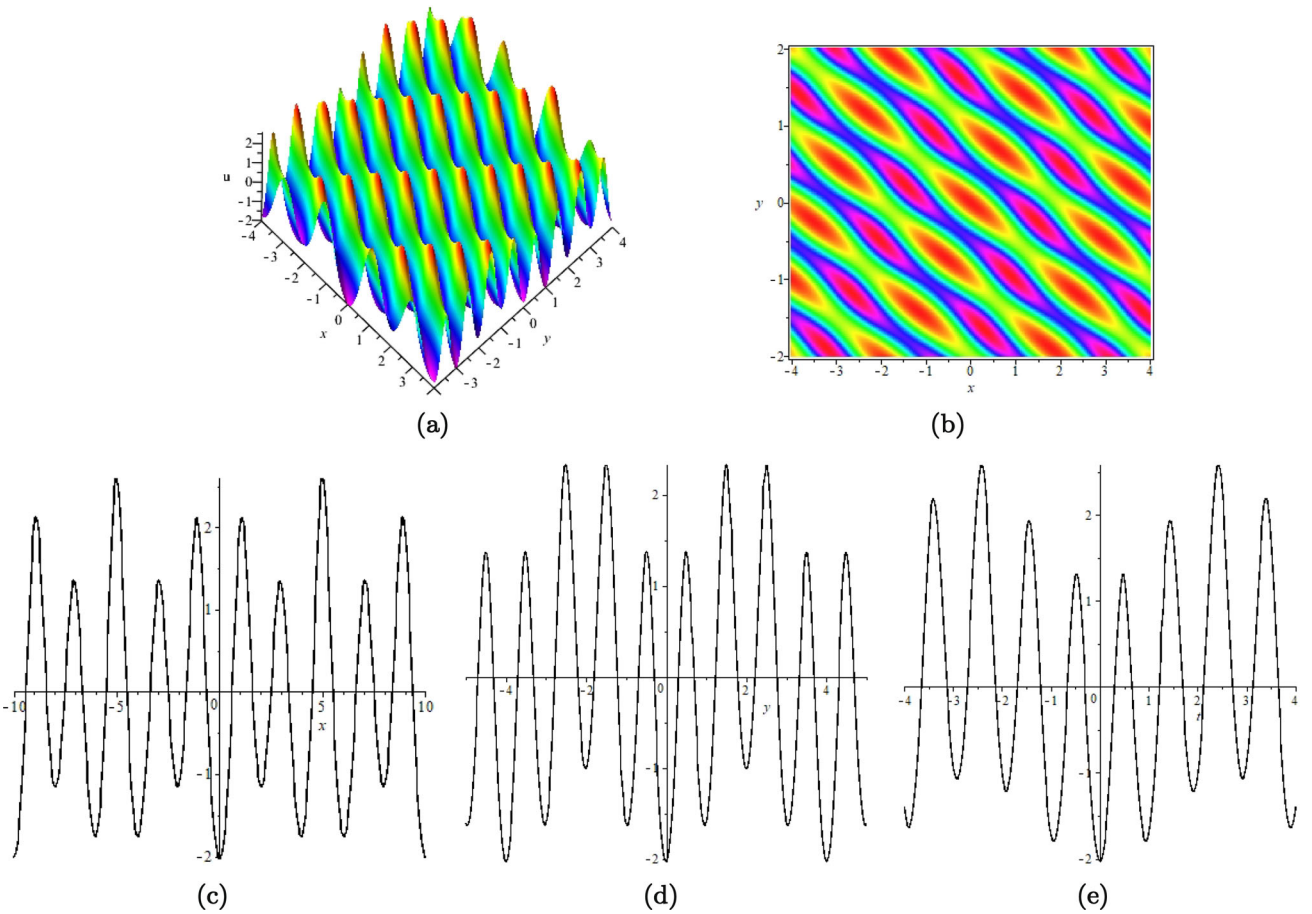

Fig. 17 (Color online) A two-periodic wave of Eq. (1) with parameters $c_1 = c_2 = c_3 = 1, \varepsilon_1 = 0.5, \eta_1 = 1, \varepsilon_2 = 0.3, \eta_2 = -0.25, a_{11} = 1, a_{12} = 0.3, a_{22} = 1$. **a** Three-dimensional stereogram of two-periodic wave when $t = 0$. **b** Vertical view of plot **a**. **c** The wave moves along the x-axis when $y = 0, t = 0$. **d** The wave moves along the y-axis when $x = 0, t = 0$. **e** The wave moves along t-axis when $x = 0, y = 0$

(ii) If we give the following relations of $\begin{vmatrix} \varepsilon_1 & \eta_1 \\ \varepsilon_2 & \eta_2 \end{vmatrix} = 0$, that is the two characteristic lines are parallel. In one case $\frac{\varepsilon_1}{\eta_1} = \frac{\varepsilon_2}{\eta_2} = k$, where k is a constant, $k \neq 1$, as shown in Fig. 18, and in the other case $\frac{\varepsilon_1}{\eta_1} = \frac{\varepsilon_2}{\eta_2} = 1$, as shown in Fig. 19. What they have in common is the parallel of phase variables τ_1, τ_2 makes the periodic wave fluctuate in parallel and propagate periodically along the x-axis and y-axis. The different is that Fig. 19 has two strict periods along x-axis and y-axis, whereas Fig. 18 has one period along x-axis and y-axis.

5.3 Asymptotic properties of two-periodic waves

In what follows, we further analyze asymptotic properties of the two-periodic wave solution by solving Eq. (33) and taking a limit condition. The expansion of matrix M has the following form of

$$
\begin{aligned}
M = &\begin{pmatrix} 0&0&0&1&0 \\ 0&0&0&0&0 \\ 0&0&0&0&0 \\ 0&0&0&0&0 \end{pmatrix} + \begin{pmatrix} 0&0&0&0&0 \\ 0&0&0&0&0 \\ -8\pi^2&0&-48\pi^2{\varepsilon_1}^2&2&0 \\ 0&0&0&0&0 \end{pmatrix}\psi_1 + \begin{pmatrix} 0&0&0&0&0 \\ 0&-8\pi^2&-48\pi^2\varepsilon_2{}^2&2&0 \\ 0&0&0&0&0 \\ 0&0&0&0&0 \end{pmatrix}\psi_2 \\
&+ \begin{pmatrix} -32\pi^2&0&-192\pi^2{\varepsilon_1}^2&2&0 \\ 0&0&0&0&0 \\ 0&0&0&0&0 \\ 0&0&0&0&0 \end{pmatrix}{\psi_1}^2 + \begin{pmatrix} 0&-32\pi^2&-192\pi^2\varepsilon_2{}^2&2&0 \\ 0&0&0&0&0 \\ 0&0&0&0&0 \\ 0&0&0&0&0 \end{pmatrix}{\psi_2}^2 \\
&+ \begin{pmatrix} 0&0&0&0&0 \\ 0&0&0&0&0 \\ 0&0&0&0&0 \\ -8\pi^2&-8\pi^2&-48\pi^2[(\varepsilon_1-\varepsilon_2)^2+(\varepsilon_1+\varepsilon_2)^2\psi_3]&2(1+\psi_3)&-16\pi^2(\psi_3-1) \end{pmatrix}\psi_1\psi_2 + o({\psi_1}^i{\psi_2}^j), \qquad (35)
\end{aligned}
$$

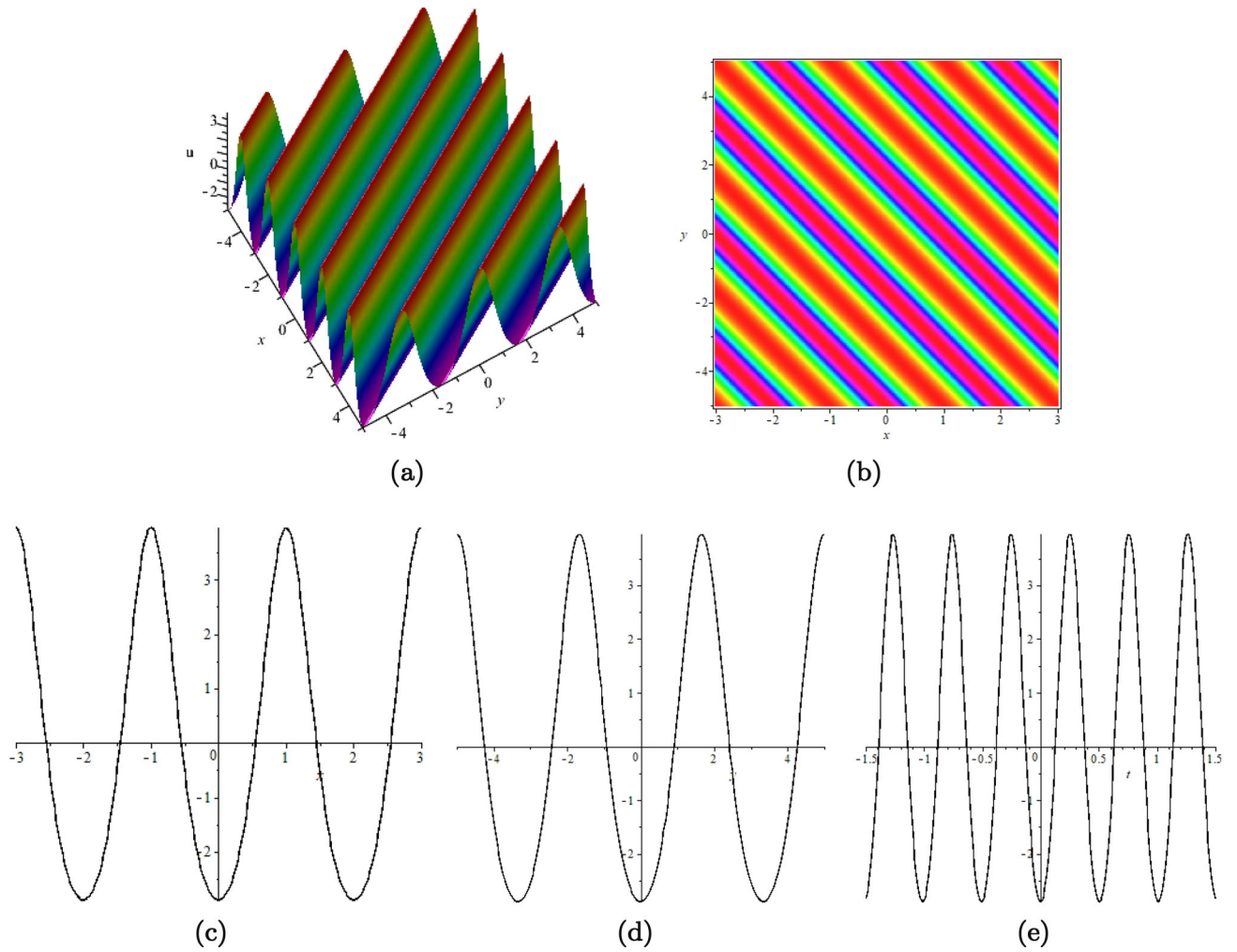

Fig. 18 (Color online) A two-periodic wave of Eq. (1) with parameters $c_1 = 1, c_2 = 2, c_3 = 3, \varepsilon_1 = 0.5, \eta_1 = 0.3, \varepsilon_2 = 0.5, \eta_2 = 0.3, a_{11} = 1, a_{12} = 0.3, a_{22} = 1$. **a** Three-dimensional stereogram of two-periodic wave when $t = 0$. **b** Vertical view of plot (**a**). **c** The wave moves along the x-axis when $y = 0, t = 0$. **d** The wave moves along the y-axis when $x = 0, t = 0$. **e** The wave moves along t-axis when $x = 0, y = 0$

where $i + j \geq 2$. and

$$b = \begin{pmatrix} 0 \\ 0 \\ \Delta_1 \\ 0 \end{pmatrix} \psi_1 + \begin{pmatrix} 0 \\ \Delta_2 \\ 0 \\ 0 \end{pmatrix} \psi_2 + \begin{pmatrix} \Delta_3 \\ 0 \\ 0 \\ 0 \end{pmatrix} {\psi_1}^2 + \begin{pmatrix} \Delta_4 \\ 0 \\ 0 \\ 0 \end{pmatrix} {\psi_2}^2 + \begin{pmatrix} 0 \\ 0 \\ 0 \\ \Delta_5 \end{pmatrix} \psi_1 \psi_2,$$

$$\Delta_1 = 8\pi^2 {\varepsilon_1}^2 c_1 + 8\pi^2 \varepsilon_1 \eta_1 c_2 - 32\pi^4 {\varepsilon_1}^4 c_3, \quad \Delta_2 = 8\pi^2 {\varepsilon_2}^2 c_1 + 8\pi^2 \varepsilon_2 \eta_2 c_2 - 32\pi^4 {\varepsilon_2}^4 c_3,$$

$$\Delta_3 = 32\pi^2 {\varepsilon_1}^2 c_1 + 32\pi^2 \varepsilon_1 \eta_1 c_2 - 512\pi^4 {\varepsilon_1}^4 c_3, \quad \Delta_4 = 8\pi^2 {\varepsilon_2}^2 c_1 + 8\pi^2 \varepsilon_2 \eta_2 c_2 - 32\pi^4 {\varepsilon_2}^4 c_3,$$

$$\Delta_5 = 8\pi^2 c_1[(\varepsilon_1 - \varepsilon_2)^2 + (\varepsilon_1 + \varepsilon_2)^2 \psi_3] + 8\pi^2 c_2[(\varepsilon_1 - \varepsilon_2)(\eta_1 - \eta_2) + (\varepsilon_1 + \varepsilon_2)(\eta_1 + \eta_2)\psi_3$$
$$- 32\pi^4 c_3[(\varepsilon_1 - \varepsilon_2)^4 + (\varepsilon_1 + \varepsilon_2)^4 \psi_3]. \tag{36}$$

Then, we assume that the solution of $M({\omega_1}^2, {\omega_2}^2, u_0, c, \omega_1\omega_2) = b$ has the following form of

$$\begin{pmatrix} {\omega_1}^2 \\ {\omega_2}^2 \\ u_0 \\ c \\ \omega_1\omega_2 \end{pmatrix} = \begin{pmatrix} {\omega_1}^{2(0)} \\ {\omega_2}^{2(0)} \\ u_0^{(0)} \\ c^{(0)} \\ \omega_1\omega_2{}^{(0)} \end{pmatrix} + \begin{pmatrix} {\omega_1}^{2(1)} \\ {\omega_2}^{2(1)} \\ u_0^{(1)} \\ c^{(1)} \\ \omega_1\omega_2{}^{(1)} \end{pmatrix} \psi_1 + \begin{pmatrix} {\omega_1}^{2(2)} \\ {\omega_2}^{2(2)} \\ u_0^{(2)} \\ c^{(2)} \\ \omega_1\omega_2{}^{(2)} \end{pmatrix} \psi_2 + \begin{pmatrix} {\omega_1}^{2(11)} \\ {\omega_2}^{2(11)} \\ u_0^{(11)} \\ c^{(11)} \\ \omega_1\omega_2{}^{(11)} \end{pmatrix} {\psi_1}^2$$

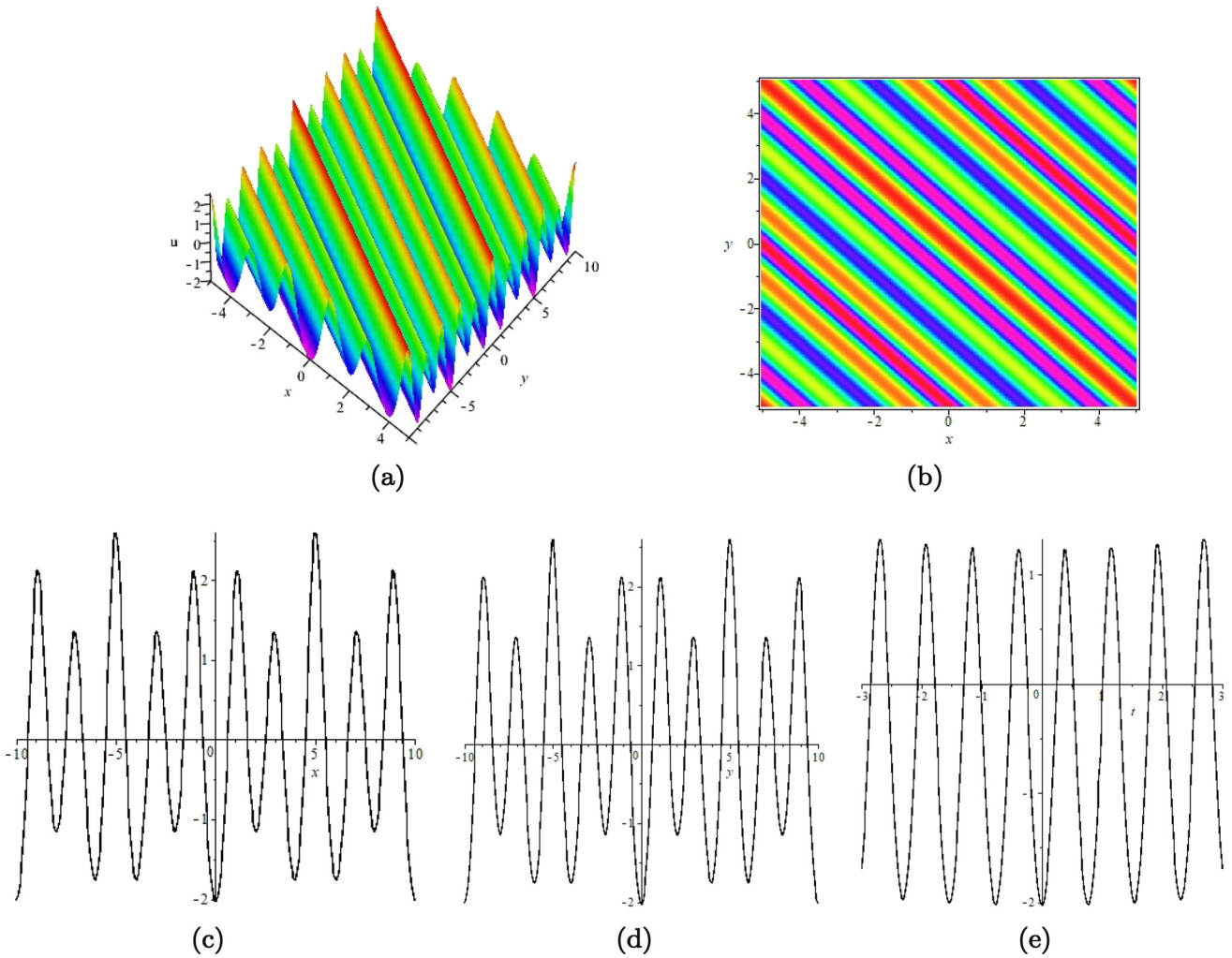

Fig. 19 (Color online) A two-periodic wave of Eq. (1) with parameters $c_1 = c_2 = c_3 = 1, \varepsilon_1 = 0.5, \eta_1 = 0.5, \varepsilon_2 = 0.3, \eta_2 = 0.3, a_{11} = 1, a_{12} = 0.3, a_{22} = 1$. **a** Three-dimensional stereogram of two-periodic wave when $t = 0$. **b** Vertical view of plot (**a**). **c** The wave moves along the x-axis when $y = 0, t = 0$. **d** The wave moves along the y-axis when $x = 0, t = 0$. **e** The wave moves along t-axis when $x = 0, y = 0$

$$+\begin{pmatrix} {\omega_1}^{2(22)} \\ {\omega_2}^{2(22)} \\ u_0^{(22)} \\ c^{(22)} \\ \omega_1\omega_2{}^{(22)} \end{pmatrix}{\psi_2}^2 + \begin{pmatrix} {\omega_1}^{2(12)} \\ {\omega_2}^{2(12)} \\ u_0^{(12)} \\ c^{(12)} \\ \omega_1\omega_2{}^{(12)} \end{pmatrix}\psi_1\psi_2 + o({\psi_1}^i{\psi_2}^j), i + j \geq 2. \tag{37}$$

Interestingly, the relation of the two-soliton wave solution and two-periodic wave solution is given as follows.

Theorem 2 If two-periodic wave solution Eq. (34) satisfies the following condition of

$$\varepsilon_j = \frac{k_j}{2\pi \mathrm{i}}, \quad \eta_j = \frac{l_j}{2\pi \mathrm{i}}, \quad \upsilon_j = \frac{\delta_j + \pi a_{jj}}{2\pi \mathrm{i}}, \quad a_{12} = \frac{A_{12}}{-2\pi}, \quad (j = 1, 2) \tag{38}$$

where k_j, l_j and δ_j $(j = 1, 2)$ are given by Eq. (5), we have the following asymptotic properties:

$$u_0 \to 0,\ c \to 0,\ \tau_j \to \frac{\sigma_j + \pi a_{jj}}{2\pi \mathrm{i}}\ (j = 1, 2),\ \varphi(\tau_1, \tau_2, a) \to 1 + \mathrm{e}^{\sigma_1} + \mathrm{e}^{\sigma_2} + \mathrm{e}^{\sigma_1+\sigma_2+A_{12}}, \quad \psi_1, \psi_2 \to 0.$$

Proof By substituting Eq. (35-37) into Eq. (33), we obtain the following relations of

$$c^{(0)} = c^{(1)} = c^{(2)} = c^{(12)} = 0,\ \ \omega_1^{2(0)} + 6\varepsilon_1 u_0^{(0)} = -\varepsilon_1^2 c_1 - \varepsilon_1\eta_1 c_2 + 4\pi^2\varepsilon_1^2 c_3,$$
$$\omega_2^{2(0)} + 6\varepsilon_2 u_0^{(0)} = -\varepsilon_2^2 c_1 - \varepsilon_2\eta_2 c_2 + 4\pi^2\varepsilon_2^2 c_3,\ \omega_1^{2(1)} + 6\varepsilon_1 u_0^{(1)} = 0,\ \ \omega_2^{2(1)} + 6\varepsilon_2 u_0^{(1)} = 0,$$
$$c^{(11)} - 32\pi^2\omega_1^{2(0)} - 192\pi^2\varepsilon_1^2 u_0^{(0)} = 32\pi^2\varepsilon_1^2 c_1 + 32\pi^2\varepsilon_1\eta_1 c_2 - 512\pi^4\varepsilon_1^4 c_3,$$

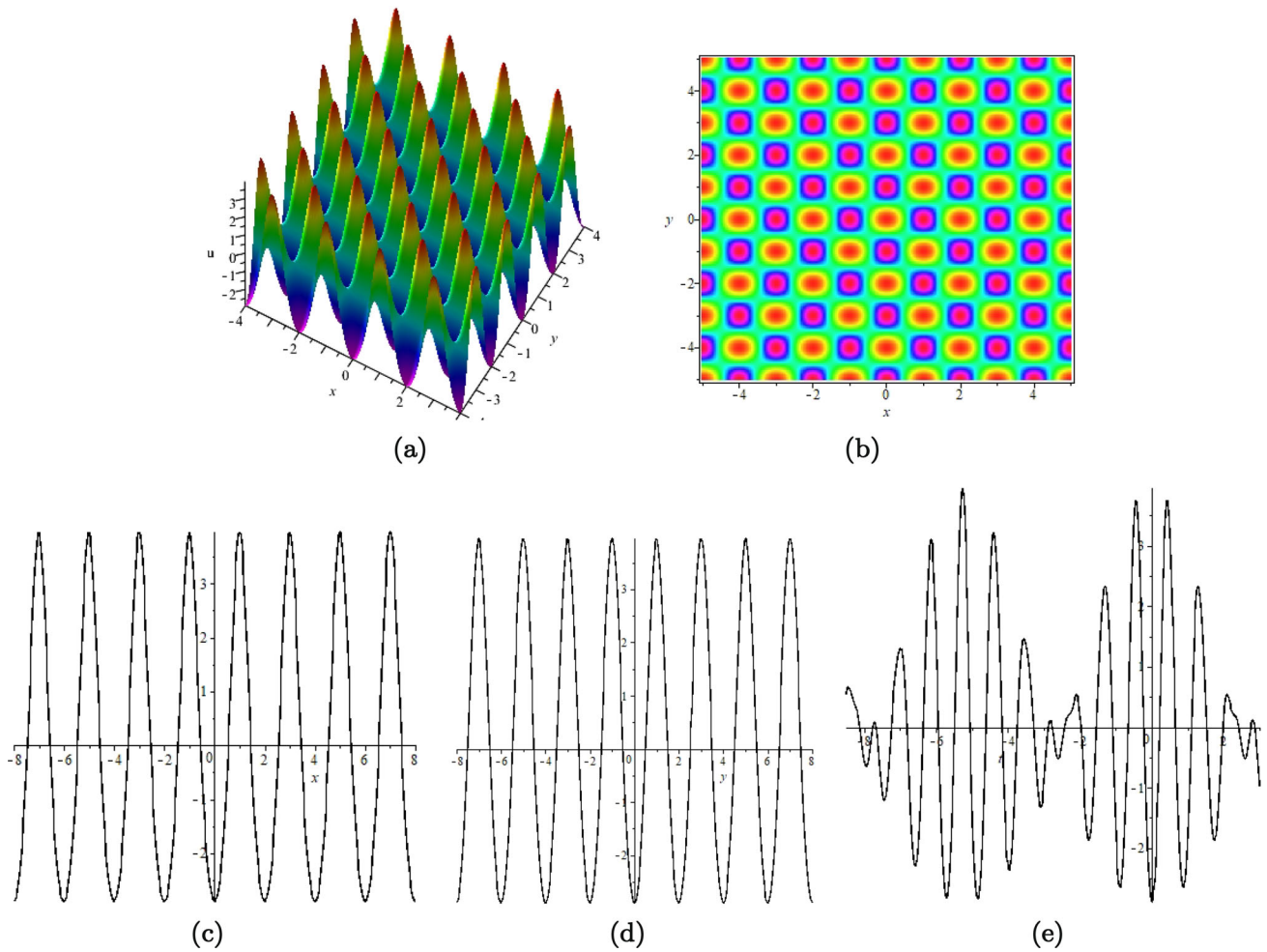

Fig. 20 (Color online) A two-periodic wave of Eq. (1) with parameters $c_1 = c_2 = c_3 = 1, \varepsilon_1 = 0.5, \eta_1 = 0.5, \varepsilon_2 = 0.5, \eta_2 = -0.5, a_{11} = 1, a_{12} = 0.3, a_{22} = 1$. **a** Three-dimensional stereogram of two-periodic wave when $t = 0$. **b** Vertical view of plot (**a**). **c** The wave moves along the x-axis when $y = 0, t = 0$. **d** The wave moves along the y-axis when $x = 0, t = 0$. **e** The wave moves along t-axis when $x = 0, y = 0$

$$c^{(22)} - 32\pi^2\omega_2^{2(0)} - 192\pi^2\varepsilon_2^2 u_0^{(0)} = 32\pi^2\varepsilon_2^2 c_1 + 32\pi^2\varepsilon_2\eta_2 c_2 - 512\pi^4\varepsilon_2^4 c_3. \tag{39}$$

□

By using condition(38), and taking $u_0^{(0)} = 0$, Eq. (39) has the following form of

$$\begin{aligned} c &= -384\pi^4{\varepsilon_1}^4 c_3{\psi_1}^2 - 384\pi^4{\varepsilon_2}^4 c_3{\psi_2}^2 + o({\psi_1}^2{\psi_2}^2), \\ 2\pi\mathrm{i}\omega_1 &= \sqrt{-4\pi^2\omega_1} = \sqrt{-4\pi^2(-{\varepsilon_1}^2 c_1 - \varepsilon_1\eta_1 c_2 + 4\pi^2{\varepsilon_1}^2 c_3)}, \\ 2\pi\mathrm{i}\omega_2 &= \sqrt{-4\pi^2\omega_2} = \sqrt{-4\pi^2(-{\varepsilon_2}^2 c_1 - \varepsilon_2\eta_2 c_2 + 4\pi^2{\varepsilon_2}^2 c_3)}, \end{aligned}$$

and using condition(38), we have

$$u_0 \to 0,\ c \to 0,\ \ 2\pi\mathrm{i}\omega_1 \to \sqrt{-{k_1}^2 c_1 - k_1 l_1 c_2 - {k_1}^2 c_3},\ \ 2\pi\mathrm{i}\omega_2 \to \sqrt{-{k_2}^2 c_1 - k_2 l_2 c_2 - {k_2}^2 c_3},\ \ \psi_1, \psi_2 \to 0.$$

By expanding the theta function

$$\varphi(\tau_1, \tau_2, a) = 1 + (\mathrm{e}^{2\pi\mathrm{i}\tau_1} + \mathrm{e}^{-2\pi\mathrm{i}\tau_1})\mathrm{e}^{-\pi a_{11}} + (\mathrm{e}^{2\pi\mathrm{i}\tau_2} + \mathrm{e}^{-2\pi\mathrm{i}\tau_2})\mathrm{e}^{-\pi a_{22}} + \left(\mathrm{e}^{2\pi\mathrm{i}(\tau_1+\tau_2)} + \mathrm{e}^{-2\pi\mathrm{i}(\tau_1+\tau_2)}\right)\mathrm{e}^{-\pi(a_{11}+2a_{12}+a_{22})} + \cdots,$$

and applying condition(38), one has

$$\begin{aligned} \varphi(\tau_1, \tau_2, a) &= 1 + \mathrm{e}^{{\tau_1}'} + \mathrm{e}^{{\tau_2}'} + \mathrm{e}^{{\tau_1}'+{\tau_2}'-2\pi a_{12}} + {\psi_1}^2\mathrm{e}^{-{\tau_1}'} + {\psi_2}^2\mathrm{e}^{-{\tau_2}'} + {\psi_1}^2{\psi_2}^2\mathrm{e}^{-{\tau_1}'-{\tau_2}'-2\pi a_{12}} + \cdots \\ &\to 1 + \mathrm{e}^{{\tau_1}'} + \mathrm{e}^{{\tau_2}'} + \mathrm{e}^{{\tau_1}'+{\tau_2}'+A_{12}}, \quad \psi_1, \psi_2 \to 0, \end{aligned} \tag{40}$$

where

$$\tau_1{}' = 2\pi \mathrm{i}\tau_1 - \pi a_{11} \to k_1 x + l_1 y + \sqrt{-c_2 k_1 l_1 - c_3 {k_1}^4 - c_1 {k_1}^2}\, t + \delta_1 = \sigma_1,$$
$$\tau_2{}' = 2\pi \mathrm{i}\tau_2 - \pi a_{22} \to k_2 x + l_2 y + \sqrt{-c_2 k_2 l_2 - c_3 {k_2}^4 - c_1 {k_2}^2}\, t + \delta_2 = \sigma_2, \quad \psi_1, \psi_2 \to 0. \tag{41}$$

Combining Eqs. (40) and (41), we obtain

$$\varphi(\tau_1, \tau_2, a) \to 1 + \mathrm{e}^{\sigma_1} + \mathrm{e}^{\sigma_2} + \mathrm{e}^{\sigma_1 + \sigma_2 + A_{12}}, \ \psi_1, \psi_2 \to 0.$$

Therefore, two-periodic wave solution tends to two-soliton solution under the condition of $\psi_1, \psi_2 \to 0$.

6 Three-periodic waves and asymptotic properties

In this section, three-periodic wave solution of Eq. (1) is more complex than the two-periodic wave solution. When $N = 3$, the theta function degenerates the following Fourier series

$$\varphi(\tau, a) = \varphi(\tau_1, \tau_2, \tau_3, a) = \sum_{n=-\infty}^{+\infty} \mathrm{e}^{2\pi \mathrm{i} < \tau, n > - \pi < an, n >}, \tag{42}$$

with phase variable $\tau_1 = \varepsilon_1 x + \eta_1 y + \omega_1 t + \upsilon_1$, $\tau_2 = \varepsilon_2 x + \eta_2 y + \omega_2 t + \upsilon_2$ and $\tau_3 = \varepsilon_3 x + \eta_3 y + \omega_3 t + \upsilon_3$, where $n = (n_1, n_2, n_3)^T \in Z^3$, $\tau = (\tau_1, \tau_2, \tau_3)^T \in C^3$, and a is a positive definite and real-valued symmetric 3×3 matrix, that is, $a = \begin{pmatrix} a_{11} & a_{12} & a_{13} \\ a_{21} & a_{22} & a_{23} \\ a_{31} & a_{32} & a_{33} \end{pmatrix}$.

6.1 Construction of three-periodic waves

The structure of three-periodic waves is similar to that of two-periodic waves, where

$$B({m_1}', {m_2}', {m_3}') = \begin{cases} B({m_1}' - 2, {m_2}', {m_3}')\mathrm{e}^{2\pi(1-{m_1}')a_{11} - 2\pi(a_{12}{m_2}' + a_{13}{m_3}')}, & l = 1, \\ B({m_1}', {m_2}' - 2, {m_3}')\mathrm{e}^{2\pi(1-{m_2}')a_{22} - 2\pi(a_{21}{m_1}' + a_{23}{m_3}')}, & l = 2, \\ B({m_1}', {m_2}', {m_3}' - 2)\mathrm{e}^{2\pi(1-{m_3}')a_{33} - 2\pi(a_{31}{m_1}' + a_{32}{m_2}')}, & l = 3, \end{cases}$$

which shows that $\overline{B}({m_1}', {m_2}', {m_3}')$ $({m_1}' \in Z^3, {m_2}' \in Z^3, {m_3}' \in Z^3)$ is entirely determined by eight formulas $\overline{B}(0, 0, 0)$, $\overline{B}(1, 0, 0)$, $\overline{B}(0, 1, 0)$, $\overline{B}(0, 0, 1)$, $\overline{B}(1, 1, 0)$, $\overline{B}(1, 0, 1)$, $\overline{B}(0, 1, 1)$, $\overline{B}(1, 1, 1)$, that is, if the following eight equations are satisfied

$$\overline{B}(0, 0, 0) = \overline{B}(1, 0, 0) = \overline{B}(0, 1, 0) = \overline{B}(0, 0, 1) = \overline{B}(1, 1, 0) = \overline{B}(1, 0, 1) = \overline{B}(0, 1, 1) = \overline{B}(1, 1, 1) = 0 \tag{43}$$

then

$$\overline{B}({m_1}', {m_2}', {m_3}') = 0 \ ({m_1}' \in Z^3, \ {m_2}' \in Z^3, \ {m_3}' \in Z^3), \quad B(D_x, D_y, D_t)\varphi(\tau_1, \tau_2, \tau_3, a)\varphi(\tau_1, \tau_2, \tau_3, a) = 0.$$

Then introducing the marks as

$$M = (a_{jl})_{8\times 11}, \ b = (b_1, b_2, b_3, b_4, b_5, b_6, b_7, b_8)^T,$$
$$a_{j1} = \sum_{n_1, n_2, n_3 \in Z^3} -4\pi^2 (2n_1 - s_1^j)^2 \upsilon_j(n),$$
$$a_{j2} = \sum_{n_1, n_2, n_3 \in Z^3} -4\pi^2 (2n_2 - s_2^j)^2 \upsilon_j(n),$$
$$a_{j3} = \sum_{n_1, n_2, n_3 \in Z^3} -4\pi^2 (2n_3 - s_3^j)^2 \upsilon_j(n),$$
$$a_{j4} = \sum_{n_1, n_2, n_3 \in Z^3} -4\pi^2 c_2 < 2n - s^j, \varepsilon > (2n_1 - s_1^j)\upsilon_j(n),$$
$$a_{j5} = \sum_{n_1, n_2, n_3 \in Z^3} -4\pi^2 c_2 < 2n - s^j, \varepsilon > (2n_2 - s_2^j)\upsilon_j(n),$$
$$a_{j6} = \sum_{n_1, n_2, n_3 \in Z^3} -4\pi^2 c_2 < 2n - s^j, \varepsilon > (2n_3 - s_3^j)\upsilon_j(n),$$

$$
\begin{aligned}
a_{j7} &= \sum_{n_1,n_2,n_3\in Z^3} -24\pi^2 < 2n - s^j, \varepsilon >^2 v_j(n),\\
a_{j8} &= \sum_{n_1,n_2,n_3\in Z^3} v_j(n),\\
a_{j9} &= \sum_{n_1,n_2,n_3\in Z^3} -8\pi^2(2n_1 - s_1^j)(2n_2 - s_2^j)v_j(n),\\
a_{j10} &= \sum_{n_1,n_2,n_3\in Z^3} -8\pi^2(2n_1 - s_1^j)(2n_3 - s_3^j)v_j(n),\\
a_{j11} &= \sum_{n_1,n_2,n_3\in Z^3} -8\pi^2(2n_2 - s_2^j)(2n_3 - s_3^j)v_j(n),\\
b_j &= \sum_{n_1,n_2,n_3\in Z^3} (4\pi^2 c_1 < 2n - s^j, \varepsilon >^2 - 16\pi^4 c_3 < 2n - s^j, \varepsilon >^4)v_j(n),\\
v_j(n) &= {\psi_1}^{{n_1}^2+(n_1-s_1^j)^2} \times {\psi_2}^{{n_2}^2+(n_2-s_2^j)^2} \times {\psi_3}^{{n_3}^2+(n_3-s_3^j)^2} \times {\psi_{12}}^{n_1n_2+(n_1-s_1^j)(n_2-s_2^j)}\\
&\quad \times {\psi_{13}}^{n_1n_3+(n_1-s_1^j)(n_3-s_3^j)} \times {\psi_{12}}^{n_2n_3+(n_2-s_2^j)(n_3-s_3^j)},\\
\psi_1 &= \mathrm{e}^{-\pi a_{11}},\ \psi_2 = \mathrm{e}^{-\pi a_{22}}, \psi_3 = \mathrm{e}^{-\pi a_{33}},\ \psi_{12} = \mathrm{e}^{-2\pi a_{12}},\ \psi_{13} = \mathrm{e}^{-2\pi a_{13}},\ \psi_{23} = \mathrm{e}^{-2\pi a_{23}},\\
s^1 &= (0,0,0),\ s^2 = (1,0,0),\ s^3 = (0,1,0),\ s^4 = (0,0,1),\ s^5 = (1,1,0),\\
s^6 &= (1,0,1),\ s^7 = (0,1,1), s^8 = (1,1,1),\ s^j = (s_1^j, s_2^j, s_3^j),
\end{aligned}
$$

Eq. (43) can be written as the form of a system of linear equations about η_1, η_2, η_3, frequency ω_1, ω_2, ω_3, constant u_0 and integration constant c, that is

$$M({\omega_1}^2, {\omega_2}^2, {\omega_3}^2, \eta_1, \eta_2, \eta_3, u_0, c, \omega_1\omega_2, \omega_1\omega_3, \omega_2\omega_3) = b, \tag{44}$$

then we obtain the three-periodic wave solution of Eq. (1)

$$u = u_0 + 2(\ln \varphi(\tau_1, \tau_2, \tau_3, a))_{xx}, \tag{45}$$

where the theta function $\varphi(\tau_1, \tau_2, \tau_3, a)$ is given by Eq. (42), u_0 is determined by formula (44), the other parameters $c_1, c_2, c_3, a_{11}, a_{12}, a_{13}, a_{23}, a_{22}, a_{33}, \varepsilon_1, \varepsilon_2, \varepsilon_3, \upsilon_1, \upsilon_2$ and υ_3 are free, the nine parameters $a_{11}, a_{12}, a_{13}, a_{23}, a_{22}, a_{33}, \varepsilon_1, \varepsilon_2$ and ε_3 play a major role in three-periodic waves.

6.2 Characteristics of three-periodic waves

(1) It is bounded for all complex variables (x, y, t).
(2) It is obvious that three-periodic waves are the direct generalization of the one- and two-periodic waves, but there are three phase variables τ_1, τ_2 and τ_3, it has three independent periods in two independent horizontal directions, respectively.
(3) $B(D_x, D_y, D_t)\varphi(\tau_1, \tau_2, \tau_3, a)\varphi(\tau_1, \tau_2, \tau_3, a)$ can be written as the form of

$$\sum_{m'=-\infty}^{+\infty} \overline{B}({m_1}', {m_2}', {m_3}')\cos(\tau_1{m_1}')\cos(\tau_2{m_2}')\cos(\tau_3{m_3}').$$

According to the above formula, three-periodic wave has three characteristic lines: $\tau_1 = \varepsilon_1 x + \eta_1 y + \omega_1 t + \upsilon_1 = 0$, $\tau_2 = \varepsilon_2 x + \eta_2 y + \omega_2 t + \upsilon_2 = 0$ and $\tau_3 = \varepsilon_3 x + \eta_3 y + \omega_3 t + \upsilon_3 = 0$.

If giving the relations $\varepsilon_1 > 0 (< 0), \varepsilon_2 > 0 (< 0), \varepsilon_3 > 0 (< 0)$, we obtain $\frac{\varepsilon_1}{\eta_1} \approx \frac{\varepsilon_2}{\eta_2} \approx \frac{\varepsilon_3}{\eta_3}$, that is the three characteristic lines are parallel, as shown in Figs. 21, 22, 23 and 24. In Fig. 21, $\varepsilon_1 \neq \varepsilon_2 \neq \varepsilon_3$, it presents three strict periods along the x-axis, y-axis and t-axis. Then we consider the special relations of $\varepsilon_1 = -\varepsilon_2$, and $\varepsilon_3 \neq \varepsilon_1, \varepsilon_2$, it presents two periods along the x-axis, y-axis and t-axis, and appears interesting Hill-shaped protrusions, as shown in Fig. 24. In Fig. 22, $\varepsilon_1 = \varepsilon_2 \neq \varepsilon_3$, it presents two periods along the x-axis, y-axis and t-axis. In Fig. 23, $\varepsilon_1 = \varepsilon_2 = \varepsilon_3$, three-periodic wave degenerates into one-periodic wave in the x-axis, y-axis and t-axis, and they are superimposed in three directions.

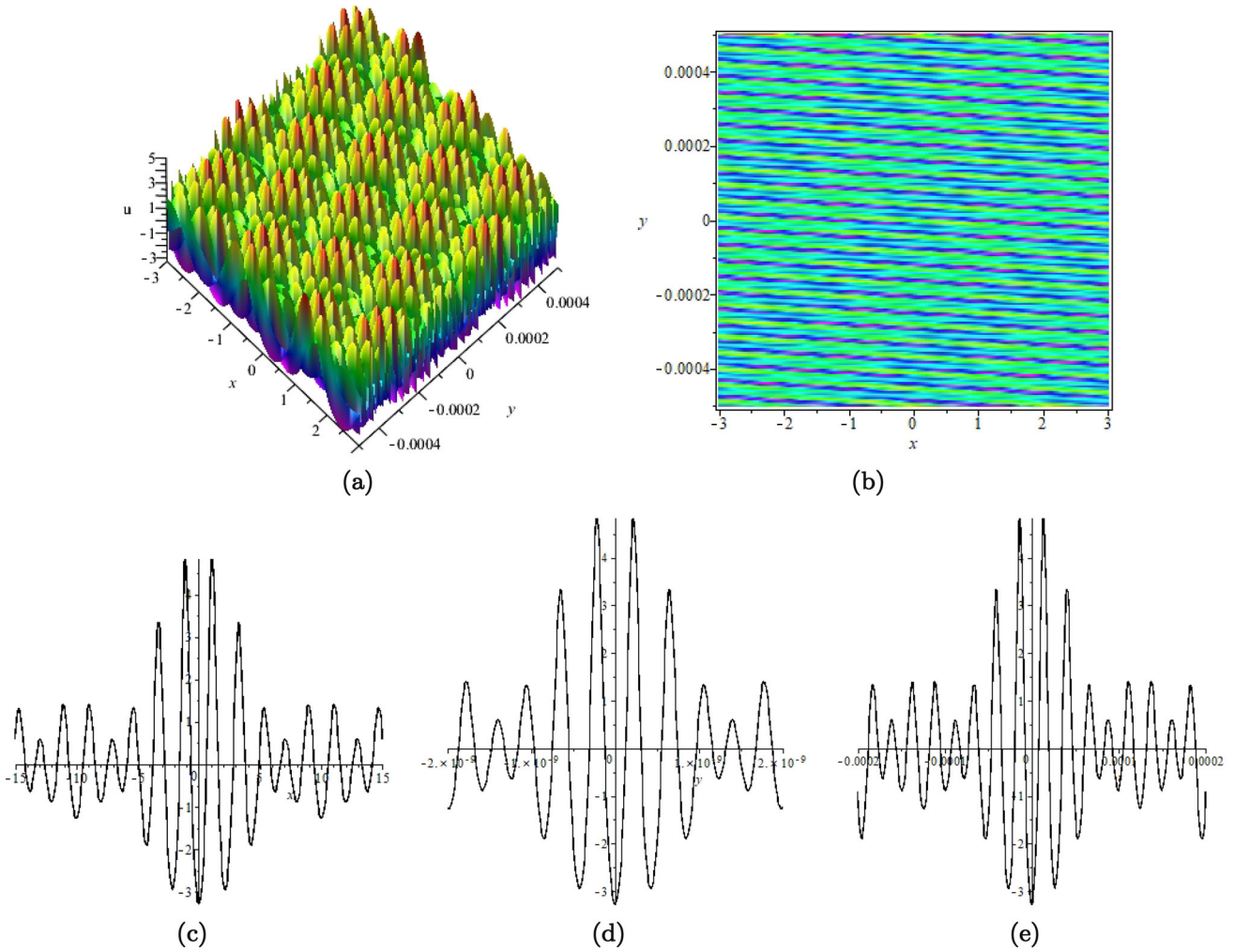

Fig. 21 (Color online) A three-periodic wave of Eq. (1) with parameters $c_1 = c_2 = c_3 = 1, \varepsilon_1 = 0.5, \varepsilon_2 = 0.45, \varepsilon_3 = 0.4, a_{11} = 1, a_{12} = 0.3, a_{13} = 0.3, a_{23} = 0.3, a_{22} = 1, a_{33} = 1$. **a** Three-dimensional stereogram of three-periodic wave when $t = 0$. **b** Vertical view of plot (**a**). **c** The wave moves along the x-axis when $y = 0, t = 0$. **d** The wave moves along the y-axis when $x = 0, t = 0$. **e** The wave moves along t-axis when $x = 0, y = 0$

6.3 Asymptotic properties of three-periodic waves

In what follows, we further analyze asymptotic properties of the three-periodic wave solution by solving Eq. (44) and taking a limit condition. The expansion of matrix M has the following form of

$$
\begin{aligned}
M = &\begin{pmatrix} \overbrace{0\cdots01\ 000}^{1\times 8} \\ \underbrace{\cdots 0\cdots}_{7\times 11} \end{pmatrix} + \begin{pmatrix} \cdots 0\cdots \\ -8\pi^2 00 -8\pi^2\varepsilon_1 c_2 00 -48\pi^2\varepsilon_1{}^2\ 20\,00 \\ \underbrace{\cdots 0\cdots}_{6\times 11} \end{pmatrix}\psi_1 \\
&+ \begin{pmatrix} \overbrace{\cdots 0\cdots}^{2\times 11} \\ 0 -8\pi^2 00 -8\pi^2\varepsilon_2 c_2 0 -48\pi^2\varepsilon_2{}^2\ 20\,00 \\ \underbrace{\cdots 0\cdots}_{5\times 11} \end{pmatrix}\psi_2 \\
&+ \begin{pmatrix} \overbrace{\cdots 0\cdots}^{3\times 11} \\ 00 -8\pi^2 00 -8\pi^2\varepsilon_3 c_2 -48\pi^2\varepsilon_3{}^2\ 20\,00 \\ \underbrace{\cdots 0\cdots}_{4\times 11} \end{pmatrix}\psi_3
\end{aligned}
$$

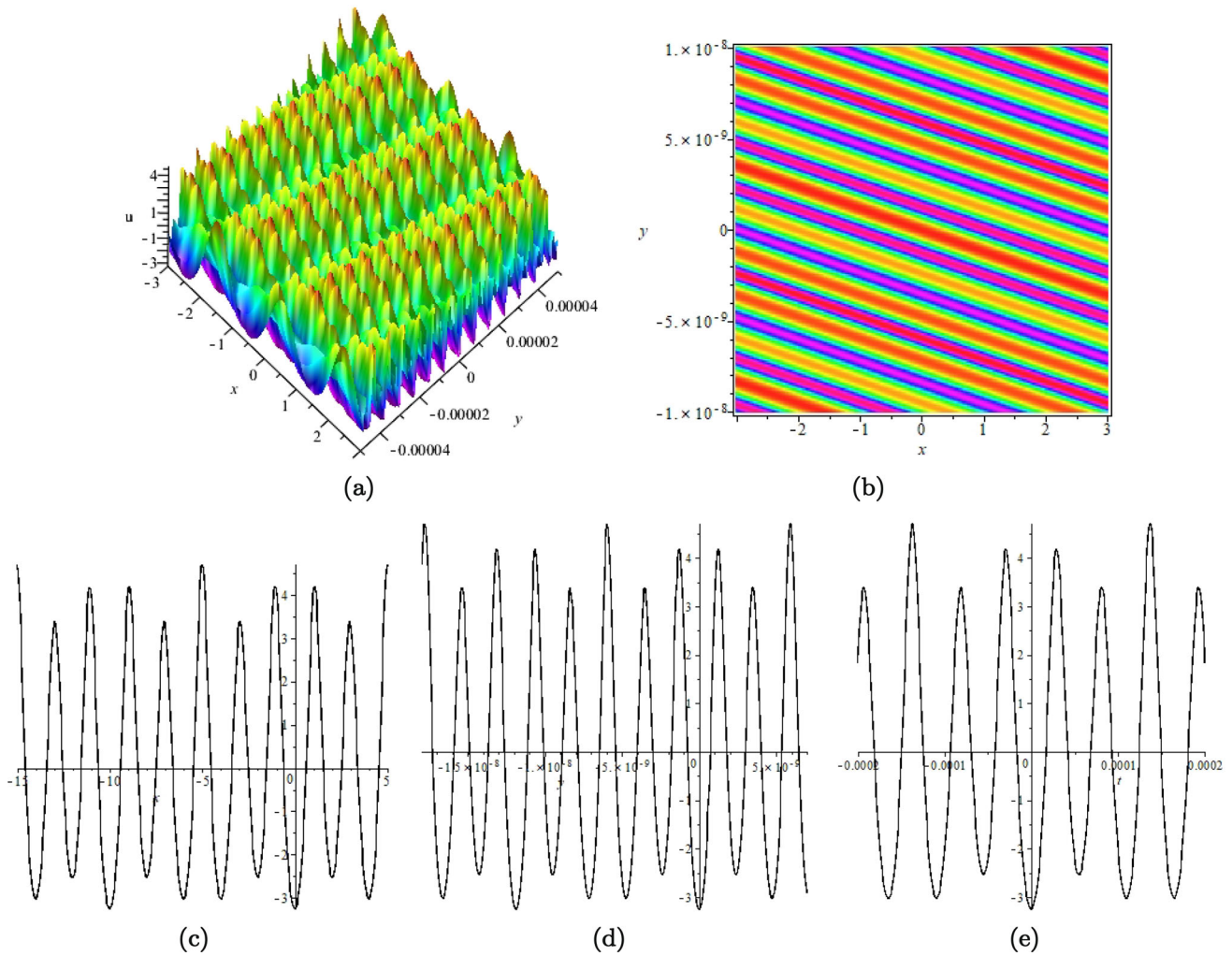

Fig. 22 (Color online) A three-periodic wave of Eq. (1) with parameters $c_1 = c_2 = c_3 = 1, \varepsilon_1 = 0.5, \varepsilon_2 = 0.5, \varepsilon_3 = 0.3, a_{11} = 1, a_{12} = 0.3, a_{13} = 0.3, a_{23} = 0.3, a_{22} = 1, a_{33} = 1$. **a** Three-dimensional stereogram of three-periodic wave when $t = 0$. **b** Vertical view of plot (**a**). **c** The wave moves along the x-axis when $y = 0, t = 0$. **d** The wave moves along the y-axis when $x = 0, t = 0$. **e** The wave moves along t-axis when $x = 0, y = 0$

$$
+\left(\begin{array}{c}\overbrace{\cdots 0\cdots}^{4\times 11}\\ -8\pi^2 -8\pi^2 0\Gamma_1\Gamma_2 0\Gamma_3\, 2(1+\psi_{12}) -16\pi^2(\psi_{12}-1)\, 00\\ \underbrace{\cdots 0\cdots}_{3\times 11}\end{array}\right)\psi_1\psi_2
$$

$$
+\left(\begin{array}{c}\overbrace{\cdots 0\cdots}^{5\times 11}\\ -8\pi^2 0 -8\pi^2\Gamma_4 0\Gamma_5\Gamma_6\, 2(1+\psi_{13}) 0 -16\pi^2(\psi_{13}-1) 0\\ \underbrace{\cdots 0\cdots}_{2\times 11}\end{array}\right)\psi_1\psi_3
$$

$$
+\left(\begin{array}{c}\overbrace{\cdots 0\cdots}^{6\times 11}\\ 0 -8\pi^2 -8\pi^2 0\Gamma_7\Gamma_8\Gamma_9\, 2(1+\psi_{23}) 0 0 -16\pi^2(\psi_{23}-1)\\ \underbrace{\cdots 0\cdots}_{1\times 11}\end{array}\right)\psi_2\psi_3
$$

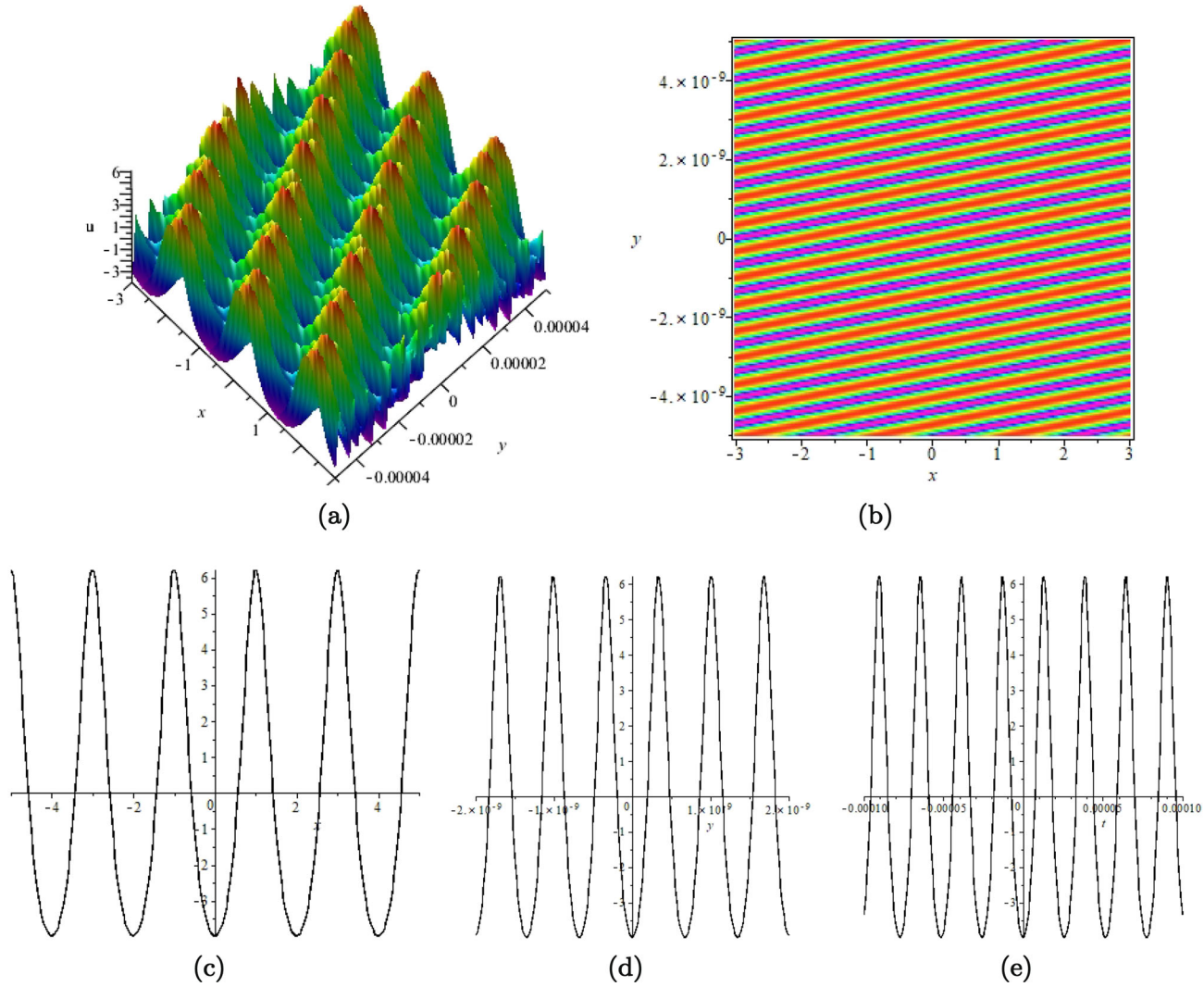

Fig. 23 (Color online) A three-periodic wave of Eq. (1) with parameters $c_1 = c_2 = c_3 = 1, \varepsilon_1 = 0.5, \varepsilon_2 = 0.5, \varepsilon_3 = 0.5, a_{11} = 1, a_{12} = 0.3, a_{13} = 0.3, a_{23} = 0.3, a_{22} = 1, a_{33} = 1$. **a** Three-dimensional stereogram of three-periodic wave when $t = 0$. **b** Vertical view of plot (**a**). **c** The wave moves along the x-axis when $y = 0, t = 0$. **d** The wave moves along the y-axis when $x = 0, t = 0$. **e** The wave moves along t-axis when $x = 0, y = 0$

$$
\begin{aligned}
&+\begin{pmatrix} -32\pi^2 00 -32\pi^2\varepsilon_1 c_2 00 -192\pi^2\varepsilon_1{}^2\, 2000 \\ \underbrace{\cdots 0 \cdots}_{7\times 11} \end{pmatrix}\psi_1{}^2 \\
&+\begin{pmatrix} 0 -32\pi^2 00 -32\pi^2\varepsilon_2 c_2 0 -192\pi^2\varepsilon_2{}^2\, 2000 \\ \underbrace{\cdots 0 \cdots}_{7\times 11} \end{pmatrix}\psi_2{}^2 \\
&+\begin{pmatrix} 00 -32\pi^2 00 -32\pi^2\varepsilon_3 c_2 -192\pi^2\varepsilon_3{}^2\, 2000 \\ \underbrace{\cdots 0 \cdots}_{7\times 11} \end{pmatrix}\psi_3{}^2 \\
&+\begin{pmatrix} \overbrace{\cdots 0 \cdots}^{7\times 11} \\ -8\pi^2 -8\pi^2 -8\pi^2\Gamma_{10}\Gamma_{11}\Gamma_{12}\Gamma_{13}\Gamma_{14}\Gamma_{15}\Gamma_{16}\Gamma_{16} \end{pmatrix}\psi_1\psi_2\psi_3 + o(\psi_1{}^i\psi_2{}^j\psi_3{}^k),\ i+j+k \geq 3,
\end{aligned}
$$

$$\Gamma_1 = \Gamma_2 = -8\pi^2 c_2[(\varepsilon_1+\varepsilon_2)\psi_{12} + (\varepsilon_1-\varepsilon_2)],\ \Gamma_3 = -48\pi^2[(\varepsilon_1+\varepsilon_2)^2\psi_{12} + (\varepsilon_1-\varepsilon_2)^2],$$

$$\Gamma_4 = \Gamma_5 = -8\pi^2 c_2[(\varepsilon_1+\varepsilon_3)\psi_{13} + (\varepsilon_1-\varepsilon_3)],\ \Gamma_6 = -48\pi^2[(\varepsilon_1+\varepsilon_3)^2\psi_{13} + (\varepsilon_1-\varepsilon_3)^2],$$

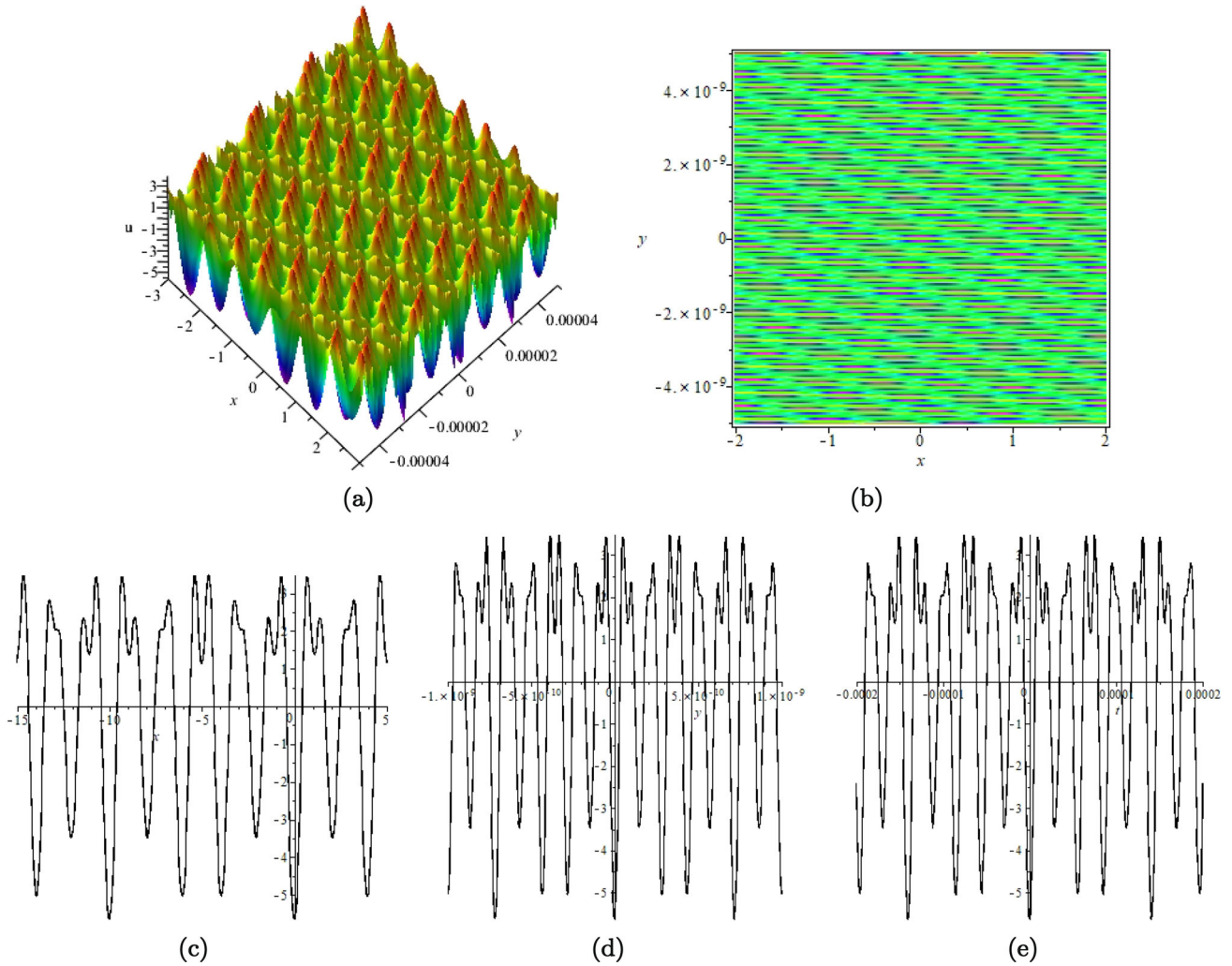

Fig. 24 (Color online) A three-periodic wave of Eq. (1) with parameters $c_1 = c_2 = c_3 = 1, \varepsilon_1 = 0.5, \varepsilon_2 = -0.5, \varepsilon_3 = 0.3, a_{11} = 1, a_{12} = 0.3, a_{13} = 0.3, a_{23} = 0.3, a_{22} = 1, a_{33} = 1$. **a** Three-dimensional stereogram of three-periodic wave when $t = 0$. **b** Vertical view of plot (**a**). **c** The wave moves along the x-axis when $y = 0, t = 0$. **d** The wave moves along the y-axis when $x = 0, t = 0$. **e** The wave moves along t-axis when $x = 0, y = 0$

$$
\begin{aligned}
&\Gamma_7 = \Gamma_8 = -8\pi^2 c_2[(\varepsilon_2+\varepsilon_3)\psi_{23} + (\varepsilon_2-\varepsilon_3)], \ \Gamma_9 = -48\pi^2[(\varepsilon_2+\varepsilon_3)^2\psi_{23} + (\varepsilon_2-\varepsilon_3)^2],\\
&\Gamma_{10} = -48\pi^2 c_2[(\varepsilon_1+\varepsilon_2+\varepsilon_3)\psi_{12}\psi_{13}\psi_{23} + (\varepsilon_1-\varepsilon_2-\varepsilon_3)\psi_{23} + (\varepsilon_1-\varepsilon_2+\varepsilon_3)\psi_{13} + (\varepsilon_1+\varepsilon_2-\varepsilon_3)\psi_{12}],\\
&\Gamma_{11} = -48\pi^2 c_2[(\varepsilon_1+\varepsilon_2+\varepsilon_3)\psi_{12}\psi_{13}\psi_{23} + (-\varepsilon_1+\varepsilon_2+\varepsilon_3)\psi_{23} + (-\varepsilon_1+\varepsilon_2-\varepsilon_3)\psi_{13} + (\varepsilon_1+\varepsilon_2-\varepsilon_3)\psi_{12}],\\
&\Gamma_{12} = -48\pi^2 c_2[(\varepsilon_1+\varepsilon_2+\varepsilon_3)\psi_{12}\psi_{13}\psi_{23} + (-\varepsilon_1+\varepsilon_2+\varepsilon_3)\psi_{23} + (\varepsilon_1-\varepsilon_2+\varepsilon_3)\psi_{13} + (-\varepsilon_1-\varepsilon_2+\varepsilon_3)\psi_{12}],\\
&\Gamma_{13} = -48\pi^2[(\varepsilon_1+\varepsilon_2+\varepsilon_3)^2\psi_{12}\psi_{13}\psi_{23} + (-\varepsilon_1+\varepsilon_2+\varepsilon_3)^2\psi_{23} + (\varepsilon_1-\varepsilon_2+\varepsilon_3)^2\psi_{13} + (\varepsilon_1+\varepsilon_2-\varepsilon_3)^2\psi_{12}],\\
&\Gamma_{14} = 2(\psi_{12}+\psi_{13}+\psi_{23}+\psi_{12}\psi_{13}\psi_{23}), \ \Gamma_{15} = -16\pi^2(\psi_{12}\psi_{13}\psi_{23} + \psi_{12} - \psi_{13} - \psi_{23}),\\
&\Gamma_{16} = -16\pi^2(\psi_{12}\psi_{13}\psi_{23} + \psi_{13} - \psi_{12} - \psi_{23}), \ \Gamma_{17} = -16\pi^2(\psi_{12}\psi_{13}\psi_{23} + \psi_{23} - \psi_{12} - \psi_{13}),
\end{aligned}
\tag{46}
$$

and

$$
b = \begin{pmatrix} 0 \\ H_1 \\ 0 \\ 0 \\ 0 \\ 0 \\ 0 \\ 0 \end{pmatrix}\psi_1 + \begin{pmatrix} 0 \\ 0 \\ H_2 \\ 0 \\ 0 \\ 0 \\ 0 \\ 0 \end{pmatrix}\psi_2 + \begin{pmatrix} 0 \\ 0 \\ 0 \\ H_3 \\ 0 \\ 0 \\ 0 \\ 0 \end{pmatrix}\psi_3 + \begin{pmatrix} H_4 \\ 0 \\ 0 \\ 0 \\ 0 \\ 0 \\ 0 \\ 0 \end{pmatrix}{\psi_1}^2 + \begin{pmatrix} H_5 \\ 0 \\ 0 \\ 0 \\ 0 \\ 0 \\ 0 \\ 0 \end{pmatrix}{\psi_2}^2 + \begin{pmatrix} H_6 \\ 0 \\ 0 \\ 0 \\ 0 \\ 0 \\ 0 \\ 0 \end{pmatrix}{\psi_3}^2
$$

$$+\begin{pmatrix}0\\0\\0\\0\\H_7\\0\\0\\0\end{pmatrix}\psi_1\psi_2+\begin{pmatrix}0\\0\\0\\0\\0\\H_8\\0\\0\end{pmatrix}\psi_1\psi_3+\begin{pmatrix}0\\0\\0\\0\\0\\0\\H_9\\0\end{pmatrix}\psi_2\psi_3+\begin{pmatrix}0\\0\\0\\0\\0\\0\\0\\H_{10}\end{pmatrix}\psi_1\psi_2\psi_3, \tag{47}$$

where

$$\begin{aligned}
&H_1=8\pi^2{\varepsilon_1}^2c_1-32\pi^4{\varepsilon_1}^4c_3,\ H_2=8\pi^2{\varepsilon_2}^2c_1-32\pi^4{\varepsilon_2}^4c_3,\ H_3=8\pi^2{\varepsilon_3}^2c_1-32\pi^4{\varepsilon_3}^4c_3,\\
&H_4=32\pi^2{\varepsilon_1}^2c_1-512\pi^4{\varepsilon_1}^4c_3,\ H_5=32\pi^2{\varepsilon_2}^2c_1-512\pi^4{\varepsilon_2}^4c_3,\ H_6=32\pi^2{\varepsilon_3}^2c_1-512\pi^4{\varepsilon_3}^4c_3,\\
&H_7=8\pi^2c_1[(\varepsilon_1+\varepsilon_2)^2\psi_{12}+(\varepsilon_1-\varepsilon_2)^2]-32\pi^4c_3[(\varepsilon_1+\varepsilon_2)^4\psi_{12}+(\varepsilon_1-\varepsilon_2)^4],\\
&H_8=8\pi^2c_1[(\varepsilon_1+\varepsilon_3)^2\psi_{13}+(\varepsilon_1-\varepsilon_3)^2]-32\pi^4c_3[(\varepsilon_1+\varepsilon_3)^4\psi_{13}+(\varepsilon_1-\varepsilon_3)^4],\\
&H_9=8\pi^2c_1[(\varepsilon_2+\varepsilon_3)^2\psi_{23}+(\varepsilon_2-\varepsilon_3)^2]-32\pi^4c_3[(\varepsilon_2+\varepsilon_3)^4\psi_{23}+(\varepsilon_2-\varepsilon_3)^4],\\
&H_{10}=8\pi^2c_1[(\varepsilon_1+\varepsilon_2+\varepsilon_3)^2\psi_{12}\psi_{13}\psi_{23}+(-\varepsilon_1+\varepsilon_2+\varepsilon_3)^2\psi_{23}\\
&\quad+(\varepsilon_1-\varepsilon_2+\varepsilon_3)^2\psi_{13}+(\varepsilon_1+\varepsilon_2-\varepsilon_3)^2\psi_{12}]-32\pi^4c_3[(\varepsilon_1+\varepsilon_2+\varepsilon_3)^4\psi_{12}\psi_{13}\psi_{23}\\
&\quad+(-\varepsilon_1+\varepsilon_2+\varepsilon_3)^4\psi_{23}+(\varepsilon_1-\varepsilon_2+\varepsilon_3)^4\psi_{13}+(\varepsilon_1+\varepsilon_2-\varepsilon_3)^4\psi_{12}].
\end{aligned}$$

Then, we assume the solution of $M({\omega_1}^2,{\omega_2}^2,{\omega_3}^2,\eta_1,\eta_2,\eta_3,u_0,c,\omega_1\omega_2,\omega_1\omega_3,\omega_2\omega_3)=b$ has the following form of

$$\begin{aligned}
&({\omega_1}^2,{\omega_2}^2,{\omega_3}^2,\eta_1,\eta_2,\eta_3,u_0,c,\omega_1\omega_2,\omega_1\omega_3,\omega_2\omega_3,)^T\\
&=({\omega_1}^{2(0)},{\omega_2}^{2(0)},{\omega_3}^{2(0)},{\eta_1}^{(0)},{\eta_2}^{(0)},{\eta_3}^{(0)},{u_0}^{(0)},c^{(0)},\omega_1{\omega_2}^{(0)},\omega_1{\omega_3}^{(0)},\omega_2{\omega_3}^{(0)})^T\\
&\quad+({\omega_1}^{2(1)},{\omega_2}^{2(1)},{\omega_3}^{2(1)},{\eta_1}^{(1)},{\eta_2}^{(1)},{\eta_3}^{(1)},{u_0}^{(1)},c^{(1)},\omega_1{\omega_2}^{(1)},\omega_1{\omega_3}^{(1)},\omega_2{\omega_3}^{(1)})^T\psi_1\\
&\quad+({\omega_1}^{2(2)},{\omega_2}^{2(2)},{\omega_3}^{2(2)},{\eta_1}^{(2)},{\eta_2}^{(2)},{\eta_3}^{(2)},{u_0}^{(2)},c^{(2)},\omega_1{\omega_2}^{(2)},\omega_1{\omega_3}^{(2)},\omega_2{\omega_3}^{(2)})^T\psi_2\\
&\quad+({\omega_1}^{2(3)},{\omega_2}^{2(3)},{\omega_3}^{2(3)},{\eta_1}^{(3)},{\eta_2}^{(3)},{\eta_3}^{(3)},{u_0}^{(3)},c^{(3)},\omega_1{\omega_2}^{(3)},\omega_1{\omega_3}^{(3)},\omega_2{\omega_3}^{(3)})^T\psi_3\\
&\quad+({\omega_1}^{2(11)},{\omega_2}^{2(11)},{\omega_3}^{2(11)},{\eta_1}^{(11)},{\eta_2}^{(11)},{\eta_3}^{(11)},{u_0}^{(11)},c^{(11)},\omega_1{\omega_2}^{(11)},\omega_1{\omega_3}^{(11)},\omega_2{\omega_3}^{(11)})^T{\psi_1}^2\\
&\quad+({\omega_1}^{2(22)},{\omega_2}^{2(22)},{\omega_3}^{2(22)},{\eta_1}^{(22)},{\eta_2}^{(22)},{\eta_3}^{(22)},{u_0}^{(22)},c^{(22)},\omega_1{\omega_2}^{(22)},\omega_1{\omega_3}^{(22)},\omega_2{\omega_3}^{(22)})^T{\psi_2}^2\\
&\quad+({\omega_1}^{2(33)},{\omega_2}^{2(33)},{\omega_3}^{2(33)},{\eta_1}^{(33)},{\eta_2}^{(33)},{\eta_3}^{(33)},{u_0}^{(33)},c^{(33)},\omega_1{\omega_2}^{(33)},\omega_1{\omega_3}^{(33)},\omega_2{\omega_3}^{(33)})^T{\psi_3}^2\\
&\quad+({\omega_1}^{2(12)},{\omega_2}^{2(12)},{\omega_3}^{2(12)},{\eta_1}^{(12)},{\eta_2}^{(12)},{\eta_3}^{(12)},{u_0}^{(12)},c^{(12)},\omega_1{\omega_2}^{(12)},\omega_1{\omega_3}^{(12)},\omega_2{\omega_3}^{(12)})^T\psi_1\psi_2\\
&\quad+({\omega_1}^{2(13)},{\omega_2}^{2(13)},{\omega_3}^{2(13)},{\eta_1}^{(13)},{\eta_2}^{(13)},{\eta_3}^{(13)},{u_0}^{(13)},c^{(13)},\omega_1{\omega_2}^{(13)},\omega_1{\omega_3}^{(13)},\omega_2{\omega_3}^{(13)})^T\psi_1\psi_3\\
&\quad+({\omega_1}^{2(23)},{\omega_2}^{2(23)},{\omega_3}^{2(23)},{\eta_1}^{(23)},{\eta_2}^{(23)},{\eta_3}^{(23)},{u_0}^{(23)},c^{(23)},\omega_1{\omega_2}^{(23)},\omega_1{\omega_3}^{(23)},\omega_2{\omega_3}^{(23)})^T\psi_2\psi_3\\
&\quad+({\omega_1}^{2(123)},{\omega_2}^{2(123)},{\omega_3}^{2(123)},{\eta_1}^{(123)},{\eta_2}^{(123)},{\eta_3}^{(123)},{u_0}^{(123)},c^{(123)},\omega_1{\omega_2}^{(123)},\omega_1{\omega_3}^{(123)},\omega_2{\omega_3}^{(123)})^T\\
&\quad\times\psi_1\psi_2\psi_3+o({\psi_1}^i{\psi_2}^j{\psi_3}^k),\ i+j+k\geq 3.
\end{aligned} \tag{48}$$

Finally, the relation of the three-soliton wave solution and three-periodic wave solution is given as follows.

Theorem 3 If three-periodic wave solution Eq. (45) satisfies the condition of

$$\varepsilon_j=\frac{k_j}{2\pi\mathrm{i}},\quad \eta_j=\frac{l_j}{2\pi\mathrm{i}},\quad \upsilon_j=\frac{\delta_j+\pi a_{jj}}{2\pi\mathrm{i}},\quad a_{js}=\frac{A_{js}}{-2\pi},\quad (j=1,2,3) \tag{49}$$

where k_j, l_j and $\delta_j (j=1,2,3)$ are given by Eq. (5), we have the following asymptotic properties:

$$\begin{aligned}
&u_0\to 0,\ c\to 0,\ \ \tau_j\to\frac{\sigma_j+\pi a_{jj}}{2\pi\mathrm{i}}\ (j=1,2,3),\\
&\varphi(\tau_1,\tau_2,\tau_3,a)\to 1+\mathrm{e}^{\sigma_1}+\mathrm{e}^{\sigma_2}+\mathrm{e}^{\sigma_3}+\mathrm{e}^{\sigma_1+\sigma_2+A_{12}}+\mathrm{e}^{\sigma_1+\sigma_3+A_{13}}+\mathrm{e}^{\sigma_2+\sigma_3+A_{23}}\\
&\qquad+\mathrm{e}^{\sigma_1+\sigma_2+\sigma_3+A_{12}+A_{13}+A_{23}},\ \ \psi_1,\psi_2,\psi_3\to 0.
\end{aligned}$$

Proof By substituting Eq. (46-48) into Eq. (44), we obtain the following relations of

$$\begin{aligned}
&c^{(0)}=c^{(1)}=c^{(2)}=c^{(3)}=c^{(12)}=c^{(13)}=c^{(23)}=c^{(123)}=0,\\
&{\omega_1}^{2(0)}+6\varepsilon_1u_0^{(0)}=-{\varepsilon_1}^2c_1-\varepsilon_1{\eta_1}^{(0)}c_2+4\pi^2{\varepsilon_1}^2c_3,
\end{aligned}$$

$$
\begin{aligned}
&{\omega_2}^{2(0)} + 6\varepsilon_2 u_0^{(0)} = -{\varepsilon_2}^2 c_1 - \varepsilon_2 {\eta_2}^{(0)} c_2 + 4\pi^2 {\varepsilon_2}^2 c_3,\\
&{\omega_3}^{2(0)} + 6\varepsilon_3 u_0^{(0)} = -{\varepsilon_3}^2 c_1 - \varepsilon_3 {\eta_3}^{(0)} c_2 + 4\pi^2 {\varepsilon_3}^2 c_3,\\
&{\omega_1}^{2(1)} + \varepsilon_1 {\eta_1}^{(1)} c_2 + 6\varepsilon_1 u_0^{(1)} = 0,\ {\omega_2}^{2(1)} + \varepsilon_2 {\eta_2}^{(1)} c_2 + 6\varepsilon_2 u_0^{(1)} = 0,\ {\omega_3}^{2(1)} + \varepsilon_3 {\eta_3}^{(1)} c_2 + 6\varepsilon_3 u_0^{(1)} = 0,\\
&c^{(11)} - 32\pi^2 {\omega_1}^{2(0)} - 32\pi^2 {\varepsilon_1}{\eta_1}^{(0)} c_2 - 192\pi^2 {\varepsilon_2}^2 u_0^{(0)} = 32\pi^2 {\varepsilon_1}^2 c_1 - 512\pi^4 {\varepsilon_1}^4 c_3,\\
&c^{(22)} - 32\pi^2 {\omega_2}^{2(0)} - 32\pi^2 {\varepsilon_2}{\eta_2}^{(0)} c_2 - 192\pi^2 {\varepsilon_2}^2 u_0^{(0)} = 32\pi^2 {\varepsilon_2}^2 c_1 - 512\pi^4 {\varepsilon_2}^4 c_3,\\
&c^{(33)} - 32\pi^2 {\omega_3}^{2(0)} - 32\pi^2 {\varepsilon_3}{\eta_3}^{(0)} c_2 - 192\pi^2 {\varepsilon_3}^2 u_0^{(0)} = 32\pi^2 {\varepsilon_3}^2 c_1 - 512\pi^4 {\varepsilon_3}^4 c_3.
\end{aligned}
\tag{50}
$$

□

Then by using condition (49), taking $u_0^{(0)} = 0,\ \eta_j^{(0)} = \eta_j, (j = 1, 2, 3)$ and letting the remaining components of η are zero, Eq. (50) has the following form of

$$
\begin{aligned}
c &= -384\pi^4 {\varepsilon_1}^4 c_3 {\psi_1}^2 - 384\pi^4 {\varepsilon_2}^4 c_3 {\psi_2}^2 - 384\pi^4 {\varepsilon_3}^4 c_3 {\psi_3}^2 + o({\psi_1}^2 {\psi_2}^2 {\psi_3}^2),\\
2\pi \mathrm{i}\omega_1 &= \sqrt{-4\pi^2 \omega_1} = \sqrt{-4\pi^2(-{\varepsilon_1}^2 c_1 - \varepsilon_1 \eta_1 c_2 + 4\pi^2 {\varepsilon_1}^2 c_3)},\\
2\pi \mathrm{i}\omega_2 &= \sqrt{-4\pi^2 \omega_2} = \sqrt{-4\pi^2(-{\varepsilon_2}^2 c_1 - \varepsilon_2 \eta_2 c_2 + 4\pi^2 {\varepsilon_2}^2 c_3)},\\
2\pi \mathrm{i}\omega_3 &= \sqrt{-4\pi^2 \omega_3} = \sqrt{-4\pi^2(-{\varepsilon_3}^2 c_1 - \varepsilon_3 \eta_3 c_2 + 4\pi^2 {\varepsilon_3}^2 c_3)}.
\end{aligned}
$$

By using condition (49), we have

$$
\begin{aligned}
u_0 \to 0,\ c \to 0,\ 2\pi \mathrm{i}\omega_1 &\to \sqrt{-{k_1}^2 c_1 - k_1 l_1 c_2 - {k_1}^2 c_3},\\
2\pi \mathrm{i}\omega_2 &\to \sqrt{-{k_2}^2 c_1 - k_2 l_2 c_2 - {k_2}^2 c_3},\\
2\pi \mathrm{i}\omega_3 &\to \sqrt{-{k_3}^2 c_1 - k_3 l_3 c_2 - {k_3}^2 c_3},\quad \psi_1, \psi_2, \psi_3 \to 0.
\end{aligned}
$$

By expanding the theta function

$$
\begin{aligned}
\varphi(\tau_1, \tau_2, \tau_3, a) = 1 &+ (\mathrm{e}^{2\pi \mathrm{i}\tau_1} + \mathrm{e}^{-2\pi \mathrm{i}\tau_1})\mathrm{e}^{-\pi a_{11}} + (\mathrm{e}^{2\pi \mathrm{i}\tau_2} + \mathrm{e}^{-2\pi \mathrm{i}\tau_2})\mathrm{e}^{-\pi a_{22}}\\
&+ (\mathrm{e}^{2\pi \mathrm{i}\tau_3} + \mathrm{e}^{-2\pi \mathrm{i}\tau_3})\mathrm{e}^{-\pi a_{33}} + \left(\mathrm{e}^{2\pi \mathrm{i}(\tau_1+\tau_2)} + \mathrm{e}^{-2\pi \mathrm{i}(\tau_1+\tau_2)}\right)\mathrm{e}^{-\pi(a_{11}+2a_{12}+a_{22})}\\
&+ \left(\mathrm{e}^{2\pi \mathrm{i}(\tau_1+\tau_3)} + \mathrm{e}^{-2\pi \mathrm{i}(\tau_1+\tau_3)}\right)\mathrm{e}^{-\pi(a_{11}+2a_{13}+a_{33})} + \left(\mathrm{e}^{2\pi \mathrm{i}(\tau_2+\tau_3)} + \mathrm{e}^{-2\pi \mathrm{i}(\tau_2+\tau_3)}\right)\mathrm{e}^{-\pi(a_{22}+2a_{23}+a_{33})}\\
&+ \left(\mathrm{e}^{2\pi \mathrm{i}(\tau_1+\tau_2+\tau_3)} + \mathrm{e}^{-2\pi \mathrm{i}(\tau_1+\tau_2+\tau_3)}\right)\mathrm{e}^{-\pi(a_{11}+2a_{12}+2a_{13}+2a_{23}+a_{22}+a_{33})} + \cdots,
\end{aligned}
$$

and applying condition(49), one yields

$$
\begin{aligned}
\varphi(\tau_1, \tau_2, \tau_3, a) = 1 &+ \mathrm{e}^{{\tau_1}'} + \mathrm{e}^{{\tau_2}'} + \mathrm{e}^{{\tau_3}'} + \mathrm{e}^{{\tau_1}'+{\tau_2}'-2\pi a_{12}} + \mathrm{e}^{{\tau_1}'+{\tau_3}'-2\pi a_{13}} + \mathrm{e}^{{\tau_2}'+{\tau_3}'-2\pi a_{23}}\\
&+ \mathrm{e}^{{\tau_1}'+{\tau_2}'+{\tau_3}'-2\pi(a_{12}+a_{13}+a_{23})} + {\psi_1}^2 \mathrm{e}^{-{\tau_1}'} + {\psi_2}^2 \mathrm{e}^{-{\tau_2}'} + {\psi_3}^2 \mathrm{e}^{-{\tau_3}'}\\
&+ \cdots \to 1 + \mathrm{e}^{{\tau_1}'} + \mathrm{e}^{{\tau_2}'} + \mathrm{e}^{{\tau_3}'} + \mathrm{e}^{{\tau_1}'+{\tau_2}'+A_{12}} + \mathrm{e}^{{\tau_1}'+{\tau_3}'+A_{13}}\\
&+ \mathrm{e}^{{\tau_2}'+{\tau_3}'+A_{23}} + \mathrm{e}^{{\tau_1}'+{\tau_2}'+{\tau_3}'+A_{12}+A_{13}+A_{23}},\quad \psi_1, \psi_2, \psi_3 \to 0,
\end{aligned}
\tag{51}
$$

where

$$
\begin{aligned}
{\tau_1}' &= 2\pi \mathrm{i}\tau_1 - \pi a_{11} \to k_1 x + l_1 y + \sqrt{-c_2 k_1 l_1 - c_3 {k_1}^4 - c_1 {k_1}^2} t + \delta_1 = \sigma_1,\\
{\tau_2}' &= 2\pi \mathrm{i}\tau_2 - \pi a_{22} \to k_2 x + l_2 y + \sqrt{-c_2 k_2 l_2 - c_3 {k_2}^4 - c_1 {k_2}^2} t + \delta_2 = \sigma_2,\\
{\tau_3}' &= 2\pi \mathrm{i}\tau_3 - \pi a_{33} \to k_3 x + l_3 y + \sqrt{-c_2 k_3 l_3 - c_3 {k_3}^4 - c_1 {k_3}^2} t + \delta_3 = \sigma_3,\quad \psi_1, \psi_2, \psi_3 \to 0.
\end{aligned}
\tag{52}
$$

Finally, combining Eqs. (51) and (52), we obtain

$$
\begin{aligned}
\varphi(\tau_1, \tau_2, \tau_3, a) \to 1 &+ \mathrm{e}^{\sigma_1} + \mathrm{e}^{\sigma_2} + \mathrm{e}^{\sigma_3} + \mathrm{e}^{\sigma_1+\sigma_2+A_{12}} + \mathrm{e}^{\sigma_1+\sigma_3+A_{13}} + \mathrm{e}^{\sigma_2+\sigma_3+A_{23}}\\
&+ \mathrm{e}^{\sigma_1+\sigma_2+\sigma_3+A_{12}+A_{13}+A_{23}},\quad \psi_1, \psi_2, \psi_3 \to 0.
\end{aligned}
$$

Therefore, three-periodic wave solution tends to three-soliton solution under the condition of $\psi_1, \psi_2, \psi_3 \to 0$.

7 Conclusion

In this paper, we have investigated the soliton solutions, breath-wave solutions and their transformations, and one-, two-, and three-periodic waves for a (2+1)-dimensional Boussinesq-type equation. Based on the Hirota's bilinear method, the soliton solutions have been derived. By taking the complex conjugate condition to the soliton solutions, the breather solutions are further obtained. And transformation mechanism of the one breather wave is systematically studied by considering the case which two characteristic lines are parallel, that is $\begin{vmatrix} a_1 & p_1 \\ a_2 & p_2 \end{vmatrix} = 0$, under this condition, a large number of types of nonlinear waves are obtained, including quasi-anti-dark soliton, M-shaped soliton, oscillation M-shaped soliton, multi-peak soliton, quasi-sine wave, quasi-periodic W-shaped wave, quasi-periodic anti-dark soliton wave and quasi-periodic wave. The transformation of two breather waves is further studied.

According to the Riemann theta function, we have got one- and two-period wave solutions. At the same time, we firstly extend the study of periodic wave to three-periodic wave solution. In addition, when studying the dynamic characteristics of periodic waves, the characteristic line method is also firstly introduced. It is obvious that the one-periodic wave solution has one characteristic line of $\tau = \varepsilon x + \eta y + \omega t + \upsilon = 0$, the propagation direction of wave is completely determined by τ, and $\frac{\upsilon_x}{\upsilon_y} = \frac{\varepsilon}{\eta}$, as shown in Fig. 16. And the two-periodic wave has two characteristic lines of $\tau_1 = \varepsilon_1 x + \eta_1 y + \omega_1 t + \upsilon_1 = 0$ and $\tau_2 = \varepsilon_2 x + \eta_2 y + \omega_2 t + \upsilon_2 = 0$. By considering whether the two characteristic lines are parallel or not, the different forms of two-periodic wave are obtained, as shown in Figs. 17, 18, 19 and 20. The three-periodic wave has three characteristic lines of $\tau_1 = \varepsilon_1 x + \eta_1 y + \omega_1 t + \upsilon_1 = 0$, $\tau_2 = \varepsilon_2 x + \eta_2 y + \omega_2 t + \upsilon_2 = 0$ and $\tau_3 = \varepsilon_3 x + \eta_3 y + \omega_3 t + \upsilon_3 = 0$. By considering the relationship between the values of ε_1, ε_2 and ε_3, the different forms of three-periodic wave are gained, as shown in Figs. 21, 22, 23 and 24.

The generalized Boussinesq equation can be reduced into some integrable equations including rich algebraic and geometric structures, and it appears in many disciplines and research fields, such as fluid mechanics, ocean waves, nonlinear optics and atmospheric science. The obtained results about the transformation mechanism of the breather waves and high-dimensional Riemann theta function quasi-periodic waves, in particular the three-periodic waves, will play an important role in explaining the nonlinear phenomena existing in Eq. (1). Furthermore, the characteristic line method has been well extended to analyze the dynamical behaviors of the quasi-periodic waves, which gives a new perspective to consider the Riemann theta function periodic waves. The analytic method presented in this paper can be applied to other integrable systems to explore rich integrable properties.

Acknowledgements This work is supported by the National Natural Science Foundation of China (No. 12101572) and Research Project Supported by Shanxi Scholarship Council of China (No. 2020-105).

Data Availability Statement Our manuscript has no associated data.

Declarations

Conflicts of interest The authors declare that they have no conflict of interest.

References

1. M.B. Riaz, A. Atangana, A. Jhangeer, S. Tahir, Soliton solutions, soliton-type solutions and rational solutions for the coupled nonlinear Schrödinger equation in magneto-optic waveguides. Eur. Phys. J. Plus **136**, 161 (2021)
2. H. Bulut, T.A. Sulaiman, H.M. Baskonus, On the new soliton and optical wave structures to some nonlinear evolution equations. Eur. Phys. J. Plus **132**, 459 (2017)
3. A. Biswas, J.M. Vega-Guzman, A.H. Kara, Q. Zhou, M. Ekici, Y. Yıldırım, H.M. Alshehri, M.R. Belic, Conservation laws for solitons in magneto-optic waveguides with dual-power law nonlinearity. Phys. Lett. A **416**, 127667 (2021)
4. X.Y. Wu, B. Tian, L. Liu, Y. Sun, Bright and dark solitons for a discrete (2+1)-dimensional Ablowitz-Ladik equation for the nonlinear optics and Bose-Einstein condensation. Commun. Nonlinear Sci. Numer. Simul. **50**, 201–210 (2017)
5. T. Pavithra, R. Ravichandran, G. Sunny, L. Kavitha, Electromagnetic lump soliton solution of (2+1) dimensional ferromagnetic nanowire with Dzyaloshinskii-Moriya interaction. Mater. Today: Proc. **25**, 192–198 (2020)
6. V. Senthil Kumar, L. Kavitha, C. Boopathy, D. Gopi, Loss-less propagation, elastic and inelastic interaction of electromagnetic soliton in an anisotropic ferromagnetic nanowire. Commun. Nonlinear Sci. Numer. Simul. **51**, 50–65 (2017)
7. L. Kavitha, M. Saravanan, V. Senthilkumar, R. Ravichandran, D. Gopi, Collision of electromagnetic solitons in a weak ferromagnetic medium. J. Magn. Magn. Mater. **355**, 37–50 (2014)
8. J. Borhanian, I. Kourakis, S. Sobhanian, Electromagnetic envelope solitons in magnetized plasma. Phys. Lett. A **373**, 3667–3677 (2009)
9. J.B. Okaly, F.I. Ndzana, R.L. Woulaché, T.C. Kofané, Solitary wavelike solutions in nonlinear dynamics of damped DNA systems. Eur. Phys. J. Plus. **134**, 598 (2019)
10. S. Issa, I. Maïna, C.B. Tabi, A. Mohamadou, H.P. Ekobena Fouda, T.C. Kofané, Long-range modulated wave patterns in certain nonlinear saturation alpha-helical proteins. Eur. Phys. J. Plus. **136**(9), 1–21 (2021)
11. D.D. Georgiev, J.F. Glazebrook, Thermal stability of solitons in protein α-helices. Chaos, Solitons Fractals **155**, 111644 (2021)
12. W. Ma, L. Yang, R. Rohs, W. Noble, DNA sequence plus shape kernel enables alignment-free modeling of transcription factor binding. Bioinformatics **33**, 3003–3010 (2017)

13. R.X. Liu, B. Tian, L.C. Liu, B. Qin, X. Lü, Bilinear forms, N-soliton solutions and soliton interactions for a fourth-order dispersive nonlinear Schrödinger equation in condensed-matter physics and biophysics. Phys. B **413**, 120–125 (2013)
14. A.F. Shchepetkin, J.C. McWilliams, Accurate Boussinesq oceanic modeling with a practical, "stiffened" equation of state. Ocean Model. **38**, 41–70 (2011)
15. S. Kumar, S. Rani, Study of exact analytical solutions and various wave profiles of a new extended (2+1)-dimensional Boussinesq equation using symmetry analysis. J. Ocean Eng. Sci. (2021). https://doi.org/10.1016/j.joes.2021.10.002
16. B.Q. Li, A.M. Wazwaz, Y.L. Ma, Two new types of nonlocal Boussinesq equations in water waves: bright and dark soliton solutions. Chin. J. Phys. **77**, 1782–1788 (2022)
17. J.G. Liu, W.H. Zhu, Multiple rogue wave solutions for (2+1)-dimensional Boussinesq equation. Chin. J. Phys. **67**, 492–500 (2020)
18. W.Y. Sun, Y.Y. Sun, The degenerate breather solutions for the Boussinesq equation. Appl. Math. Lett. **128**, 107884 (2021)
19. X.G. Geng, T. Su, Discrete coupled derivative nonlinear Schrödinger equations and their quasi-periodic solutions. J. Phys. A: Math. Theor. **40**, 433–453 (2007)
20. E.G. Fan, Supersymmetric KdV-Sawada-Kotera-Ramani equation and its quasi-periodic wave solutions. Phys. Lett. A **374**, 744–749 (2010)
21. L. Luo, E.G. Fan, Quasi-periodic waves of the N=1 supersymmetric modified Korteweg-de Vries equation. Nonlinear Anal. **74**, 666–675 (2011)
22. S.F. Tian, H.Q. Zhang, A kind of explicit Riemann theta functions periodic waves solutions for discrete soliton equations. Commun. Nonlinear Sci. Numer. Simul. **16**, 173–186 (2011)
23. H. Jin, B. Liu, Y. Wang, The existence of quasiperiodic solutions for coupled Duffing-type equations. J. Math. Anal. Appl. **374**, 429–441 (2011)
24. F. Veerman, F. Verhulst, Quasiperiodic phenomena in the Vanderpol-Mathieu equation. J. Sound Vib. **326**, 314–320 (2009)
25. V.T. Yatsyuk, The existence of quasiperiodic solutions of systems of differential equations of the second order. Ukr. Math. J. **26**, 578–584 (1974)
26. P. Poláčik, D.A. Valdebenito, The existence of partially localized periodic-quasiperiodic solutions and related KAM-type results for elliptic equations on the entire space. J. Dynam. Differ. Equ. (2021). https://doi.org/10.1007/s10884-020-09925-5
27. P. Zhao, E.G. Fan, A unified construction for the algebro-geometric quasiperiodic solutions of the Lotka-Volterra and relativistic Lotka-Volterra hierarchy. J. Math. Phys. **56**, 043501 (2015)
28. P. Zhao, E.G. Fan, L. Luo, Quasiperiodic solutions of the Kadomtsev-Petviashvili equation via the multidimensional Baker-Akhiezer function generated by the Broer-Kaup hierarchy. J. Math. Anal. Appl. **435**, 38–60 (2016)
29. M.J. Xu, S.F. Tian, J.M. Tu, P.L. Ma, T.T. Zhang, Quasi-periodic wave solutions with asymptotic analysis to the Saweda-Kotera-Kadomtsev-Petviashvili equation. Eur. Phys. J. Plus **130**, 174 (2015)
30. Z.L. Zhao, B. Han, Quasiperiodic wave solutions of a (2+1)-dimensional generalized breaking soliton equation via bilinear Bäcklund transformation. Eur. Phys. J. Plus. **131**, 128 (2016)
31. Z.L. Zhao, B. Han, The Riemann-Bäcklund method to a quasiperiodic wave solvable generalized variable coefficient (2+1)-dimensional KdV equation. Nonlinear Dyn. **87**, 2661–2676 (2017)
32. E.G. Fan, Y.C. Hon, Quasiperiodic waves and asymptotic behavior for Bogoyavlenskii's breaking soliton equation in (2+1) dimensions. Phys. Rev. E **78**, 036607 (2008)
33. L. Luo, E.G. Fan, Bilinear approach to the quasi-periodic wave solutions of modified Nizhnik-Novikov-Vesselov equation in (2+1) dimensions. Phys. Lett. A **374**, 3001–3006 (2010)
34. J. Wei, X.G. Geng, X. Zeng, Quasi-periodic solutions to the hierarchy of four-component Toda lattices. J. Geom. Phys. **106**, 26–41 (2016)
35. J.V. Boussinesq, Theorie de L'intumescence liguide appelee onde solitaire ou de translation se propageant dans un canal rectangulaire. Comptes rendus de l' Académie des Sci. **72**, 755–759 (1871)
36. J.V. Boussinesq, Théorie des ondes et des remous qui se propagent le long d'un canal rectangu-laire horizontal, en communiquant au liquide contenu dans ce canal des vitesses sensiblement pareilles de la surface au fond. J. Math. Pures Appl. **17**, 55–108 (1872)
37. P.A. Clarkson, M.D. Kruskal, New similarity reductions of the Boussinesq equation. J. Math. Phys. **30**, 2201–2213 (1989)
38. M. Boiti, F. Pempinelli, Similarity solutions and Bäcklund transformations of the Boussinesq equation. Nuov. Cim. B **56**, 148–156 (1980)
39. J. Weiss, The Painlevé property and Bäcklund transformations for the sequence of Boussinesq equations. J. Math. Phys. **26**, 258–269 (1985)
40. Y. Zhou, S. Manukure, M. McAnally, Lump and rogue wave solutions to a (2+1)-dimensional Boussinesq type equation. J. Geom. Phys. **167**, 104275 (2021)
41. X. Lü, J.P. Wang, F.H. Lin, X.W. Zhou, Lump dynamics of a generalized two-dimensional Boussinesq equation in shallow water. Nonlinear Dyn. **91**, 1249–1259 (2018)
42. Z.L. Zhao, B. Han, Nonlocal symmetry and explicit solutions from the CRE method of the Boussinesq equation. Eur. Phys. J. Plus **133**, 144 (2018)
43. R. Hirota, Exact solution of the Korteweg-de Vries equation for multiple collisions of solitons. Phys. Rev. Lett. **27**, 1192 (1971)
44. R. Hirota, *The Direct Method in Soliton Theory* (Cambridge University Press, Cambridge, 2004)
45. Z.L. Zhao, L.C. He, M-lump and hybrid solutions of a generalized (2+1)-dimensional Hirota-Satsuma-Ito equation. Appl. Math. Lett. **111**, 106612 (2021)
46. Z.L. Zhao, L.C. He, Resonance Y-type soliton and hybrid solutions of a (2+1)-dimensional asymmetrical Nizhnik-Novikov-Veselov equation. Appl. Math. Lett. **122**, 107497 (2021)
47. G.Q. Xu, A.M. Wazwaz, Integrability aspects and localized wave solutions for a new (4+1)-dimensional Boiti-Leon-Manna-Pempinelli equation. Nonlinear Dyn. **98**, 1379–1390 (2019)
48. G.Q. Xu, Y.P. Liu, W.Y. Cui, Painlevé analysis, integrability property and multiwave interaction solutions for a new (4+1)-dimensional KdV-Calogero-Bogoyavlenkskii-Schiff equation. Appl. Math. Lett. **132**, 108184 (2022)
49. X. Zhang, L. Wang, C. Liu, M. Li, Y.C. Zhao, High-dimensional nonlinear wave transitions and their mechanisms. Chaos **30**, 113107 (2020)